Immunogenicity and protection mediated by next-generation EBV gH/gL vaccines in non-human primate and humanized mouse models of infection

Kristina Edwards

A dissertation

submitted in partial fulfillment of the

requirements for the degree of

Doctor of Philosophy

University of Washington

2024

Reading Committee:

Andrew T. McGuire, Chair

Noah Sather

Jim Boonyaratanakornkit

Program Authorized to Offer Degree:

Pathobiology

University of Washington

Abstract

Immunogenicity and protection mediated by next-generation EBV gH/gL vaccines in non-human primate and humanized mouse models of infection

Kristina Edwards

Chair of the Supervisory Committee:

Andrew T. McGuire
Department of Global Health

Epstein Barr Virus (EBV) is an orally transmitted, γ-herpesvirus infecting 90% of adults worldwide. Infection is associated with various cancers and development of multiple sclerosis. A vaccine that prevents infection and reduce the global burden of EBV-associated disease is an urgent, yet unmet need. EBV infects epithelial cells and B cells, therefore an effective vaccine would likely have to block infection of both these cell types. The viral gH/gL glycoprotein complex is essential for entry, making it an attractive vaccine target. Additionally, antibodies against gH/gL have been shown to be protective against infection in vitro and in vivo. In this work we evaluate two different next-generation vaccine platforms to immunize animals with EBV gH/gL.

In one project we evaluated the immunogenicity of a multimeric gH/gL nanoparticle vaccine administered with two different adjuvants, Sigma Adjuvant System (SAS) and Saponin/MPLA nanoparticles (SMNP), in rhesus macaques. Formulation with SMNP elicited higher titers of binding and neutralizing antibodies, and higher frequency of vaccine-specific $IFN\gamma^{+}IL2^{+}$ $CD4^{+}$ T cells. After oral challenge with the EBV orthologue rhesus lymphocryptovirus

(rhLCV), all macaques in the control and SAS groups became infected, while one of four animals in the SMNP group remained aviremic and were seronegative against non-vaccine antigens, indicating protection. Further study revealed considerable antigenic disparity between the rhLCV gH/gL and EBV gH/gL. We found that our protected animal displayed a broader pattern of epitope recognition, as visualized by electron microscopy polyclonal epitope mapping, which may be linked to protection. The observed prevention of rhLCV infection in one macaque, despite the substantial antigenic disparity between the vaccine and challenge strain, supports the further pursuit of gH/gL nanoparticle vaccines against EBV.

In a second project, we have developed and optimized an alphavirus-derived self-amplifying mRNA vaccine platform (repRNA) to immunize mice with EBV gH/gL. The lead candidate tested was able to elicit a vaccine-specific $CD8^+$ T cell response as well as high-titers of neutralizing antibodies that persisted for at least 8 months post immunization. Transfer of vaccine-elicited IgG protected humanized mice from EBV-driven tumor formation and death following high-dose viral challenge. These data demonstrate that repRNA-gH/gL formulated with a localizing cationic nanocarrier (LION) is a promising candidate vaccine for preventing EBV infection and/or related malignancies in humans and encourage clinical development of vaccines targeting EBV gH/gL.

A third work-in-progress section describes a potential route of Fc-mediated EBV infection. In sum, this work describes the generation of immunogenic next-generation vaccines targeting EBV gH/gL and highlights some of the challenges and considerations of using the two most common animal models for EBV to evaluate vaccine-elicited protection.

Table of Contents

List of Figures ---------- ix

Chapter 1. Introduction To Epstein-Barr Virus ---------- 1

1.1 Global Burden of the virus ---------- 1
1.2 Factors Influencing Global Burden of EBV ---------- 2
1.3 Major Proteins Involved in EBV Infection ---------- 3
1.4 How EBV Infects: ---------- 4
1.5 The Immune Response to EBV Infection ---------- 5
1.5.1 Innate Immune Responses ---------- 5
1.5.2 Cellular Immune Response ---------- 5
1.5.3 Antibody Response to EBV ---------- 7
1.6 Vaccine Development: ---------- 8
1.6.1 Antigen Selection: ---------- 8
1.6.2 Types of vaccine platforms: ---------- 10
1.6.3 Vaccine Adjuvants: ---------- 12
1.6.4 Other considerations for vaccine development: ---------- 13
1.7 Animal models for evaluating EBV vaccines ---------- 14
1.7.1 Rhesus Macaques ---------- 14
1.7.2 Humanized Mice ---------- 15
1.7.3 Other Animal Models ---------- 17
1.8 Thesis Goals ---------- 17
1.9 Chapter 1 Bibliography ---------- 18

Chapter 2. Vaccination with nanoparticles displaying gH/gL from Epstein-Barr virus elicits limited cross-protection against rhesus lymphocryptovirus ---------- 28

2.1 Abstract ---------- 29
2.2 Introduction ---------- 30
2.3 Results ---------- 32
2.3.1 Immunogenicity of gH/gL 60-mer formulated with two different adjuvants in rhesus macaques ---------- 32
2.3.2 Immunization with gH/gL 60-mer formulated with SMNP protected 1 of 4 animals from oral rhLCV challenge ---------- 39
2.3.3 Cross reactivity of vaccine-elicited EBV gH/gL plasma antibodies with rhLCV gH/gL ----- 42
2.3.4 Electron microscopy polyclonal epitope mapping of vaccinated animals ---------- 44
2.4 Discussion ---------- 56
2.5 Materials and Methods ---------- 60
Study Design ---------- 60
Rhesus macaque PBMC isolation ---------- 61
Rhesus macaque oral swabs ---------- 62
Plasmids ---------- 62
rhLCV smallVCA protein expression and purification ---------- 62
Lentiviral Transduction ---------- 63
Purification of gH/gL 60-mer ---------- 63
Purification of rhLCV gH/gL-HIS ---------- 64

Purification of untagged monomeric EBV gH/gL ---- 64
Biotinylation of recombinant proteins ---- 64
rhLCV virus production ---- 64
rhLCV titration ---- 65
Preparation of EBV Reporter Viruses ---- 65
Digital droplet PCR ---- 66
EBV neutralization assay in B cells ---- 66
EBV Neutralization Assay in Epithelial Cells: ---- 67
gH/gL Neutravidin Capture ELISA ---- 67
rhLCV-smallVCA and EBV gB ELISAs ---- 68
Virus-free fusion assay ---- 69
Staining of antigen specific B cells ---- 69
T Cell Stimulation and ICS ---- 70
Biolayer Interferometry (BLI) ---- 71
mAb binding to EBV and rhLCV gH/gL ---- 71
Competition BLI ---- 72
Polyclonal IgG purification from sera ---- 72
pFAb-gH/gL complex formation ---- 72
Negative stain electron microscopy sample preparation, data processing and analysis ---- 73
Statistical Analysis ---- 73
2.6 Acknowledgments: ---- 73
2.7 Author Contributions ---- 74
2.8 Chapter 2 Bibliography ---- 74

Chapter 3. An Alphavirus Replicon Vaccine Encoding gH/gL Elicits Neutralizing Antibodies That Protect Against EBV Challenge In Humanized Mice. ---- 78

3.1 Abstract ---- 79
3.2 Introduction: ---- 79
3.3 Results: ---- 82
3.3.1 Initial characterization: ---- 82
3.3.2 Dose optimization for LION/repRNA gH/gL vaccination ---- 84
3.3.3 repRNA encoding membrane anchored gH/gL monomer is more immunogenic than the gH/gL ectodomain ---- 89
3.3.4.Membrane retained gH/gL monomer repRNA immunization is more immunogenic than secreted gH/gL multimers ---- 91
3.3.5 Passive transfer of IgG elicited by LION/repRNA gH/gL protects humanized mice from lethal EBV challenge ---- 94
3.3.6 LION/repRNA gH/gL elicits higher cellular responses than immunization with adjuvanted recombinant gH/gL ---- 103
3.4 Discussion ---- 105
3.6 Methods: ---- 108
Cell lines ---- 108
Mice ---- 109
Plasmids ---- 109
repRNA production ---- 110
Recombinant Proteins ---- 110
Preparation of EBV Reporter Viruses ---- 111
EBV neutralization assay in B cells ---- 111
EBV Neutralization Assay in Epithelial Cells ---- 112

Immunizations in C57BL/6 mice ----------113
IgG purification from murine plasma ----------113
Measurement of plasma antibody endpoint binding titers by anti-His capture ELISA ----------114
Measure of competitive binding titers by ELISA----------115
Stimulation of splenocytes ----------116
Intracellular staining (ICS)----------116
EBV infection in humanized mice ----------117
Quantitative PCR analysis EBV DNA in huCD34 engrafted mice----------118
3.7 Chapter 3 Bibliography ----------119

Chapter 4. Defining a Novel Pathway of Epstein-Barr Virus Infection With Implications for Vaccine Development ----------123

4.1 Abstract:----------123
4.2 Introduction ----------124
4.3 Results and Discussion: ----------127
4.3.1 'Humanized' 72A1 mediates worsened disease in humanized mice----------127
4.3.2 72A1 mediates worsened disease in Fc-dependent manner ----------129
4.3.3 Otherwise resistant B cells become susceptible to 72A1-mediated EBV attachment in an Fc-dependent manner ----------131
4.3.4 Fc mediated infection is limited to 72A1 ----------133
4.4 Conclusions and future directions: ----------135
4.5 Methods: ----------137
Antibody production:----------137
Mice ----------137
EBV infection in humanized mice ----------138
Quantitative PCR analysis EBV DNA in huCD34 engrafted mice----------139
Plasmids ----------140
Lentiviral Production: ----------140
Lentiviral Transduction: ----------140
Antibody mediated attachment staining----------141
Preparation of EBV Reporter Viruses ----------141
Antibody mediated infection assay----------141
4.6 Chapter 4 Bibliography ----------142

Chapter 5. Concluding Remarks on EBV gH/gL Vaccines ----------147

List of Figures

Chapter 2:

Figure S1: Monitoring for rhLCV infection prior to challenge....35
Figure 1: Immunogenicity of EBV gH/gL nanoparticle in rhesus macaques....36
Figure S2: Gating strategy to identify EBV gH/gL specific B cells....37
Figure S3: rhLCV titration curves....39
Figure 2: Outcome of oral rhLCV challenge in immunized animals....40
Figure 3: Serum cross-reactivity between EBV gH/gL and rhLCV gH/gL....42
Figure S4: rhLCV gH/gL binding titers for gH/gL + SMNP immunized animals....43
Figure 4: Electron microscopy polyclonal epitope mapping (EMPEM) analysis of polyclonal Fab fragments purified from animals A21137, A21138 and A21139 binding to EBV gH/gL and rhLCV gH/gL as indicated....45
Figure S5: Representative views of electron microscopy polyclonal epitope mapping (EMPEM) analysis of polyclonal Fab fragments purified from animals A21137, A21138 and A21139 binding to EBV gH/gL and rhLCV gH/gL....47
Figure 5: Neutralizing epitopes on EBV gH/gL are poorly conserved on rhLCV gH/gL....50
Figure 6: T cell responses elicited by gH/gL vaccination....52
Figure S6: Gating strategy for T cells after peptide stimulation and ICS....53
Figure S7: TNFα and IFNɣ production in CD8+ T cells in response to stimulation with peptide pools....54

Chapter 3:

Figure 1: Development and immunogenicity studies of repRNAs encoding EBV gH/gL....82
Figure 2: Dose optimization of gH/gL repRNA immunizations....85
Table S1: Statistical differences from data shown in Figure 2....87
Figure 3: Full-length gH/gL delivered by LION/repRNA elicits higher neutralizing titers than the gH/gL ectodomain....89
Figure 4: Full-length monomeric gH/gL elicits higher neutralizing titers than gH/gL multimers when delivered by LION/repRNA....91
Table S2: Statistical differences from data shown in Figure 4....92
Figure 5: IgG elicited by LION/repRNA- gH/gL protects humanized mice from lethal EBV challenge....96
Figure S1: gH/gL binding of purified IgG after two immunizations with full length gH/gL encoded by repRNA or the recombinant gH/gL ectodomain as indicated....98
Figure S2: Cell engraftment in humanized mice....99
Figure S3: Weight of mice from Figure 5 after EBV challenge....100
Figure S4: Spleens from individual animals from Figure 5 collected at time of euthanasia....101
Figure 6: LION/repRNA-gH/gL immunization elicits stronger vaccine-specific CD8+ T cell responses than protein monomer immunization....102
Figure S5: Gating strategy for evaluating IFNɣ+ CD4+ and CD8+ T cells....103

Chapter 4:

Figure 1: Transfer of 72A1 leads to enhanced disease in humanized mouse challenge model....127
Figure 2: Humanized mouse challenge after treatment with 72A1 or 72A1 silent Fc mAb....129
Figure 3: Fc-dependent attachment of EBV glycoproteins....131
Figure 4: Fc-mediated attachment facilitates EBV infection in vitro....133

ACKNOWLEDGEMENTS

First, I'd like the thank the members of the McGuire lab, former and present, for making the lab a fun and supportive environment and being great coworkers and friends. My fellow grad students, Harman, Crystal, and Sam for becoming good friends over the years and being amazing people to learn from. Leah and Karina were instrumental in performing experiments for my projects, and also great people to work with. From happy hours and lab hikes and pizza making parties, the McGuire lab is a great environment with great people and its hard to imagine a better place to be a grad student.

Next, none of this would have been possible without my mentor, Andy McGuire. He's been a terrific mentor during grad school, holding high expectations for my work and productivity while also letting me have flexibility and maintain a work life balance. Seeing the balance Andy has between being a great PI and being constantly busy with grants and papers, but still making time to do cool things outside of lab is a major reason why I want to continue in academia. Andy is a great scientist and all around cool guy who I feel lucky to have as a mentor.

My committee has also been invaluable during this process, thank you to Drs. Jenny Lund, Noah Sather, David Veesler, Jim Boonyaratanakornkit, and Leslie Goo. Thank you especially to Jenny for being someone outside of my lab that I can go to for advice. I'd also like to thank Noah and Jim for being on the reading committee and giving thoughtful feedback on this dissertation. Other people at UW and Fred Hutch have also been supportive during this journey, I'd specifically like to thank Karen Peterson and Ernie Lefler.

Finally, I'd like to thank all of my friends, family, and partner who have supported me during this process. Thank you to my parents, who may not understand what I do or why I want to study it, but support me in the process anyways. Thank you to my brother Erik. Thank you to my partner Tim, who has an inspiring work ethic and always encourages me to accomplish my next goal. Thank you to Tyler, Lucy, Kyle, and Kayla for their love and support over the years.

Chapter 1. Introduction To Epstein-Barr Virus

1.1 Global Burden of the virus

Epstein-Barr virus (EBV) is a ubiquitous gamma herpesvirus that infects over 90% of adults globally[1]. EBV infection is typically asymptomatic, however during primary infection, the virus can cause infectious mononucleosis (IM)[2–4]. IM is characterized by fever and lymphadenopathy, driven by a massive expansion of $CD8^+$ T cells[5–7]. IM typically develops when primary infection occurs after adolescence, but it is not well understood why some people develop symptoms yet others remain asymptomatic[2–5]. Symptoms typically resolve in 4-6 weeks[5–7].

Beyond IM, EBV is also associated with a variety of cancers including, but not limited to, gastric cancer, nasopharyngeal carcinoma, Hodgkin's and non-Hodgkin's lymphoma[8]. In fact, EBV was the first virus to be linked to development of cancer in humans and the discovery of EBV came from the culture of lymphoblasts from a Burkitt lymphoma patient[9]. Estimations of the global burden of EBV-associated malignancies range from 239,700–357,900 new cases of cancer and 137,900–208,700 deaths annually[8,10]. EBV associated B cell malignancies are thought to be related in part to the virus's ability to persist in and transform these cells. Mechanistic causes behind EBV-associated epithelial cell cancers are less understood[11]. Interactions between viral lytic genes and environmental and genetic factors are suspected[5,11]. While there are many factors involved in EBV's role in the development of malignancy, there is clear evidence for EBV driving a notable proportion of these cancers, leading to global morbidity and mortality[5,8,10,11].

In addition to cancer, EBV has been implicated in certain autoimmune disorders including rheumatoid arthritis[12] and multiple sclerosis (MS)[13–15]. A clear mechanism by which

EBV can cause or enhance the risk of developing these autoimmune conditions remains to be determined[12,16]. A link between EBV and development of MS had long been suspected[17–19], and a recent longitudinal study including over ten million people serving in the US military strengthened the connection, finding that the risk of MS increased over 30-fold after EBV infection[13,16].

1.2 Factors Influencing Global Burden of EBV

There are regional differences in prevalence and presentation of EBV infection[20]. Serological studies show a high prevalence of the virus in adults worldwide[21–26], yet the age of primary infection differs in different geographic regions[22]. Infectious mononucleosis is more prevalent when primary infection occurs at or past the age of adolescence[27,28]. Delayed primary infection is frequently observed in higher income countries[27–30]. Factors influencing the age of EBV acquisition are complex, but include socioeconomic status, ethnicity, and day-care attendance[31]. In contrast, children in the African subcontinent tend to have earlier primary infections, which is thought to contribute to higher rates of endemic Burkitt lymphoma[32–34].

Another contributing factor to different regional presentations of EBV-associated malignancies is co-infections. Co-infection with the pathogen causing malaria, *Plasmodium falciparum*, is linked to the development of endemic Burkitt lymphoma[35,36]. Immune dysregulation arising from co-infection with HIV-1 is linked to higher risks of developing some EBV associated B cell lymphomas[37]. Persons with untreated HIV-1 can have higher levels of EBV-specific $CD8^+$ T cells, higher levels of virus shed in saliva, and higher antibody levels compared to HIV-negative people and HIV-positive people under treatment [5]. HIV infection of mothers is also linked to earlier age of acquisition of newborns[38]. Other geographic differences in presentation occur as well. Nasopharyngeal carcinoma is an EBV associated malignancy that

is highly prevalent in Eastern and Southeastern Asia[39,40]. Possible explanations include environmental factors, genetic differences[41,42], and strain variation[43].

1.3 Major Proteins Involved in EBV Infection

During primary infection, EBV infects B cells and epithelial cells. Infection of these two cell types involves different viral proteins and entry pathways[44,45]. In EBV infection of epithelial cells, the viral protein BMRF2 has been implicated as an attachment protein[46–48]. BMRF2 contains an RGD motif, known to facilitate binding to host integrins, and further work has shown interactions between BMRF2 and α3, α5, and β1 integrins[48]. After attachment, the viral proteins gH, gL, and gB comprise the core fusion machinery[45]. The proteins gH/gL form a heterodimeric 1:1 complex, and act as a trigger for the fusion protein gB to undergo a massive conformational change and mediate fusion[45]. It has been suggested that gH/gL could potentially mediate attachment to integrins on host cells, as it also contains a KGD domain[49,50]. Additionally, potential interactions between gH/gL and non-muscle myosin heavy chain IIA[51] or ephrin A2[52] have been identified. The binding of gH/gL to the host cell through one or more of these proteins is thought to trigger gB to mediate fusion and allow infection to proceed. It has also been theorized that gB could bind to neuropilin 1, playing a role in triggering fusion to epithelial cells[53].

For B cell infection, the viral protein gp350 can bind to CD21 or CD35 (also known as complement receptors 2 and 1, respectively) on the B cell surface for the initial attachment step of infection[54,55]. Following this, the EBV protein gp42, in a 1:1:1 complex with gH/gL, binds to MHC class II on the B cell which then acts to trigger the downstream fusion protein gB[56–58]. This binding of gH/gL/gp42 to MHC II , through an as-of-yet undefined mechanism, triggers the fusion protein gB to undergo a major conformational change and mediate cell fusion[5]. An interesting feature of the virus is the abundance of the viral protein gp42 on the virion surface

can influence tropism[59]. When EBV is produced in B cells, gp42 can bind to HLA class II inside the cell, leading to its sequestration and degradation, resulting in progeny virions with less gp42[60]. This is not the case with virus produced in epithelial cells as they lack MHC class II[59]. An abundance of gp42 in the virion limits infection of epithelial cells, while being necessary for infection of B cells[61,62]. In short, EBV produced in B cells has a tropism for epithelial cells, and vice versa.

1.4 How EBV Infects:

EBV is an orally transmitted virus, spread via saliva[5]. During primary infection, EBV can replicate in the oral epithelium[63] and locally infiltrating B cells[5]. Some evidence suggests B cells are the first cell type infected after the initial exposure, including the fact that EBV in saliva contains progeny virions with a high abundance of gp42, indicating a tropism for B cells[64]. Despite some ambiguity of the exact order of events after exposure, the general consensus is that EBV undergoes lytic replication and viral amplification in the oral epithelia, and both lytic and latent infection of local B cells[5]. It is also unclear if certain B cell subtypes are preferentially targeted [5,45,65]. Infection of B cells can lead to lifelong viral persistence in the host through latent infection of memory B cells [66,67]. EBV encodes a complex series of genes that regulate latency, aiding in persistence, proliferation, and evading immune recognition[68]. These latently infected B cells can periodically reactivate and re-enter lytic replication in response to various factors, including differentiation to plasma cells[69] and expression of the lytic switch gene BZLF1[70,71]**.** Spontaneous lytic replication can seed new epithelial cell infection and shedding of the virus into the oral mucosa and into saliva, allowing for further transmission of the virus[68]. In a healthy person, spontaneous reactivation to lytic replication can be kept in check by the immune system.

1.5 The Immune Response to EBV Infection

1.5.1 Innate Immune Responses

Both innate and adaptive immune responses are important to control EBV infection. Studying initial immune responses after infection is difficult, as primary infection is often asymptomatic. As such, much of what has been studied in humans is in those presenting with IM[72]. NK cells have been shown to be particularly important to the control of EBV, demonstrated in IM[68,73,74], in those with primary immunodeficiencies that are related to more severe EBV symptoms[75–77], and in a humanized mouse model of EBV[78]. The humanized mouse model will be discussed in more detail later in this thesis. One study found a subset of NK cells ($CD56^{dim}$ $NKG2A^+$ KIR^-) that preferentially degranulate in response to host cells with lytic EBV infection[79]. Additionally, another study found a subset of tonsillar-enriched NK cells ($CD56^{bright}$ $CD16^-$) increase secretion of IFNɣ in response to stimulation of dendritic cells by EBV[80].

1.5.2 Cellular Immune Response

Both the cellular and humoral arms of the adaptive immune system have been shown to be important to control of EBV. In the cellular arm, $CD8^+$ T cells have been observed to massively expand during IM, to the degree where EBV-specific cells make up over 50% of the $CD8^+$ T cell repertoire[68]. After resolution of IM, the $CD8^+$ T cell compartment contracts to its usual size[68]. Infection in asymptomatic individuals also elicits $CD8^+$ T cell responses, without the massive expansion observed in IM[81]. During persistent infection, similar frequencies of EBV-specific $CD8^+$ T cells are seen between those who had IM or an asymptomatic primary infection—up to 2% of $CD8^+$ T cell responses directed towards individual lytic antigens, and less (0.5%) towards latent antigens[68,81]. $CD8^+$ T cells can directly lyse infected B cells, controlling

infection during IM and during spontaneous reactivation to lytic phase of EBV in latently infected B cells[81]. An additional factor to consider is that studies often sample peripheral blood and look at EBV specific responses in PBMCs, however this neglects the role for local tissue memory T cells[81]. In the tonsils of healthy carriers there is often an enrichment for EBV-specific $CD8^+$ T cells, and $CD8^+$ T cells are found to localize near the tonsillar epithelium where infected B cells can be found[81,82].

An EBV associated malignancy that highlights the role of $CD8^+$ T cells in the infected host is posttransplant lymphoproliferative disease (PTLD). PTLD is lymphoma driven by the uncontrolled proliferation of EBV infected B cells[68]. In the context of transplant (either solid organ or hematopoietic stem cell transplantation), patients undergo immunosuppression to prevent rejection of the transplant[68]. This depletes EBV-specific $CD8^+$ T cells and prevents them from lysing infected cells, leading to the unchecked proliferation characteristic of PTLD[68]. Additionally, certain malignancies occur much more frequently in patients with untreated HIV infection than in uninfected persons, likely due in part to impaired T cell responses in AIDS patients[68].

In healthy carriers, after primary infection, the $CD4^+$ T cell response is commonly about 10x lower than the $CD8^+$ response against the same antigen (as measured by a frequency of cells reacting to the antigen)[68]. The direct role of EBV-specific $CD4^+$ T cells on infected cells is not well established[68], however upon *ex vivo* stimulation EBV-specific $CD4^+$ T cells from healthy carriers have polyfunctional cytokine production with a marked increase in TNFα[81]. *In vitro*, isolated $CD4^+$ T cells are able to kill EBV-transformed cells, but the importance of these cells in controlling infection *in vivo* needs further research[68]. In addition, $CD4^+$ T cells facilitate the development of potent antibody responses against EBV by providing B cell help[83].

1.5.3 Antibody Response to EBV

After infection, people develop neutralizing antibodies (nAbs) against EBV[84]. These nAbs can take a while to develop, with on study finding that neutralizing titers peak around six months post-infection[84]. Neutralizing antibodies have been isolated against many of the different glycoproteins involved in infection of both B cells and epithelial cells. In sera from healthy carriers the majority of the antibody response able to neutralize B cell infection targets gp350, while the majority of the epithelial cell neutralizing antibody response binds gH/gL[85]**.** Several neutralizing antibodies against gH/gL have been isolated from healthy carries, the first of which was AMMO1[86,87]. Since then, several other nAbs targeting gH/gL have been identified from humans, including 769B10[85], 1D8[88], among others[89]. These are in addition to previous nAbs isolated from mice (E1D1[90], CL40[91] and CL59[91]). Antibodies against gH/gL typically neutralize epithelial cell infection better than B cell infection, as observed in serum antibodies from healthy donors[85] as well as in vaccine trials with gH/gL[85,92,93].

Similarly, antibodies against gB have been isolated with variable neutralization depending on the epitope targeted. The majority of mAbs against EBV gB isolated have been non-neutralizing[86,94]. However, the human mAb AMMO5[86] and murine mAbs 8A9 and 8C12[94] all target different epitopes on gB, and have variable neutralization capacity against epithelial cells and/or B cells.

The major target of the neutralizing antibody response to EBV is gp350, the attachment protein for B cell infection[95]. Neutralizing mAbs against gp350 and gp42 have been isolated from mice[96,97] and rabbits[98] after immunization with these glycoproteins. The murine nAb 72A1 is a particularly well characterized mAb against gp350 that is highly potent against B cell infection[99–102], and has even been tested in humans for its ability to control PTLD[103].

Antibodies have protective mechanisms beyond neutralization, including triggering antibody dependent cellular cytotoxicity (ADCC), antibody dependent cellular phagocytosis involving macrophages via opsonization (ADCP), antibody dependent neutrophil phagocytosis (ADNP), and others[104,105]. Non-neutralizing functional antibodies have been identified against EBV, including antibodies able to mediate ADCC against EBV infected cells[106–109] as well as ADCP[105,110], and ADNP[105]. These antibodies seem to appear after the resolution of acute infection[105,106,110] although one study observed some functionality during acute IM[105]. Increased study of the role of functional antibodies is warranted, particularly in the context of studying protective antibody responses from maternal antibody transfer[111].

1.6 Vaccine Development:

Studying immune responses to EBV can help inform vaccine design. By determining what antigens are targeted by cellular responses, and how antibodies can neutralize infection, we can identify promising targets for vaccination and key cell populations that can play a role in mediating protection. Ways to optimize candidate vaccines include: inclusion of different viral antigens, the type of vaccine given, the route of administration, and inclusion of different adjuvants. Each choice influences the type of immune response elicited after vaccination.

1.6.1 Antigen Selection:

EBV is a complex virus that encodes many different potential vaccine targets. One way to decide what proteins to target is to look at the antibody response after infection. Antibodies are the major correlate of protection for many successful vaccines[112,113]. We can look at the neutralizing antibody response elicited by natural infection to identify what proteins would be advantageous to include in candidate vaccines. The glycoprotein gp350 has historically been

the major target of EBV vaccine design[114–118] due to it being the most abundant glycoprotein on the surface of the virion[119], making up the majority of the humoral response[95], and early depletion studies showing antibodies against gp350 make up a large proportion of the neutralizing antibody response[95].

There have been a handful of human trials of gp350 vaccines[120–123]. In a phase II study of a soluble monomer gp350 vaccine, there was demonstrated protection against development of IM, but no protection against EBV infection[121]. It is possible better results would be observed with a more immunogenic vaccine, and gp350 vaccines are still being developed and evaluated either alone or in combination with other antigens in animals[124–127], and humans (NCT04645147, NCT05164094). Some potential drawbacks of focusing on gp350 as a vaccine immunogen include the fact that it is only involved in B cell infection[128], and that virus lacking gp350 is still infectious, albeit at a lower level[129], but inclusion of other antigens could overcome these. Additionally, a highly potent mAb against gp350 was found to lead to enhanced infection of epithelial cells *in vitro*, and this same effect could be mediated by saliva antibodies from infected individuals[130].

Many current vaccine candidates in development include proteins involved in fusion (gH/gL, gp42, and gB)[85,92,93,131,132] **(**NCT05164094). This has the advantage of potentially protecting against both epithelial cell and B cell infection. Work outlined later in this thesis will discuss the evaluation of different gH/gL vaccines. In addition to gH/gL, some vaccine candidates also include gp42, which is necessary for triggering fusion in B cells[85,93]. Antibodies against gp42 in plasma correlate with the ability of that plasma to neutralize B cell infection, however the correlation is weaker than what is observed with antibodies against gp350[128]. The fusion protein gB is also targeted in some candidate vaccines[131–133]. However, as a metastable fusion protein, EBV gB exists in pre-fusion and post-fusion conformations[94]. The difference in

the availability in neutralizing epitopes between these two conformations has not been well characterized, as the prefusion gB structure remains unsolved[134]. Further structural analysis of EBV gB and its neutralizing epitopes is warranted.

Many candidate EBV vaccines focus on the inclusion of antigens that will elicit neutralizing antibody responses, but some approaches also aim to elicit protective T cell responses[135]. A potential benefit of T cell vaccines is the potential to prevent or treat EBV associated malignancies[136–138]. Neutralizing antibody responses have also been associated with favorable outcomes in EBV associated malignancies, so this potential benefit is not solely limited to vaccines targeting T cell responses[136,139]. Many of the same glycoproteins that are targets of the neutralizing antibody response can also be targeted by T cells[68,140]. Additional antigens involved in latent infection and proteins that are expressed in EBV-associated tumors, including but not limited to EBNA1, EBNA-2, EBNA-LP, and LMP1, have been included in vaccines aiming to provoke protective T cell responses[68,141–143].

1.6.2 Types of vaccine platforms:

There are multiple platforms for vaccination, each with their own advantages and disadvantages. Many vaccines currently in development for EBV are protein based. Protein vaccines characteristically induce strong humoral responses but little/no $CD8^+$ T cell responses[144]. Soluble monomeric gp350 has been used as a vaccine candidate in humans, but none were protective against EBV infection[120–122]. A strategy to increase the immunogenicity of protein vaccines is to use multimeric nanoparticles rather than monomeric subunits[85,92,124,145,146]. This is often done by using a protein scaffold, either a naturally occurring scaffold such as ferritin[147] or one computationally designed[148–150], as a backbone to display multiple copies of the vaccine antigen(s). Benefits of multimerization include better BCR stimulation and germinal center responses, and higher affinity antibody production[146,151]. Similar to protein nanoparticle

vaccines are virus-like particles, or VLPs. These vaccines are based on viral structural proteins that can self-assemble and elicit many of the same advantages as nanoparticle subunit vaccines[144,152]. VLP vaccines for EBV are under development as well[153–155].

mRNA vaccines against EBV are also currently being developed and evaluated (NCT05164094, NCT05831111). In short, mRNA encoding the antigen(s) of interest is formulated in a nanocarrier allowing the mRNA to enter the host cell, leading to the transcription of the mRNA and production of the encoded antigen by the host cell[144]. As a platform, mRNA vaccines have been shown to elicit strong humoral responses and are able to elicit cellular responses, including $CD8^+$ T cells[144]. The vaccine antigen encoded by mRNA is produced by the host cell, where it can be degraded by the proteasome and loaded onto MHC class I for display to CD8+ T cells, leading to efficient induction of vaccine-specific CD8+ T cell responses[156]. Another type of mRNA vaccine, termed self-amplifying mRNA (saRNA), has the potential to be a promising vaccine platform. In theory saRNA allows for lower vaccine doses to be administered, as the mRNA entering the cell can be amplified, leading to increased antigen production by the host cell as compared to conventional mRNA vaccines[157]**.** saRNA vectors are typically based on single stranded RNA virus genomes, retaining the ability to self amplify but without the ability to form infectious particles[157]. Within the field of mRNA vaccines, there are many factors that can be optimized further including sequence modifications that may affect secondary structures of the mRNA[158], chemical or structural modifications of the mRNA, modifying the mRNA vector, and optimizing the formulation and delivery of the mRNA[157,159]**.**

Other vaccine platforms also exist and are being utilized for EBV vaccine candidates, including viral vector vaccines[141–143]. Some platforms, like live attenuated virus vaccines, do not lend themselves well to EBV vaccine design because of EBV's oncogenic potential and the risk of reversion[138,160].

1.6.3 Vaccine Adjuvants:

Inclusion of an adjuvant can help to boost the immunogenicity of vaccination[161]. Only a handful of adjuvants are currently approved for use in the clinic, including alum, MF59, $AS01_B$, AS04, CpG 1018, and Matrix M[162]. While the mechanism of action of adjuvants is not always well characterized or understood, modes of operation include triggering innate immune responses through activating antigen presenting cells, targeting antigen to lymph nodes, activate innate immune receptors, or by causing the localization and slow release of antigen at an injection site, called depot effect[161].

Despite being discovered nearly 100 years ago, the mechanism of action of alum adjuvants remains unclear[163,164] . These tend to elicit a more Th2 skewed immune response (at least in mice), with IgG antibody responses but poor cellular immunity[164]. As detailed below, many newer adjuvants include alum in their formulation.

Some adjuvants target innate immune sensors. For example, AS04 consists of MPL, a TLR4-stimulating compound derived from bacteria, and an aluminum salt[162,165]. The adjuvant CpG 1018 is a short single stranded synthetic DNA molecule that stimulates TLR9[161].

Many kinds of adjuvants are emulsions, for example MF59 is an oil-in-water emulsion that contains squalene[161]. It's mode of action was initially thought to be through depot effect and slow release of antigen, however it also induces beneficial innate immune responses like recruitment of phagocytic cells to increase antigen trafficking to lymph nodes, stimulation of DCs, and chemokine production that benefits T cell migration to LN[161,166]. AS01 is a liposome-based adjuvant which contains MPL and the saponin QS-21 isolated from tree bark[162,163,167]. Liposome-based adjuvants help to protect immunogen from degradation *in vivo* and aid uptake by APCs[161]. Saponins are very immunostimulatory and can elicit strong humoral and cellular

responses[161]. In some adjuvants, saponins are formulated with immunostimulatory complexes (ISCOMs)[161], for example Matrix M[168].

Additional adjuvants are currently under development. Sigma adjuvant systems (SAS, also known as RIBI) is a squalene oil-in-water emulsion containing MPL that is commonly used in immunogenicity studies in animals[169–172]. Saponin MPLA nanoparticles (SMNP)[173] is another highly immunogenic adjuvant under development that our group and others use to assess vaccine immunogenicity[173–177]. This adjuvant contains saponins that self-assemble with MPL to form ISCOM like structures, leading to potent antibody responses, even outperforming another saponin MPL adjuvant, $AS01_B$[173].

In short, many vaccine adjuvants use multiple approaches (TLR stimulation, emulsion, aluminum, saponins, ISCOMS) to improve immunogenicity, making adjuvant selection an important consideration for vaccine evaluation. Work in this thesis evaluates the same protein nanoparticle vaccine formulated with two different adjuvants, SAS and SMNP, in a non human primate (NHP) model. We aimed to investigate the role of adjuvant selection on the immunogenicity of our vaccine and its impact on efficacy against oral viral challenge, detailed further in chapter 2.

1.6.4 Other considerations for vaccine development:

Another consideration for vaccine design is the route of infection. EBV is primarily spread via saliva, so designing a vaccine that can protect against oral infection is important[178]. Eliciting potent mucosal responses is of interest in vaccine design for many different respiratory and sexually transmitted pathogens[179], so as the field of vaccinology moves towards a better understanding of how to elicit these responses, the design of EBV vaccines will also benefit . We do know that the route of vaccine administration can have strong influences on the resulting resident memory T cell populations in mucosal tissues as well as eliciting protective IgA

responses[180,181]. Most vaccines are delivered by intramuscular injection, but oral vaccination, skin microneedle patch, and intranasal vaccination are all other possible avenues to explore[179,182].

An additional factor to consider is the dose of an immunization. Previous work in vaccine design for other pathogens has highlighted the importance of the dose given in eliciting optimal immune responses, with both a low prime/high boost[183,184] and high boost/low prime[185] approaches showing better immunogenicity than matched prime/boost in their respective studies. Work outlined in this thesis will evaluate the impact of variable prime and boost doses on immunogenicity of an mRNA EBV gH/gL vaccine. The timing between doses also plays a role in the immunogenicity, as observed in study of HIV vaccines[186,187] as well as in our own work, detailed in chapter 3, where delay of boost immunization was required to see an increase in antibody titers following vaccination.

1.7 Animal models for evaluating EBV vaccines

1.7.1 Rhesus Macaques

After creating a candidate EBV vaccine, good animal models are needed to evaluate vaccine immunogenicity and efficacy. This is complicated by the fact that humans are the only natural host for EBV[188]. Old World monkeys have orthologous gamma-herpesviruses that are species specific[189,190]. For example, one animal model used to study EBV infection *in vivo* are rhesus macaques, and the EBV homologue rhesus lymphocryptovirus (rhLCV)[190–192]. rhLCV infection of rhesus macaques is a promising model for EBV infection of humans, as several key features are replicated: the route of infection, typical age of primary infection, typical

asymptomatic infection, and high homology between the rhLCV and EBV viral genomes[188,192–197].

Despite these similarities, there are still some differences between the two viruses. Work in this thesis highlights important antigenic disparity between rhLCV and EBV gH/gL, despite their ~90% amino acid similarity[196]. In addition, the EBV gp350 is very divergent from rhLCV gp350[193].

Challenge studies with rhLCV can be difficult as rhesus macaques typically get infected with rhLCV at a young age, so rhLCV negative animals have to be acquired. This can happen either from the use of infant macaques prior to infection, or by using animals from rhLCV negative colonies[192]. If infant macaques are used, animals must be isolated from rhLCV positive animals at a young age and consistently tested to ensure they truly are rhLCV negative[192]. If a vaccine or antibody or some sort of intervention is to be tested in a challenge model, the infant animals have to be monitored for the waning of maternal antibodies against rhLCV that could interfere prior to study start[192]. The cost of housing these animals for the ~6 months it takes for maternal antibodies to wane prior to the start of a study is not insignificant. Establishment and maintenance of specific rhLCV negative colonies also present their own challenges. As mentioned, to isolate rhLCV negative macaques they are isolated at a young age to prevent acquisition of the virus. This isolation can impact their socialization and complicate later breeding efforts[198] with other rhLCV negative macaques, making the establishment of a rhLCV negative colony difficult.

1.7.2 Humanized Mice

Humanized mice allow for the in vivo study of EBV in a small animal model. In this model highly immunocompromised mice, often nonobese diabetic-*scid* IL2Rgamma^{null} (NSG) mice, are engrafted with human CD34^{+} peripheral blood stem cells (PBSC)[188,199–202]. The PBSC

transferred into the mice can then reconstitute the human hematopoietic system, allowing for the recapitulation of *in vivo* infection of B cells but not epithelial cells[201]. To infect these mice, the natural oral route of transmission is not possible so instead they are infected with EBV by IP, IV, or RO injection of the virus[199]. Some groups have even managed to model asymptomatic latent EBV infection by giving a low challenge dose of EBV[199].

With this model, some human immune cell function is impaired. There's evidence of some T cell and NK cell functionality in these mice, but whether the populations that develop are comparable to populations found in humans remains incompletely characterized[78,201]. There is also an observable lytic $CD8^+$ T cell response that results in the lysis of infected $CD19^+$ B cells [199,203,204]. The B cells in these mice are also not able to produce strong antibody responses[205]. Evidence has shown that they may develop limited IgM response to infection[199], though to evaluate vaccine efficacy we would ideally want the ability to develop strong IgG and IgA responses. To get around this, we can vaccinate immune competent mice and passively transfer vaccine elicited antibodies into humanized mice prior to EBV challenge to be able to model vaccine efficacy[89,92,93]. While not perfect, humanized mice are a very useful preclinical model of vaccine efficacy. These mice appear to develop T cell responses to vaccination[199,201], leading to a potential model where humanized mice could be both directly vaccinated to elicit T cell responses as well as given passively transferred vaccine elicited antibodies to study humoral protection[201].

In addition to PBSC engrafted NSG mice, other kinds of humanized mice also exist. Some studies use NSG mice engrafted with PBMC (either EBV+ or not) to study infection in vivo[206]. Other groups have used HLA-A2[207] or human IL-6[205] transgenic NSG mice for engraftment with PBSC and seen better development of immune responses of those engrafted

cells. Another approach to humanization includes transfer of bone marrow, liver and thymus to create “BLT” mice[206]. This leads to more complete human immune development in these mice.

1.7.3 Other Animal Models

Other animal models for EBV do exist, but they are less commonly used[188]. Cottontop tamarins and common marmosets can both be infected with EBV[188,208–210], however instead of a typical asymptomatic presentation these animals develop lethal B cell malignancies[188,208]. Cottontop tamarins also stopped being used as a model animal as they are critically endangered[211]. Rabbits have also been intravenously infected with EBV, leading to persistent infection and B cell lymphoma following immune suppression[212]**.** Mice can be infected with the mouse orthologue murine gamma herpesvirus 68, which persists in memory B cells in infected mice but lacks the transforming ability of EBV, having more homology to Kaposi’s scarcoma-associated herpesvirus than EBV[188].

1.8 Thesis Goals

As detailed above, EBV is a ubiquitous virus that has a clear global burden of disease and no available vaccine. In this thesis, I will detail the evaluation of several candidate vaccines targeting gH/gL. We are focused on gH/gL as a vaccine target as (1) it is critical for infection of both B cells and epithelial cells[45], and (2) antibodies against gH/gL have been isolated from humans that can neutralize B cell and epithelial cell infection *in vitro* and *in vivo* using humanized mice[87–89] and rhesus macaque models[87]. Antibodies are the major correlate of protection for vaccines[112] and have been used to guide vaccine development by identifying promising vaccine targets[112] .

In chapter two, I will detail the testing of a protein nanoparticle displaying 60 copies of EBV gH/gL in a rhesus macaque model. Using two different adjuvants, SAS and SMNP, we evaluated the immunogenicity of the 60mer nanoparticle vaccine and the protection elicited against oral challenge with rhLCV. In addition to immunogenicity and protection, I also characterized antigenic differences between the rhLCV and EBV gH/gL, with implications for the design of future vaccine trials using this model. In the second project, mice were immunized with different gH/gL mRNA vaccine constructs, and the most immunogenic construct was evaluated in a humanized mouse model. This work is detailed in chapter three.

In addition to this, I will outline ongoing work investigating paradoxical behavior of a neutralizing antibody against EBV in chapter four. This antibody, 72A1, appears to mediate disease enhancement in an Fc dependent manner in a humanized mouse model for EBV. This work is still ongoing, but I will describe collected data, current projects, and the future directions and implications this work has for the future of EBV vaccine design.

1.9 Chapter 1 Bibliography

1. Cohen, J. I. Epstein–Barr Virus Infection. *New England Journal of Medicine* **343**, 481–492 (2000).
2. Henle, G., Henle, W. & Diehl, V. Relation of Burkitt's tumor-associated herpes-ytpe virus to infectious mononucleosis. *Proceedings of the National Academy of Sciences* **59**, 94–101 (1968).
3. Sylvester, J. E., Buchanan, B. K. & Silva, T. W. Infectious Mononucleosis: Rapid Evidence Review. *Am Fam Physician* **107**, 71–78 (2023).
4. Rostgaard, K. *et al.* Primary Epstein-Barr virus infection with and without infectious mononucleosis. *PLoS One* **14**, e0226436 (2019).
5. Howley, P. M., Knipe, D. M., Cohen, J. L. & Damania, B. A. Fields Virology: DNA Viruses. in *Fields Virology.* (eds. Howley, P. M. & Knipe, D. M.) vol. 2 806–945 (Wolters Kluwer, Philadelphia, 2021).
6. Cameron, B. *et al.* Prolonged illness after infectious mononucleosis is associated with altered immunity but not with increased viral load. *J Infect Dis* **193**, 664–71 (2006).
7. Abbott, R. J. *et al.* Asymptomatic Primary Infection with Epstein-Barr Virus: Observations on Young Adult Cases. *J Virol* **91**, (2017).
8. Khan, G., Fitzmaurice, C., Naghavi, M. & Ahmed, L. A. Global and regional incidence, mortality and disability-adjusted life-years for Epstein-Barr virus-attributable malignancies, 1990-2017. *BMJ Open* **10**, e037505 (2020).
9. Epstein, M. A., Achong, B. G. & Barr, Y. M. VIRUS PARTICLES IN CULTURED LYMPHOBLASTS FROM BURKITT'S LYMPHOMA. *The Lancet* **283**, 702–703 (1964).

10. Wong, Y., Meehan, M. T., Burrows, S. R., Doolan, D. L. & Miles, J. J. Estimating the global burden of Epstein-Barr virus-related cancers. *J Cancer Res Clin Oncol* **148**, 31–46 (2022).
11. Young, L. S., Yap, L. F. & Murray, P. G. Epstein-Barr virus: more than 50 years old and still providing surprises. *Nat Rev Cancer.* **16**, 789–802 (2016).
12. Callan, M. F. C. Epstein-Barr virus, arthritis, and the development of lymphoma in arthritis patients. *Curr Opin Rheumatol* **16**, 399–405 (2004).
13. Bjornevik, K. *et al.* Longitudinal analysis reveals high prevalence of Epstein-Barr virus associated with multiple sclerosis. *Science (1979)* **375**, 296–301 (2022).
14. Balandraud, N. & Roudier, J. Epstein-Barr virus and rheumatoid arthritis. *Joint Bone Spine* vol. 85 165–170 Preprint at https://doi.org/10.1016/j.jbspin.2017.04.011 (2018).
15. Ascherio, A. & Munger, K. L. EBV and Autoimmunity. *Curr Top Microbiol Immunol* **390**, 365–85 (2015).
16. Bjornevik, K., Münz, C., Cohen, J. I. & Ascherio, A. Epstein-Barr virus as a leading cause of multiple sclerosis: mechanisms and implications. *Nat Rev Neurol* **19**, 160–171 (2023).
17. Larsen, P. D., Bloomer, L. C. & Bray, P. F. Epstein-Barr nuclear antigen and viral capsid antigen antibody titers in multiple sclerosis. *Neurology* **35**, 435–8 (1985).
18. Sumaya, C. V, Myers, L. W. & Ellison, G. W. Epstein-Barr virus antibodies in multiple sclerosis. *Arch Neurol* **37**, 94–6 (1980).
19. Bray, P. F., Bloomer, L. C., Salmon, V. C., Bagley, M. H. & Larsen, P. D. Epstein-Barr virus infection and antibody synthesis in patients with multiple sclerosis. *Arch Neurol* **40**, 406–8 (1983).
20. Chang, C. M., Yu, K. J., Mbulaiteye, S. M., Hildesheim, A. & Bhatia, K. The extent of genetic diversity of Epstein-Barr virus and its geographic and disease patterns: a need for reappraisal. *Virus Res* **143**, 209–21 (2009).
21. Kuri, A. *et al.* Epidemiology of Epstein-Barr virus infection and infectious mononucleosis in the United Kingdom. *BMC Public Health* **20**, 912 (2020).
22. de-Thé, G. *et al.* Sero-epidemiology of the Epstein-Barr virus: preliminary analysis of an international study - a review. *IARC Sci Publ* 3–16 (1975).
23. Venkitaraman, A. R., Lenoir, G. M. & John, T. J. The seroepidemiology of infection due to Epstein-Barr virus in southern India. *J Med Virol* **15**, 11–6 (1985).
24. Fourcade, G. *et al.* Evolution of EBV seroprevalence and primary infection age in a French hospital and a city laboratory network, 2000-2016. *PLoS One* **12**, e0175574 (2017).
25. de Castro Alves, C. E. *et al.* Seroprevalence of Epstein-Barr virus and cytomegalovirus infections in Presidente Figueiredo, Amazonas, Brazil. *J Immunoassay Immunochem* **43**, 67–77 (2022).
26. Xiong, G. *et al.* Epstein-Barr virus (EBV) infection in Chinese children: a retrospective study of age-specific prevalence. *PLoS One* **9**, e99857 (2014).
27. Dunmire, S. K., Hogquist, K. A. & Balfour, H. H. Infectious Mononucleosis. *Curr Top Microbiol Immunol* **390**, 211–40 (2015).
28. Hallee, T. J., Evans, A. S., Niederman, J. C., Brooks, C. M. & Voegtly, j H. Infectious mononucleosis at the United States Military Academy. A prospective study of a single class over four years. *Yale J Biol Med* **47**, 182–95 (1974).
29. Crawford, D. H. *et al.* A cohort study among university students: identification of risk factors for Epstein-Barr virus seroconversion and infectious mononucleosis. *Clin Infect Dis* **43**, 276–82 (2006).
30. Fourcade, G. *et al.* Evolution of EBV seroprevalence and primary infection age in a French hospital and a city laboratory network, 2000-2016. *PLoS One* **12**, e0175574 (2017).
31. Condon, L. M. *et al.* Age-specific prevalence of Epstein-Barr virus infection among Minnesota children: effects of race/ethnicity and family environment. *Clin Infect Dis* **59**, 501–8 (2014).
32. de-Thé, G. Epstein-Barr virus behavior in different populations and implications for control of Epstein-Barr virus-associated tumors. *Cancer Res* **36**, 692–5 (1976).
33. de-Thé, G. Epstein-Barr virus and Burkitt's lymphoma worldwide: the causal relationship revisited. *IARC Sci Publ* 165–76 (1985).
34. Piriou, E. *et al.* Early age at time of primary Epstein-Barr virus infection results in poorly controlled viral infection in infants from Western Kenya: clues to the etiology of endemic Burkitt lymphoma. *J Infect Dis* **205**, 906–13 (2012).

35. Reynaldi, A. *et al.* Impact of Plasmodium falciparum Coinfection on Longitudinal Epstein-Barr Virus Kinetics in Kenyan Children. *J Infect Dis* **213**, 985–91 (2016).
36. Piriou, E. *et al.* Early age at time of primary Epstein-Barr virus infection results in poorly controlled viral infection in infants from Western Kenya: clues to the etiology of endemic Burkitt lymphoma. *J Infect Dis* **205**, 906–13 (2012).
37. Grogg, K. L., Miller, R. F. & Dogan, A. HIV infection and lymphoma. *J Clin Pathol* **60**, 1365–72 (2007).
38. Gantt, S. *et al.* Prospective Characterization of the Risk Factors for Transmission and Symptoms of Primary Human Herpesvirus Infections Among Ugandan Infants. *J Infect Dis* **214**, 36–44 (2016).
39. Roy Chattopadhyay, N., Das, P., Chatterjee, K. & Choudhuri, T. Higher incidence of nasopharyngeal carcinoma in some regions in the world confers for interplay between genetic factors and external stimuli. *Drug Discov Ther* **11**, 170–180 (2017).
40. Chen, Y.-P. *et al.* Nasopharyngeal carcinoma. *Lancet* **394**, 64–80 (2019).
41. Chang, E. T. & Adami, H.-O. The enigmatic epidemiology of nasopharyngeal carcinoma. *Cancer Epidemiol Biomarkers Prev* **15**, 1765–77 (2006).
42. Roy Chattopadhyay, N., Das, P., Chatterjee, K. & Choudhuri, T. Higher incidence of nasopharyngeal carcinoma in some regions in the world confers for interplay between genetic factors and external stimuli. *Drug Discov Ther* **11**, 170–180 (2017).
43. Kanda, T., Yajima, M. & Ikuta, K. Epstein-Barr virus strain variation and cancer. *Cancer Sci* **110**, 1132–1139 (2019).
44. Shannon-Lowe, C. & Rowe, M. Epstein Barr virus entry; kissing and conjugation. *Curr Opin Virol* **4**, 78–84 (2014).
45. Bu, G.-L., Xie, C., Kang, Y.-F., Zeng, M.-S. & Sun, C. How EBV Infects: The Tropism and Underlying Molecular Mechanism for Viral Infection. *Viruses* **14**, (2022).
46. Xiao, J., Palefsky, J. M., Herrera, R. & Tugizov, S. M. Characterization of the Epstein-Barr virus glycoprotein BMRF-2. *Virology* **359**, 382–96 (2007).
47. Xiao, J., Palefsky, J. M., Herrera, R., Berline, J. & Tugizov, S. M. The Epstein–Barr virus BMRF-2 protein facilitates virus attachment to oral epithelial cells. *Virology* **370**, 430–442 (2008).
48. Tugizov, S. M., Berline, J. W. & Palefsky, J. M. Epstein-Barr virus infection of polarized tongue and nasopharyngeal epithelial cells. *Nat Med* **9**, 307–314 (2003).
49. Chesnokova, L. S. & Hutt-Fletcher, L. M. Fusion of Epstein-Barr virus with epithelial cells can be triggered by αvβ5 in addition to αvβ6 and αvβ8, and integrin binding triggers a conformational change in glycoproteins gHgL. *J Virol* **85**, 13214–23 (2011).
50. Chesnokova, L. S., Nishimura, S. L. & Hutt-Fletcher, L. M. Fusion of epithelial cells by Epstein-Barr virus proteins is triggered by binding of viral glycoproteins gHgL to integrins alphavbeta6 or alphavbeta8. *Proc Natl Acad Sci U S A* **106**, 20464–9 (2009).
51. Xiong, D. *et al.* Nonmuscle myosin heavy chain IIA mediates Epstein–Barr virus infection of nasopharyngeal epithelial cells. *Proceedings of the National Academy of Sciences* **112**, 11036–11041 (2015).
52. Chen, J. *et al.* Ephrin receptor A2 is a functional entry receptor for Epstein–Barr virus. *Nat Microbiol* **3**, 172–180 (2018).
53. Wang, H.-B. *et al.* Neuropilin 1 is an entry factor that promotes EBV infection of nasopharyngeal epithelial cells. *Nat Commun* **6**, 6240 (2015).
54. Fingeroth, J. D. *et al.* Epstein-Barr virus receptor of human B lymphocytes is the C3d receptor CR2. *Proceedings of the National Academy of Sciences* **81**, 4510–4514 (1984).
55. Ogembo, J. G. *et al.* Human Complement Receptor Type 1/CD35 Is an Epstein-Barr Virus Receptor. *Cell Rep* **3**, 371–385 (2013).
56. Li, Q. *et al.* Epstein-Barr virus uses HLA class II as a cofactor for infection of B lymphocytes. *J Virol* **71**, 4657–4662 (1997).
57. Spriggs, M. K. *et al.* The extracellular domain of the Epstein-Barr virus BZLF2 protein binds the HLA-DR beta chain and inhibits antigen presentation. *J Virol* **70**, 5557–5563 (1996).
58. Mullen, M. M., Haan, K. M., Longnecker, R. & Jardetzky, T. S. Structure of the Epstein-Barr Virus gp42 Protein Bound to the MHC Class II Receptor HLA-DR1. *Mol Cell* **9**, 375–385 (2002).
59. Borza, C. M. & Hutt-Fletcher, L. M. Alternate replication in B cells and epithelial cells switches tropism of Epstein-Barr virus. *Nat Med* **8**, 594–9 (2002).

60. Möhl, B. S., Chen, J., Sathiyamoorthy, K., Jardetzky, T. S. & Longnecker, R. Structural and Mechanistic Insights into the Tropism of Epstein-Barr Virus. *Mol Cells* **39**, 286–91 (2016).
61. Kirschner, A. N., Omerović, J., Popov, B., Longnecker, R. & Jardetzky, T. S. Soluble Epstein-Barr Virus Glycoproteins gH, gL, and gp42 Form a 1:1:1 Stable Complex That Acts Like Soluble gp42 in B-Cell Fusion but Not in Epithelial Cell Fusion. *J Virol* **80**, 9444–9454 (2006).
62. Sathiyamoorthy, K. *et al.* Structural basis for Epstein-Barr virus host cell tropism mediated by gp42 and gHgL entry glycoproteins. *Nat Commun* **7**, 13557 (2016).
63. Sixbey, J. W., Nedrud, J. G., Raab-Traub, N., Hanes, R. A. & Pagano, J. S. Epstein–Barr Virus Replication in Oropharyngeal Epithelial Cells. *New England Journal of Medicine* **310**, 1225–1230 (1984).
64. Jiang, R., Scott, R. S. & Hutt-Fletcher, L. M. Epstein-Barr virus shed in saliva is high in B-cell-tropic glycoprotein gp42. *J Virol* **80**, 7281–3 (2006).
65. Thorley-Lawson, D. A., Hawkins, J. B., Tracy, S. I. & Shapiro, M. The pathogenesis of Epstein-Barr virus persistent infection. *Curr Opin Virol* **3**, 227–32 (2013).
66. Babcock, G. J., Decker, L. L., Volk, M. & Thorley-Lawson, D. A. EBV Persistence in Memory B Cells In Vivo. *Immunity* **9**, 395–404 (1998).
67. Miyashita, E. M., Yang, B., Babcock, G. J. & Thorley-Lawson, D. A. Identification of the site of Epstein-Barr virus persistence in vivo as a resting B cell. *J Virol* **71**, 4882–91 (1997).
68. Taylor, G. S., Long, H. M., Brooks, J. M., Rickinson, A. B. & Hislop, A. D. The immunology of Epstein-Barr virus-induced disease. *Annu Rev Immunol* **33**, 787–821 (2015).
69. Laichalk, L. L. & Thorley-Lawson, D. A. Terminal differentiation into plasma cells initiates the replicative cycle of Epstein-Barr virus in vivo. *J Virol* **79**, 1296–307 (2005).
70. Kraus, R. J., Mirocha, S. J., Stephany, H. M., Puchalski, J. R. & Mertz, J. E. Identification of a novel element involved in regulation of the lytic switch BZLF1 gene promoter of Epstein-Barr virus. *J Virol* **75**, 867–77 (2001).
71. Murata, T. & Tsurumi, T. Switching of EBV cycles between latent and lytic states. *Rev Med Virol* **24**, 142–53 (2014).
72. Hislop, A. D. & Taylor, G. S. T-Cell Responses to EBV. *Curr Top Microbiol Immunol* **391**, 325–53 (2015).
73. Azzi, T. *et al.* Role for early-differentiated natural killer cells in infectious mononucleosis. *Blood* **124**, 2533–43 (2014).
74. Balfour, H. H. *et al.* Behavioral, virologic, and immunologic factors associated with acquisition and severity of primary Epstein-Barr virus infection in university students. *J Infect Dis* **207**, 80–8 (2013).
75. Gineau, L. *et al.* Partial MCM4 deficiency in patients with growth retardation, adrenal insufficiency, and natural killer cell deficiency. *J Clin Invest* **122**, 821–32 (2012).
76. Joncas, J. *et al.* Brief report: killer cell defect and persistent immunological abnormalities in two patients with chronic active Epstein-Barr virus infection. *J Med Virol* **28**, 110–7 (1989).
77. Kimura, H. & Cohen, J. I. Chronic Active Epstein-Barr Virus Disease. *Front Immunol* **8**, 1867 (2017).
78. Chijioke, O. *et al.* Human natural killer cells prevent infectious mononucleosis features by targeting lytic Epstein-Barr virus infection. *Cell Rep* **5**, 1489–98 (2013).
79. Azzi, T. *et al.* Role for early-differentiated natural killer cells in infectious mononucleosis. *Blood* **124**, 2533–43 (2014).
80. Strowig, T. *et al.* Tonsilar NK cells restrict B cell transformation by the Epstein-Barr virus via IFN-gamma. *PLoS Pathog* **4**, e27 (2008).
81. Long, H. M., Meckiff, B. J. & Taylor, G. S. The T-cell Response to Epstein-Barr Virus-New Tricks From an Old Dog. *Front Immunol* **10**, 2193 (2019).
82. Hislop, A. D. *et al.* Tonsillar homing of Epstein-Barr virus-specific CD8+ T cells and the virus-host balance. *J Clin Invest* **115**, 2546–55 (2005).
83. Liu, M., Wang, R. & Xie, Z. T cell-mediated immunity during Epstein-Barr virus infections in children. *Infect Genet Evol* **112**, 105443 (2023).
84. Bu, W. *et al.* Kinetics of Epstein-Barr Virus (EBV) Neutralizing and Virus-Specific Antibodies after Primary Infection with EBV. *Clinical and Vaccine Immunology* **23**, 363–369 (2016).

85. Bu, W. *et al.* Immunization with Components of the Viral Fusion Apparatus Elicits Antibodies That Neutralize Epstein-Barr Virus in B Cells and Epithelial Cells. *Immunity* **50**, 1305-1316.e6 (2019).
86. Snijder, J. *et al.* An Antibody Targeting the Fusion Machinery Neutralizes Dual-Tropic Infection and Defines a Site of Vulnerability on Epstein-Barr Virus. *Immunity* **48**, 799-811.e9 (2018).
87. Singh, S. *et al.* Neutralizing Antibodies Protect against Oral Transmission of Lymphocryptovirus. *Cell Rep Med* **1**, 100033 (2020).
88. Zhu, Q.-Y. *et al.* A potent and protective human neutralizing antibody targeting a novel vulnerable site of Epstein-Barr virus. *Nat Commun* **12**, 6624 (2021).
89. Chen, W.-H. *et al.* Epstein-Barr virus gH/gL has multiple sites of vulnerability for virus neutralization and fusion inhibition. *Immunity* **55**, 2135-2148.e6 (2022).
90. Oba, D. E. & Hutt-Fletcher, L. M. Induction of antibodies to the Epstein-Barr virus glycoprotein gp85 with a synthetic peptide corresponding to a sequence in the BXLF2 open reading frame. *J Virol* **62**, 1108–14 (1988).
91. Molesworth, S. J., Lake, C. M., Borza, C. M., Turk, S. M. & Hutt-Fletcher, L. M. Epstein-Barr Virus gH Is Essential for Penetration of B Cells but Also Plays a Role in Attachment of Virus to Epithelial Cells. *J Virol* **74**, 6324–6332 (2000).
92. Malhi, H. *et al.* Immunization with a self-assembling nanoparticle vaccine displaying EBV gH/gL protects humanized mice against lethal viral challenge. *Cell Rep Med* **3**, 100658 (2022).
93. Wei, C.-J. *et al.* A bivalent Epstein-Barr virus vaccine induces neutralizing antibodies that block infection and confer immunity in humanized mice. *Sci Transl Med* **14**, eabf3685 (2022).
94. Hong, J. *et al.* Glycoprotein B Antibodies Completely Neutralize EBV Infection of B Cells. *Front Immunol* **13**, 920467 (2022).
95. Thorley-Lawson, D. A. & Poodry, C. A. Identification and isolation of the main component (gp350-gp220) of Epstein-Barr virus responsible for generating neutralizing antibodies in vivo. *J Virol* **43**, 730–736 (1982).
96. Mutsvunguma, L. Z. *et al.* Identification of multiple potent neutralizing and non-neutralizing antibodies against Epstein-Barr virus gp350 protein with potential for clinical application and as reagents for mapping immunodominant epitopes. *Virology* **536**, 1–15 (2019).
97. Hong, J. *et al.* Antibody Generation and Immunogenicity Analysis of EBV gp42 N-Terminal Region. *Viruses* **13**, (2021).
98. Wu, Q. *et al.* Neutralizing antibodies against EBV gp42 show potent in vivo protection and define novel epitopes. *Emerg Microbes Infect* **12**, 2245920 (2023).
99. Hoffman, G. J., Lazarowitz, S. G. & Hayward, S. D. Monoclonal antibody against a 250,000-dalton glycoprotein of Epstein-Barr virus identifies a membrane antigen and a neutralizing antigen. *Proceedings of the National Academy of Sciences* **77**, 2979–2983 (1980).
100. Thorley-Lawson, D. A. & Geilinger, K. Monoclonal antibodies against the major glycoprotein (gp350/220) of Epstein-Barr virus neutralize infectivity. *Proceedings of the National Academy of Sciences* **77**, 5307–5311 (1980).
101. Miller, G., Heston, L. & Hoffman, G. Neutralization of lymphocyte immortalization by different strains of Epstein-Barr virus with a murine monoclonal antibody. *Infect Immun* **37**, 1028–31 (1982).
102. Sairenji, T. *et al.* Inhibition of Epstein-Barr virus (EBV) release from P3HR-1 and B95-8 cell lines by monoclonal antibodies to EBV membrane antigen gp350/220. *J Virol* **62**, 2614–21 (1988).
103. Haque, T. *et al.* A Mouse Monoclonal Antibody against Epstein-Barr Virus Envelope Glycoprotein 350 Prevents Infection Both In Vitro and In Vivo. *J Infect Dis* **194**, 584–587 (2006).
104. Lu, L. L., Suscovich, T. J., Fortune, S. M. & Alter, G. Beyond binding: antibody effector functions in infectious diseases. *Nat Rev Immunol* **18**, 46–61 (2018).
105. Karsten, C. B. *et al.* Evolution of functional antibodies following acute Epstein-Barr virus infection. *PLoS Pathog* **18**, e1010738 (2022).
106. Jondal, M. Antibody-dependent cellular cytotoxicity (ADCC) against Epstein-Barr virus-determined membrane antigens. I. Reactivity in sera from normal persons and from patients with acute infectious mononucleosis. *Clin Exp Immunol* **25**, 1–5 (1976).
107. Khyatti, M., Patel, P. C., Stefanescu, I. & Menezes, J. Epstein-Barr virus (EBV) glycoprotein gp350 expressed on transfected cells resistant to natural killer cell activity serves as a target antigen for EBV-specific antibody-dependent cellular cytotoxicity. *J Virol* **65**, 996–1001 (1991).

108. Patarroyo, M., Blazar, B., Pearson, G., Klein, E. & Klein, G. Induction of the EBV cycle in B-lymphocyte-derived lines is accompanied by increased natural killer (NK) sensitivity and the expression of EBV-related antigen(s) detected by the ADCC reaction. *Int J Cancer* **26**, 365–71 (1980).
109. López-Montañés, M. *et al.* Antibody-Dependent NK Cell Activation Differentially Targets EBV-Infected Cells in Lytic Cycle and Bystander B Lymphocytes Bound to Viral Antigen-Containing Particles. *J Immunol* **199**, 656–665 (2017).
110. Weiss, E. R. *et al.* High Epstein-Barr Virus Load and Genomic Diversity Are Associated with Generation of gp350-Specific Neutralizing Antibodies following Acute Infectious Mononucleosis. *J Virol* **91**, (2017).
111. Minab, R. *et al.* Maternal Epstein-Barr Virus-Specific Antibodies and Risk of Infection in Ugandan Infants. *J Infect Dis* **223**, 1897–1904 (2021).
112. Plotkin, S. A. Correlates of Protection Induced by Vaccination. *Clinical and Vaccine Immunology* **17**, 1055–1065 (2010).
113. Earle, K. A. *et al.* Evidence for antibody as a protective correlate for COVID-19 vaccines. *Vaccine* **39**, 4423–4428 (2021).
114. Emini, E. A. *et al.* Antigenic analysis of the Epstein-Barr virus major membrane antigen (gp350/220) expressed in yeast and mammalian cells: implications for the development of a subunit vaccine. *Virology* **166**, 387–93 (1988).
115. Morgan, A. J., Finerty, S., Lovgren, K., Scullion, F. T. & Morein, B. Prevention of Epstein-Barr (EB) virus-induced lymphoma in cottontop tamarins by vaccination with the EB virus envelope glycoprotein gp340 incorporated into immune-stimulating complexes. *J Gen Virol* **69 (Pt 8)**, 2093–6 (1988).
116. Finerty, S. *et al.* Immunization of cottontop tamarins and rabbits with a candidate vaccine against the Epstein-Barr virus based on the major viral envelope glycoprotein gp340 and alum. *Vaccine* **12**, 1180–4 (1994).
117. Jackman, W. T., Mann, K. A., Hoffmann, H. J. & Spaete, R. R. Expression of Epstein-Barr virus gp350 as a single chain glycoprotein for an EBV subunit vaccine. *Vaccine* **17**, 660–8 (1999).
118. Epstein, M. A., Morgan, A. J., Finerty, S., Randle, B. J. & Kirkwood, J. K. Protection of cottontop tamarins against Epstein–Barr virus-induced malignant lymphoma by a prototype subunit vaccine. *Nature* **318**, 287–289 (1985).
119. Johannsen, E. *et al.* Proteins of purified Epstein-Barr virus. *Proc Natl Acad Sci U S A* **101**, 16286–91 (2004).
120. Moutschen, M. *et al.* Phase I/II studies to evaluate safety and immunogenicity of a recombinant gp350 Epstein–Barr virus vaccine in healthy adults. *Vaccine* **25**, 4697–4705 (2007).
121. Sokal, E. M. *et al.* Recombinant gp350 Vaccine for Infectious Mononucleosis: A Phase 2, Randomized, Double-Blind, Placebo-Controlled Trial to Evaluate the Safety, Immunogenicity, and Efficacy of an Epstein-Barr Virus Vaccine in Healthy Young Adults. *J Infect Dis* **196**, 1749–1753 (2007).
122. Rees, L. *et al.* A phase I trial of epstein-barr virus gp350 vaccine for children with chronic kidney disease awaiting transplantation. *Transplantation* **88**, 1025–9 (2009).
123. Gu, S. Y. *et al.* First EBV vaccine trial in humans using recombinant vaccinia virus expressing the major membrane antigen. *Dev Biol Stand* **84**, 171–7 (1995).
124. Kanekiyo, M. *et al.* Rational Design of an Epstein-Barr Virus Vaccine Targeting the Receptor-Binding Site. *Cell* **162**, 1090–100 (2015).
125. Zhao, B. *et al.* Immunization With Fc-Based Recombinant Epstein-Barr Virus gp350 Elicits Potent Neutralizing Humoral Immune Response in a BALB/c Mice Model. *Front Immunol* **9**, 932 (2018).
126. Heeke, D. S. *et al.* Identification of GLA/SE as an effective adjuvant for the induction of robust humoral and cell-mediated immune responses to EBV-gp350 in mice and rabbits. *Vaccine* **34**, 2562–9 (2016).
127. Kang, Y.-F. *et al.* Immunization with a Self-Assembled Nanoparticle Vaccine Elicits Potent Neutralizing Antibody Responses against EBV Infection. *Nano Lett* **21**, 2476–2486 (2021).
128. Sashihara, J., Burbelo, P. D., Savoldo, B., Pierson, T. C. & Cohen, J. I. Human antibody titers to Epstein–Barr Virus (EBV) gp350 correlate with neutralization of infectivity better than antibody

titers to EBV gp42 using a rapid flow cytometry-based EBV neutralization assay. *Virology* **391**, 249–256 (2009).
129. Janz, A. *et al.* Infectious Epstein-Barr Virus Lacking Major Glycoprotein BLLF1 (gp350/220) Demonstrates the Existence of Additional Viral Ligands. *J Virol* **74**, 10142–10152 (2000).
130. Turk, S. M., Jiang, R., Chesnokova, L. S. & Hutt-Fletcher, L. M. Antibodies to gp350/220 Enhance the Ability of Epstein-Barr Virus To Infect Epithelial Cells. *J Virol* **80**, 9628–9633 (2006).
131. Cui, X. *et al.* Immunization with Epstein–Barr Virus Core Fusion Machinery Envelope Proteins Elicit High Titers of Neutralizing Activities and Protect Humanized Mice from Lethal Dose EBV Challenge. *Vaccines (Basel)* **9**, 285 (2021).
132. Cui, X. *et al.* Rabbits immunized with Epstein-Barr virus gH/gL or gB recombinant proteins elicit higher serum virus neutralizing activity than gp350. *Vaccine* **34**, 4050–5 (2016).
133. Sun, C. *et al.* A gB nanoparticle vaccine elicits a protective neutralizing antibody response against EBV. *Cell Host Microbe* **31**, 1882-1897.e10 (2023).
134. Backovic, M., Longnecker, R. & Jardetzky, T. S. Structure of a trimeric variant of the Epstein-Barr virus glycoprotein B. *Proc Natl Acad Sci U S A* **106**, 2880–5 (2009).
135. Brooks, J. M. *et al.* Early T Cell Recognition of B Cells following Epstein-Barr Virus Infection: Identifying Potential Targets for Prophylactic Vaccination. *PLoS Pathog* **12**, e1005549 (2016).
136. Cohen, J. I. Vaccine Development for Epstein-Barr Virus. *Adv Exp Med Biol* **1045**, 477–493 (2018).
137. Cui, X. & Snapper, C. M. Epstein Barr Virus: Development of Vaccines and Immune Cell Therapy for EBV-Associated Diseases. *Front Immunol* **12**, 734471 (2021).
138. Cai, J. *et al.* Prophylactic and Therapeutic EBV Vaccines: Major Scientific Obstacles, Historical Progress, and Future Direction. *Vaccines (Basel)* **9**, (2021).
139. Coghill, A. E. *et al.* High Levels of Antibody that Neutralize B-cell Infection of Epstein-Barr Virus and that Bind EBV gp350 Are Associated with a Lower Risk of Nasopharyngeal Carcinoma. *Clin Cancer Res* **22**, 3451–7 (2016).
140. Forrest, C., Hislop, A. D., Rickinson, A. B. & Zuo, J. Proteome-wide analysis of CD8+ T cell responses to EBV reveals differences between primary and persistent infection. *PLoS Pathog* **14**, e1007110 (2018).
141. Hui, E. P. *et al.* Phase I trial of recombinant modified vaccinia ankara encoding Epstein-Barr viral tumor antigens in nasopharyngeal carcinoma patients. *Cancer Res* **73**, 1676–88 (2013).
142. Brooks, J. M. *et al.* Early T Cell Recognition of B Cells following Epstein-Barr Virus Infection: Identifying Potential Targets for Prophylactic Vaccination. *PLoS Pathog* **12**, e1005549 (2016).
143. Si, Y. *et al.* The Safety and Immunological Effects of rAd5-EBV-LMP2 Vaccine in Nasopharyngeal Carcinoma Patients: A Phase I Clinical Trial and Two-Year Follow-Up. *Chem Pharm Bull (Tokyo)* **64**, 1118–23 (2016).
144. Jeyanathan, M. *et al.* Immunological considerations for COVID-19 vaccine strategies. *Nat Rev Immunol* **20**, 615–632 (2020).
145. López-Sagaseta, J., Malito, E., Rappuoli, R. & Bottomley, M. J. Self-assembling protein nanoparticles in the design of vaccines. *Comput Struct Biotechnol J* **14**, 58–68 (2016).
146. Nguyen, B. & Tolia, N. H. Protein-based antigen presentation platforms for nanoparticle vaccines. *NPJ Vaccines* **6**, 70 (2021).
147. Weidenbacher, P. A.-B. *et al.* A ferritin-based COVID-19 nanoparticle vaccine that elicits robust, durable, broad-spectrum neutralizing antisera in non-human primates. *Nat Commun* **14**, 2149 (2023).
148. Wargacki, A. J. *et al.* Complete and cooperative in vitro assembly of computationally designed self-assembling protein nanomaterials. *Nat Commun* **12**, 883 (2021).
149. López-Sagaseta, J., Malito, E., Rappuoli, R. & Bottomley, M. J. Self-assembling protein nanoparticles in the design of vaccines. *Comput Struct Biotechnol J* **14**, 58–68 (2016).
150. Hsia, Y. *et al.* Design of a hyperstable 60-subunit protein icosahedron. *Nature* **535**, 136–139 (2016).
151. Kato, Y. *et al.* Multifaceted Effects of Antigen Valency on B Cell Response Composition and Differentiation In Vivo. *Immunity* **53**, 548-563.e8 (2020).
152. Mohsen, M. O., Zha, L., Cabral-Miranda, G. & Bachmann, M. F. Major findings and recent advances in virus-like particle (VLP)-based vaccines. *Semin Immunol* **34**, 123–132 (2017).

153. Reguraman, N. *et al.* Assessing the Efficacy of VLP-Based Vaccine against Epstein-Barr Virus Using a Rabbit Model. *Vaccines (Basel)* **11**, (2023).
154. Ruiss, R. *et al.* A virus-like particle-based Epstein-Barr virus vaccine. *J Virol* **85**, 13105–13 (2011).
155. Perez, E. M., Foley, J., Tison, T., Silva, R. & Ogembo, J. G. Novel Epstein-Barr virus-like particles incorporating gH/gL-EBNA1 or gB-LMP2 induce high neutralizing antibody titers and EBV-specific T-cell responses in immunized mice. *Oncotarget* **8**, 19255–19273 (2017).
156. Hou, X., Zaks, T., Langer, R. & Dong, Y. Lipid nanoparticles for mRNA delivery. *Nat Rev Mater* **6**, 1078–1094 (2021).
157. Bloom, K., van den Berg, F. & Arbuthnot, P. Self-amplifying RNA vaccines for infectious diseases. *Gene Ther* **28**, 117–129 (2021).
158. Kim, S. C. *et al.* Modifications of mRNA vaccine structural elements for improving mRNA stability and translation efficiency. *Mol Cell Toxicol* **18**, 1–8 (2022).
159. Blakney, A. K., Ip, S. & Geall, A. J. An Update on Self-Amplifying mRNA Vaccine Development. *Vaccines (Basel)* **9**, (2021).
160. Johannsen, E. C. & Kaye, K. M. Epstein-Barr Virus (Infectious Mononucleosis, Epstein-Barr Virus–Associated Malignant Diseases, and Other Diseases). in *Mandell, Douglas, and Bennett's Principles and Practice of Infectious Diseases* 1754-1771.e6 (Elsevier, 2015). doi:10.1016/B978-1-4557-4801-3.00141-7.
161. Firdaus, F. Z., Skwarczynski, M. & Toth, I. Developments in Vaccine Adjuvants. *Methods Mol Biol* **2412**, 145–178 (2022).
162. CDC.gov. Adjuvants and Vaccines. *Vaccine Safety* https://www.cdc.gov/vaccinesafety/concerns/adjuvants.html (2022).
163. Pulendran, B., S Arunachalam, P. & O'Hagan, D. T. Emerging concepts in the science of vaccine adjuvants. *Nat Rev Drug Discov* **20**, 454–475 (2021).
164. Laera, D., HogenEsch, H. & O'Hagan, D. T. Aluminum Adjuvants-'Back to the Future'. *Pharmaceutics* **15**, (2023).
165. Wang, Y.-Q., Bazin-Lee, H., Evans, J. T., Casella, C. R. & Mitchell, T. C. MPL Adjuvant Contains Competitive Antagonists of Human TLR4. *Front Immunol* **11**, 577823 (2020).
166. O'Hagan, D. T., Ott, G. S., De Gregorio, E. & Seubert, A. The mechanism of action of MF59 - an innately attractive adjuvant formulation. *Vaccine* **30**, 4341–8 (2012).
167. Didierlaurent, A. M. *et al.* Adjuvant system AS01: helping to overcome the challenges of modern vaccines. *Expert Rev Vaccines* **16**, 55–63 (2017).
168. Stertman, L. *et al.* The Matrix-M™ adjuvant: A critical component of vaccines for the 21st century. *Hum Vaccin Immunother* **19**, 2189885 (2023).
169. Sigma-Aldrich. Sigma Adjuvant System®. *https://www.sigmaaldrich.com/US/en/product/sigma/s6322* (2024).
170. Serradell, M. C. *et al.* Efficient oral vaccination by bioengineering virus-like particles with protozoan surface proteins. *Nat Commun* **10**, 361 (2019).
171. Ní Eidhin, D. B., O'Brien, J. B., McCabe, M. S., Athié-Morales, V. & Kelleher, D. P. Active immunization of hamsters against Clostridium difficile infection using surface-layer protein. *FEMS Immunol Med Microbiol* **52**, 207–18 (2008).
172. Kamp, H. D. *et al.* Design of a broadly reactive Lyme disease vaccine. *NPJ Vaccines* **5**, 33 (2020).
173. Silva, M. *et al.* A particulate saponin/TLR agonist vaccine adjuvant alters lymph flow and modulates adaptive immunity. *Sci Immunol* **6**, eabf1152 (2021).
174. Cottrell, C. A. *et al.* Focusing antibody responses to the fusion peptide in rhesus macaques. *bioRxiv* (2023) doi:10.1101/2023.06.26.545779.
175. Gristick, H. B. *et al.* CD4 binding site immunogens elicit heterologous anti-HIV-1 neutralizing antibodies in transgenic and wild-type animals. *Sci Immunol* **8**, eade6364 (2023).
176. He, W.-T. *et al.* Broadly neutralizing antibodies to SARS-related viruses can be readily induced in rhesus macaques. *Sci Transl Med* **14**, eabl9605 (2022).
177. Phung, I. *et al.* A combined adjuvant approach primes robust germinal center responses and humoral immunity in non-human primates. *Nat Commun* **14**, 7107 (2023).
178. Zhong, L. *et al.* Urgency and necessity of Epstein-Barr virus prophylactic vaccines. *NPJ Vaccines* **7**, 159 (2022).

179. Lavelle, E. C. & Ward, R. W. Mucosal vaccines — fortifying the frontiers. *Nat Rev Immunol* **22**, 236–250 (2022).
180. Künzli, M. *et al.* Route of self-amplifying mRNA vaccination modulates the establishment of pulmonary resident memory CD8 and CD4 T cells. *Sci Immunol* **7**, eadd3075 (2022).
181. Ackerman, M. E. *et al.* Route of immunization defines multiple mechanisms of vaccine-mediated protection against SIV. *Nat Med* **24**, 1590–1598 (2018).
182. Czerkinsky, C. & Holmgren, J. Mucosal delivery routes for optimal immunization: targeting immunity to the right tissues. *Curr Top Microbiol Immunol* **354**, 1–18 (2012).
183. Voysey, M. *et al.* Single-dose administration and the influence of the timing of the booster dose on immunogenicity and efficacy of ChAdOx1 nCoV-19 (AZD1222) vaccine: a pooled analysis of four randomised trials. *Lancet* **397**, 881–891 (2021).
184. Voysey, M. *et al.* Safety and efficacy of the ChAdOx1 nCoV-19 vaccine (AZD1222) against SARS-CoV-2: an interim analysis of four randomised controlled trials in Brazil, South Africa, and the UK. *Lancet* **397**, 99–111 (2021).
185. Regules, J. A. *et al.* Fractional Third and Fourth Dose of RTS,S/AS01 Malaria Candidate Vaccine: A Phase 2a Controlled Human Malaria Parasite Infection and Immunogenicity Study. *Journal of Infectious Diseases* **214**, 762–771 (2016).
186. Tam, H. H. *et al.* Sustained antigen availability during germinal center initiation enhances antibody responses to vaccination. *Proc Natl Acad Sci U S A* **113**, E6639–E6648 (2016).
187. Lee, J. H. *et al.* Long-primed germinal centres with enduring affinity maturation and clonal migration. *Nature* **609**, 998–1004 (2022).
188. Fujiwara, S. & Nakamura, H. Animal Models for Gammaherpesvirus Infections: Recent Development in the Analysis of Virus-Induced Pathogenesis. *Pathogens* **9**, 116 (2020).
189. Frank, A., Andiman, W. A. & Miller, G. Epstein-Barr virus and nonhuman primates: natural and experimental infection. *Adv Cancer Res* **23**, 171–201 (1976).
190. Moghaddam, A. *et al.* An Animal Model for Acute and Persistent Epstein-Barr Virus Infection. *Science (1979)* **276**, 2030–2033 (1997).
191. Wang, F. Nonhuman primate models for Epstein-Barr virus infection. *Curr Opin Virol* **3**, 233–237 (2013).
192. Carville, A. & Mansfield, K. G. Comparative pathobiology of macaque lymphocryptoviruses. *Comp Med* **58**, 57–67 (2008).
193. Rivailler, P., Jiang, H., Cho, Y., Quink, C. & Wang, F. Complete nucleotide sequence of the rhesus lymphocryptovirus: genetic validation for an Epstein-Barr virus animal model. *J Virol* **76**, 421–6 (2002).
194. Wang, F., Rivailler, P., Rao, P. & Cho, Y. Simian homologues of Epstein-Barr virus. *Philos Trans R Soc Lond B Biol Sci* **356**, 489–97 (2001).
195. Omerović, J. & Longnecker, R. Functional homology of gHs and gLs from EBV-related γ-herpesviruses for EBV-induced membrane fusion. *Virology* **365**, 157–165 (2007).
196. Wu, L. & Hutt-Fletcher, L. M. Compatibility of the gH homologues of Epstein–Barr virus and related lymphocryptoviruses. *Journal of General Virology* **88**, 2129–2136 (2007).
197. Cho, Y. G., Gordadze, A. V, Ling, P. D. & Wang, F. Evolution of two types of rhesus lymphocryptovirus similar to type 1 and type 2 Epstein-Barr virus. *J Virol* **73**, 9206–12 (1999).
198. Hannibal, D. L., Bliss-Moreau, E., Vandeleest, J., McCowan, B. & Capitanio, J. Laboratory rhesus macaque social housing and social changes: Implications for research. *Am J Primatol* **79**, 1–14 (2017).
199. Yajima, M. *et al.* A new humanized mouse model of Epstein-Barr virus infection that reproduces persistent infection, lymphoproliferative disorder, and cell-mediated and humoral immune responses. *Journal of Infectious Diseases* **198**, 673–682 (2008).
200. Fujiwara, S., Imadome, K.-I. & Takei, M. Modeling EBV infection and pathogenesis in new-generation humanized mice. *Exp Mol Med* **47**, e135–e135 (2015).
201. Münz, C. EBV Infection of Mice with Reconstituted Human Immune System Components. *Curr Top Microbiol Immunol* **391**, 407–23 (2015).
202. Münz, C. Humanized mouse models for Epstein Barr virus infection. *Curr Opin Virol* **25**, 113–118 (2017).

203. Fujiwara, S. Reproduction of epstein-barr virus infection and pathogenesis in humanized mice. *Immune Netw* **14**, 1–6 (2014).
204. Yajima, M. *et al.* T cell-mediated control of Epstein-Barr virus infection in humanized mice. *J Infect Dis* **200**, 1611–5 (2009).
205. Yu, H. *et al.* A novel humanized mouse model with significant improvement of class-switched, antigen-specific antibody production. *Blood* **129**, 959–969 (2017).
206. Fujiwara, S., Matsuda, G. & Imadome, K.-I. Humanized mouse models of epstein-barr virus infection and associated diseases. *Pathogens* **2**, 153–76 (2013).
207. van Zyl, D. G. *et al.* Immunogenic particles with a broad antigenic spectrum stimulate cytolytic T cells and offer increased protection against EBV infection ex vivo and in mice. *PLoS Pathog* **14**, e1007464 (2018).
208. Johannessen, I. & Crawford, D. H. In vivo models for Epstein-Barr virus (EBV)-associated B cell lymphoproliferative disease (BLPD). *Rev Med Virol* **9**, 263–77 (1999).
209. Shope, T., Dechairo, D. & Miller, G. Malignant lymphoma in cottontop marmosets after inoculation with Epstein-Barr virus. *Proc Natl Acad Sci U S A* **70**, 2487–91 (1973).
210. Young, L. S. *et al.* Epstein-Barr virus gene expression in malignant lymphomas induced by experimental virus infection of cottontop tamarins. *J Virol* **63**, 1967–74 (1989).
211. IUCN Red List. Cotton-headed Tamarin. *https://www.iucnredlist.org/species/19823/192551067* https://www.iucnredlist.org/species/19823/192551067.
212. Khan, G., Ahmed, W., Philip, P. S., Ali, M. H. & Adem, A. Healthy rabbits are susceptible to Epstein-Barr virus infection and infected cells proliferate in immunosuppressed animals. *Virol J* **12**, 28 (2015).

Chapter 2. Vaccination with nanoparticles displaying gH/gL from Epstein-Barr virus elicits limited cross-protection against rhesus lymphocryptovirus

This work is under review at Cell Reports Medicine as of Feb 01, 2024

Authors:
Kristina R. Edwards[1,2], Karina Schmidt[1], Leah J. Homad[1], Gargi M. Kher[1], Guoyue Xu[1,2], Kristen A. Rodrigues[5,6], Elana Ben-Akiva[5,6,8], Joe Abbott[1], Martin Prlic[1,2,3], Evan W. Newell[1,2], Stephen C. De Rosa[1,4], Darrell J. Irvine[5,6,7,9], Marie Pancera[1] and Andrew T. McGuire[1,2,4*]

[1]Vaccine and Infectious Disease Division, Fred Hutchinson Cancer Center, Seattle WA, USA.
[2]Department of Global Health, University of Washington, Seattle, WA, USA.
[3]Department of Immunology, University of Washington, Seattle, WA, USA.
[4]Department of Laboratory Medicine and Pathology, University of Washington, Seattle WA, USA.
[5]Koch Institute for Integrative Cancer Research, Massachusetts Institute of Technology, Cambridge, MA, USA.
[6]Ragon Institute of Massachusetts General Hospital, Massachusetts Institute of Technology, and Harvard University, Cambridge, MA, USA.
[7]Harvard-MIT Health Sciences and Technology Program, Institute for Medical Engineering and Science, Massachusetts Institute of Technology, Cambridge, MA 02139 USA.
[8]Departments of Biological Engineering and Materials Science and Engineering, Massachusetts Institute of Technology, Cambridge, MA, USA.
[9]Howard Hughes Medical Institute, Chevy Chase, MD, USA.

*Corresponding author. Email: amcguire@fredhutch.org.

2.1 Abstract

Epstein Barr Virus (EBV) is an orally transmitted, γ-herpesvirus associated with various cancers and development of multiple sclerosis. A vaccine that prevents infection and/or EBV-associated malignancies and morbidity is an unmet need. EBV infects epithelial cells and B cells, therefore an effective vaccine would likely have to block infection of both. The viral gH/gL glycoprotein complex is essential for entry, making it an attractive vaccine target. Here we evaluated the immunogenicity of a multimeric gH/gL nanoparticle vaccine administered with two different adjuvants, Sigma Adjuvant System (SAS) and Saponin/MPLA nanoparticles (SMNP), in rhesus macaques. Formulation with SMNP elicited higher titers of antibodies capable of neutralizing infection of epithelial and B cells and a higher frequency of vaccine-specific $CD4^+$ T cells. Study animals were subjected to oral challenge with the EBV orthologue, rhesus lymphocryptovirus (rhLCV). All macaques in the control and SAS groups became infected, while one of four animals in the SMNP group remained aviremic and failed to seroconvert to non-vaccine antigens. A subsequent investigation of the immune plasma revealed a 10-100 fold lower reactivity against rhLCV gH/gL compared to EBV gH/gL. Similarly, anti-EBV neutralizing monoclonal antibodies showed reduced binding to rhLCV gH/gL, demonstrating that critical neutralizing epitopes on EBV gH/gL are not well conserved on rhLCV gH/gL. The protected animal displayed a broader pattern of epitope recognition as visualized by electron microscopy polyclonal epitope mapping which may be linked to protection. Prevention of rhLCV infection in one macaque despite substantial antigenic disparity between the vaccine and challenge strain supports clinical development of gH/gL nanoparticle vaccines against EBV.

2.2 Introduction

Epstein-Barr Virus (EBV) is a member of the *Lymphocryptovirus* genus that infects over 90% of adults worldwide[1]. Acute infection is typically asymptomatic but can cause infectious mononucleosis, particularly if acquired in adolescence[2,3]. EBV is associated with ~209,000 deaths and ~358,000 new cases of cancer annually[4–9] and can lead to lymphoproliferative disorder in the context of immune suppression[10]. In addition to its oncogenic potential, EBV infection is linked to autoimmune conditions including rheumatoid arthritis and multiple sclerosis[11–15]. EBV reactivation is thought to contribute to the severity of COVID-19 and post-acute sequelae of COVID-19[16–20]. Thus, a vaccine that protects against EBV infection and/or the development of associated morbidities would have a substantial global health benefit.

EBV most commonly transmits from saliva to the nasopharynx where it infects B cells and epithelial cells[21] therefore, a protective vaccine would likely have to prevent infection of both. Neutralizing antibodies are the correlate of protection for most successful vaccines[22,23]. Hence it is likely that they will be an important immune response elicited by an EBV vaccine. Host cell entry is a complex process mediated by several viral glycoproteins that define tropism and facilitate membrane fusion. Among these the glycoproteins gH, gL, and gB compose the core fusion machinery and are essential for entry irrespective of cell type [24,25]. In principle, antibodies that inhibit the activity of the core fusion machinery could prevent EBV infection of both cell types.

Several monoclonal antibodies (mAbs) have been isolated that bind gH/gL and potently neutralize EBV infection of both B cells and epithelial cells *in vitro*, implicating gH/gL as a promising vaccine target[26–29]. Passive delivery of gH/gL mAbs, including AMMO1, 769B10 and 1D8, provide robust protection in humanized mouse models of EBV infection[27,29,30].

Although humanized mice provide a tractable small animal model to evaluate the in vivo efficacy of antibodies in preventing EBV infection, they do not support epithelial cell infection and the virus must be administered parenterally. Rhesus lymphocryptovirus (rhLCV) is an ortholog of EBV that naturally infects rhesus macaques[31–35]. rhLCV infection of rhesus macaques recapitulates several aspects of EBV infection in humans including a natural route of oral transmission and a similar course of infection in the host[31,32]. The rhLCV/macaque model has been used to evaluate experimental vaccines based on the rhLCV gp350 protein[36]. The anti-gH/gL mAb AMMO1, isolated from an EBV-infected donor cross-neutralizes rhLCV and passive transfer protected rhesus macaques against oral challenge with rhesus lymphocryptovirus (rhLCV), demonstrating that antibodies against EBV gH/gL can mediate cross-protection in this infection model[30]. However, it is unknown whether vaccines derived from the EBV gH/gL glycoprotein complex can elicit neutralizing antibodies that can cross-protect against rhLCV. A vaccine that could do so would presumably be efficacious at preventing EBV infection in humans.

The recombinant gH/gL ectodomain is poorly immunogenic in small animal models[26,37,38], however fusing gH/gL to protein scaffold domains that self-assemble into multimeric nanoparticles substantially boosts immunogenicity[26,37–39]. In line with this, we previously demonstrated that wildtype mice vaccinated with a computationally designed nanoparticle scaffold displaying 60 copies of gH/gL elicited high titers of neutralizing antibodies[38]. Here we evaluate the immunogenicity of the gH/gL 60-mer in rhesus macaques formulated with two different adjuvants, Sigma Adjuvant System (SAS), a squalene emulsion formulated with monophosphoryl lipid A (MPLA); and SMNP, a saponin-based immune-stimulating complex co-formulated with MPLA[40].

Formulation of the gH/gL 60-mer with SMNP led to higher antibody binding and neutralizing titers as compared to SAS. Animals in both groups were subsequently challenged

with rhLCV. All control animals and animals from the SAS group became infected following challenge. In contrast, one of four animals in the SMNP group remained aviremic and did not seroconvert, consistent with protection. A subsequent serological analysis revealed substantial antigenic disparity between EBV-derived gH/gL in the vaccine and rhLCV gH/gL from the challenge virus. The partial protection observed encourages further development of gH/gL-based nanoparticle immunogens, but also highlights the limitation of using rhesus lymphocryptovirus challenge in the evaluation of EBV vaccines.

2.3 Results

2.3.1 Immunogenicity of gH/gL 60-mer formulated with two different adjuvants in rhesus macaques

We previously developed a computationally designed self-assembling nanoparticle displaying 60 copies of EBV gH/gL[38]. Here we assessed the immunogenicity of the nanoparticle vaccine in rhesus macaques. Ten rhesus macaques were acquired within 48 hours of birth and housed separately from other colony animals to avoid natural transmission of rhLCV[32]. From 2 to 6 months of age, we monitored the waning of maternally acquired antibodies against the rhLCV small viral capsid antigen (sVCA,)[41] and the EBV gB ectodomain, which is 86% identical to rhLCV gB (Fig. S1A and B). PBMC and saliva samples collected longitudinally during this period were negative for the presence of rhLCV DNA using a sensitive ddPCR assay[28,30,36] (Figs. S1C and S1D), confirming the animals were rhLCV-negative.

Once maternal antibodies had waned, animals were immunized with gH/gL 60-mer formulated with two different adjuvants. Eight rhesus macaques received intramuscular vaccinations of 50 μg gH/gL 60-mer, four adjuvanted with SAS and four with SMNP (hereafter referred to as the SAS and SMNP groups, respectively), at weeks 0, 4, and 12. The selection of

SAS adjuvant and the dosing schedule of 0, 4, and 12 weeks were based on previous EBV vaccine immunogenicity studies in macaques[26,42]. SMNP was evaluated as an alternative adjuvant here because it leads to enhanced B cell germinal centers, increased T_{FH} help, and better neutralizing antibody responses in mice[43]. Two animals received an injection with SMNP alone (control group) (Fig. 1A). Plasma was collected at the time of, and two weeks after, each immunization (Fig. 1A) and endpoint binding titers to EBV gH/gL were measured by ELISA (Fig. 1B). At the time of the second immunization, the reciprocal endpoint binding titers in the SMNP group were approximately 1:10,000, which were 100-fold higher than those measured in animals in the SAS group (Fig. 1B). Two weeks after the second immunization, the binding titers in the SMNP group were boosted 100-fold to 1:1,000,000. Titers in the SAS group were boosted by a similar magnitude but remained 100-fold lower than the SMNP group. At week 12, animals were given a third immunization which resulted in a modest boost in binding titers by week 14.

Fluorescent gH/gL tetramers were used to identify vaccine-specific B cells by flow cytometry (Fig. S2). In line with the higher titers of binding antibodies, the frequency of gH/gL-specific B cells was approximately 5-fold higher in the SMNP compared to the SAS group (Fig. 1C).

In agreement with the absence of EBV-specific antibodies (Fig. S1), none of the animals had neutralizing titers against epithelial, or B cell infection at the time of the first immunization (Fig. 1D and E). In the epithelial cell infection assay, a single immunization with gH/gL + SAS elicited low levels of neutralizing titers in two animals at the time of the second immunization that were boosted to a reciprocal plasma dilution capable of neutralizing 50% infectivity (ID_{50}) of ~1:1,000 2 weeks later in all animals in this group (Fig. 1D). In contrast, immunization with gH/gL + SMNP achieved ID_{50} titers of ~1:1,000 by 2 weeks after a single immunization in all animals, while a second immunization boosted them nearly 100-fold (Fig. 1D). The epithelial cell neutralizing titers in two of the animals from the SAS group (A20129 and A20130) waned to

undetectable levels between weeks 6 to 12, but a third immunization boosted all epithelial cell neutralizing titers to comparable levels in the SAS group, ~ 1:1,000 ID_{50} of roughly (Fig. 1D). The neutralizing titers in the SMNP group waned by about a half-log between weeks 6 and 12, but were boosted back to peak levels after a third immunization (Fig. 1D).

Consistent with previous immunogenicity studies of gH/gL nanoparticles in non-human primates and mice, the neutralizing titers in the B cell infection assay were lower than those in the epithelial cell infection assay (Fig. 1E)[26,38]. Two immunizations were required to elicit low (ID_{50} <1:100) titers of antibodies capable of neutralizing EBV infection of B cells in the SAS group. These waned to undetectable levels by week 12 but were boosted back by a third immunization in 3 of 4 animals (Fig. 1E). The animal who did not respond to the third immunization (A20129) had several unresolved health issues throughout the study period. In contrast, two immunizations with gH/gL + SMNP elicited significantly higher B cell neutralizing titers that reached an ID_{50} of ~1:2,000 at week 6. These waned ~10-fold over the following 6 weeks but were boosted to peak levels following a third immunization (Fig. 1E).

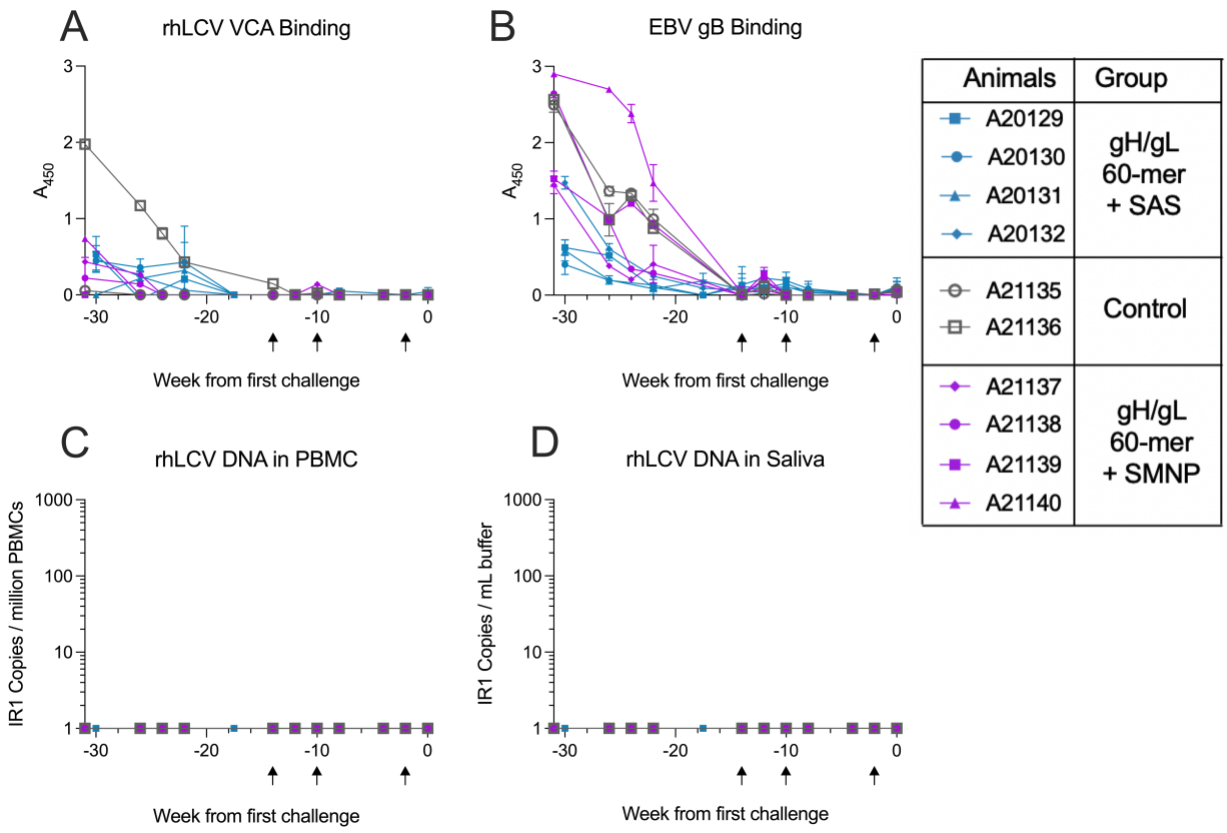

Figure S1: Monitoring for rhLCV infection prior to challenge.

(**A)** A 1:20 dilution of plasma from study animals was screened for reactivity against rhLCV VCA by ELISA at the indicated timepoints prior to challenge at week 0. (**B**) A 1:50 dilution of plasma from study animals was screened for reactivity against EBV gB prior to immunization and challenge at week 0. (**C** and **D**) Viral titers of rhLCV in the blood (C) and saliva (D) were measured by ddPCR for the rhLCV gene IR1 at the indicated timepoints prior to challenge. Arrows indicate the times of immunization in (A-D).

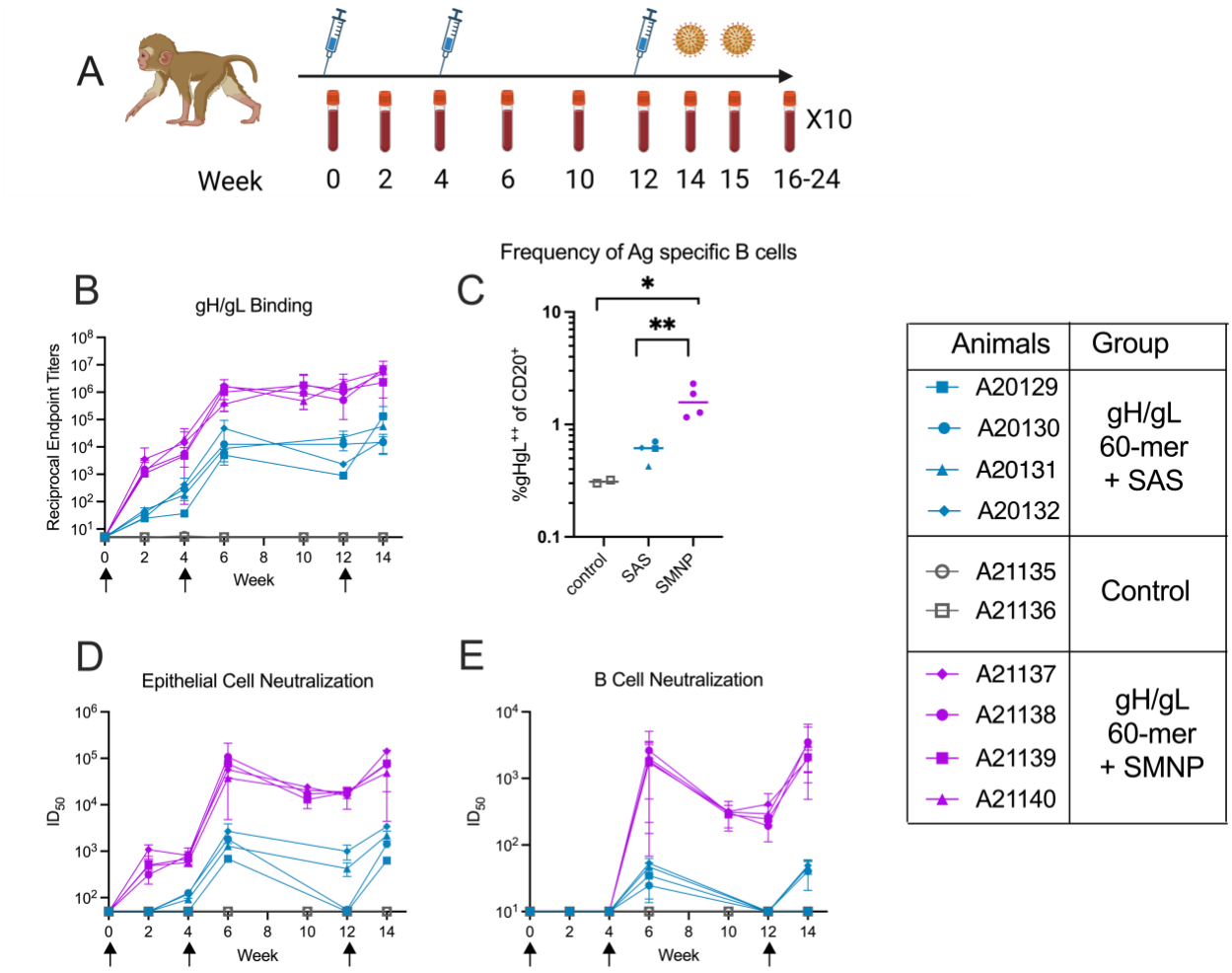

Figure 1: Immunogenicity of EBV gH/gL nanoparticle in rhesus macaques.

(**A**) Rhesus macaques were immunized with 50 µg of gH/gL 60-mer formulated in 50% (v/v) SAS (n=4, blue squares), 50ug of gH/gL 60-mer plus 400 µg SMNP (n=4, purple), or SMNP alone (n=2, black) at weeks 0, 4, and 12 indicated by syringes. Blood tubes represent collection of blood and oral swabs at the indicated timepoints. (**B**) The reciprocal gH/gL binding endpoint titers in plasma were measured by ELISA at the indicated timepoints. Each data point represents an individual animal as indicated in the legend. Arrows correspond to the immunizations. (**C**) The frequency of EBV gH/gL specific B cells in each group at week 14. Each dot represents one (control) or the average of two (SMNP and SAS) independent experiments. (**D** and **E**) The ability of plasma to inhibit EBV infection of (D) SVKCR2 epithelial cells or (E) Raji

B cells. Each dot represents the reciprocal half-maximal inhibitory plasma dilution (ID_{50}). Statistical differences between the SMNP and SAS groups were determined at each timepoint using a Mann-Whitney U-test in B-E. * indicates a p value below 0.05.

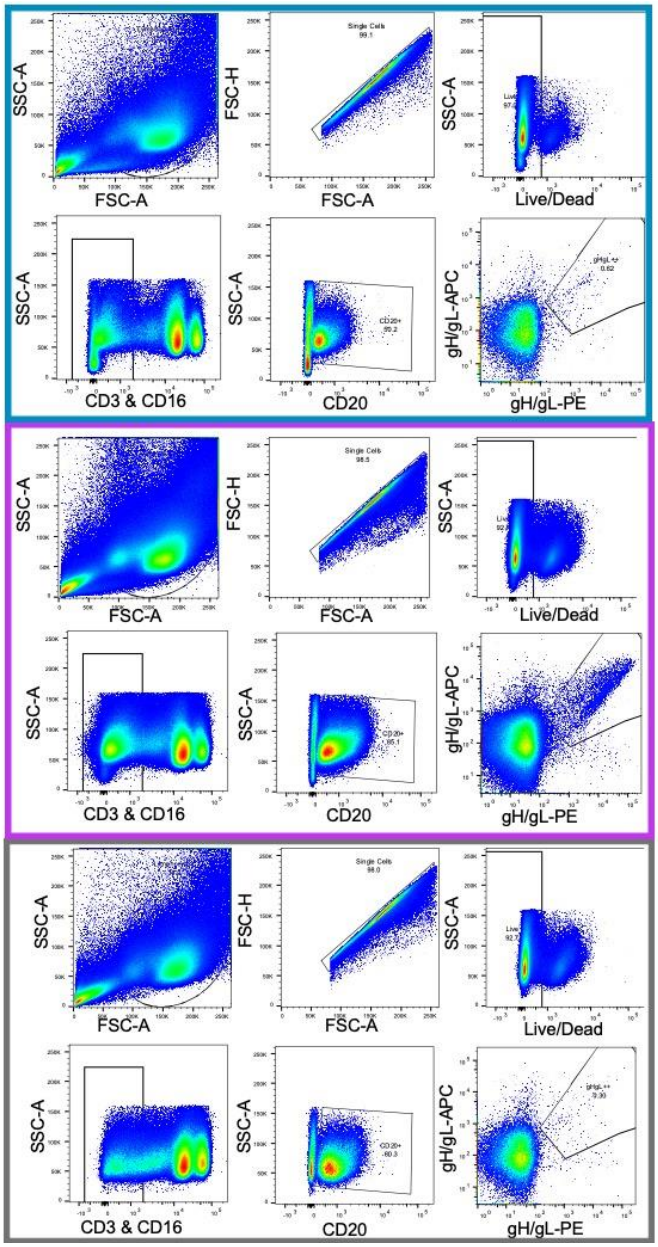

Figure S2: Gating strategy to identify EBV gH/gL specific B cells.

Single, live, $CD3^-$, $CD4^-$, $CD8^-$, $CD14^-$, $CD20^+$, lymphocytes collected at week 14 were analyzed for frequency of gH/gL-APC^+ gH/gL-PE^+ double positive events. The plots within the blue and purple boxes are from representative animals immunized with the gH/gL 60-mer formulated with SAS or SMNP, respectively. The plots within the grey box correspond to a control animal.

2.3.2 Immunization with gH/gL 60-mer formulated with SMNP protected 1 of 4 animals from oral rhLCV challenge

After demonstrating that the gH/gL 60-mer was immunogenic in rhesus macaques and formulation with SMNP elicits higher titers, we next assessed whether either vaccine formulation conferred cross-protection against rhLCV. Two and three weeks after the third immunization (weeks 14 and 15, Fig. 1A), all animals were orally challenged with 50 transforming units of rhLCV (Fig. S3A and B). Following challenge, oral swabs and peripheral blood was collected weekly for up to 12 weeks to monitor for rhLCV infection. We used a ddPCR assay that detects the IR1 gene[30], which is present at multiple copies on the rhLCV genome and is more sensitive than assays based on single copy genes[36].

All animals in the SAS group, as well as the control animals, shed virus in the saliva at repeated timepoints after challenge (Fig. 2A). Viral DNA was not detected in the saliva of animal A21139 from the SMNP group at any timepoint tested (Fig. 2A). Following challenge, rhLCV DNA was detected in PBMC at multiple timepoints in all study animals except A21139 from the SMNP group, and A21335 from the control group (Fig. 2B).

To confirm the infection status of the animals with an orthogonal assay, we monitored plasma for seroconversion to the non-vaccine antigens rhLCV-VCA (Fig. 2C) and EBV gB (Fig. 2D) by ELISA. All animals were initially seronegative for smallVCA, and all but A21139 from the SMNP group, and A21335 from the control group, seroconverted between weeks 3 and 12 after initial challenge (Fig. 2C). Initially, all animals were seronegative for gB but seroconverted by 12 weeks after the first challenge, with the exception of A21139 (Fig. 2D). To verify that A21139 was not inherently resistant to challenge we confirmed that B cells from this animal were readily transformed by the rhLCV challenge strain in culture (not shown).

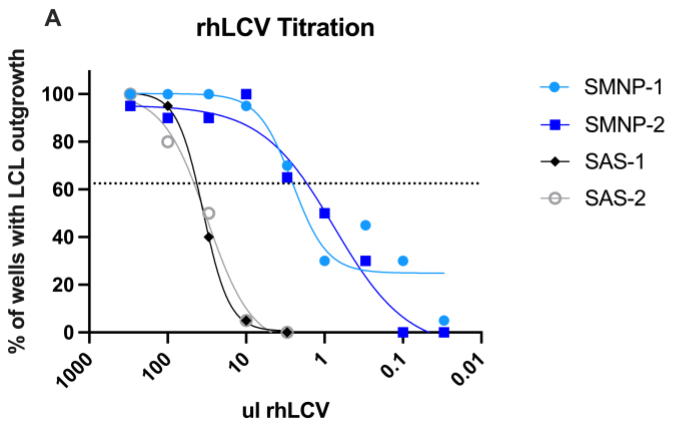

B

	1 Transforming Unit (TU)	Average of Two replicates	Challenge Dose (50 TU)
SAS- PBMC 1	42.45 µl		
SAS- PBMC 2	46.09 µl	43.38 µl	2169 µl
SMNP- PBMC 1	2.55 µl		
SMNP- PBMC 2	1.68 µl	2.11 µl	106 µl

Figure S3: rhLCV titration curves.

(**A**) Two different batches of rhLCV were titrated using PBMC from two different macaques for use in challenge studies. SMNP and SAS indicates batch of virus used for oral challenge in each vaccine group. -1 and -2 indicate replicate PBMC collected from two different macaques used for titration of each stock. Dashed line at 62.5% indicates 1 transforming unit. (**B**) Calculation of challenge dose used in each group Volume for 1 transforming unit interpolated from the curves in (**A**).

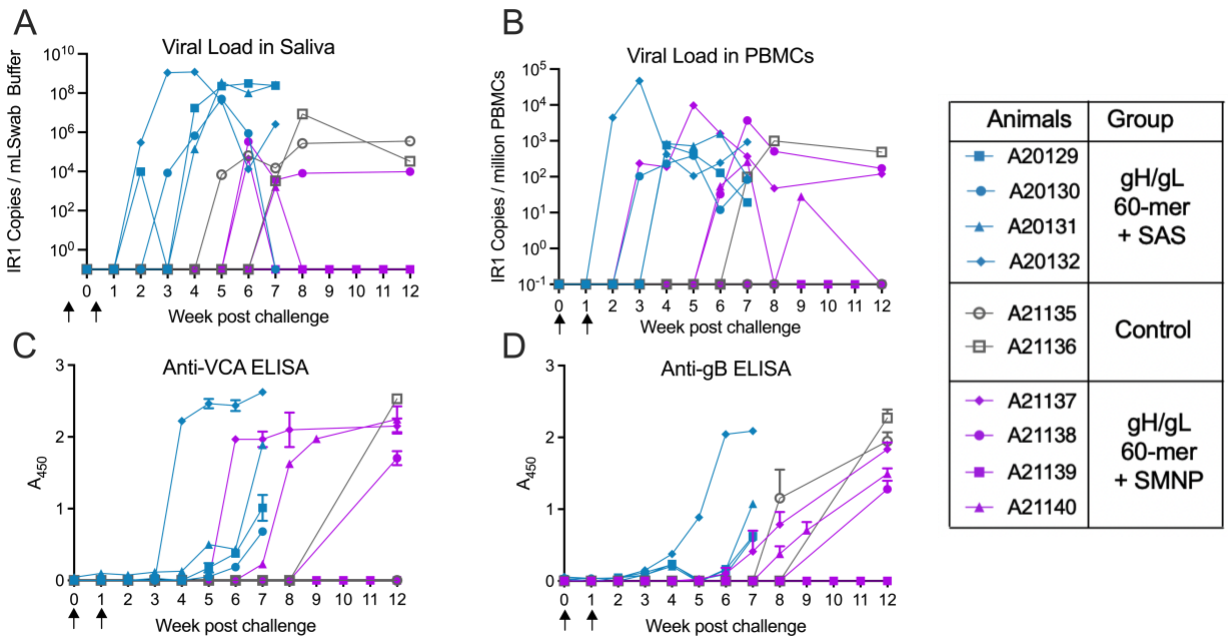

Figure 2: Outcome of oral rhLCV challenge in immunized animals.

At 2 and 3 weeks following the final immunization with gH/gL 60-mer or adjuvant alone (see Figure 1A for timeline), all study animals were challenged orally with 50 transforming units of rhLCV, indicated by arrows. (**A** and **B**) Viral DNA was quantitated in oral swabs (A) and PMBC (B) using a digital droplet PCR assay with primers and probes specific for the internal repeat (IR1) of rhLCV at the indicated time points. (**C** and **D**). Plasma from study animals was evaluated for binding to the rhLCV small viral capsid antigen (VCA) (C) and EBV-gB (D) by ELISA at the indicated timepoints. Each point represents the average A_{450} signal of a 1:20 (C) or 1:50 (D) plasma dilution measured in triplicate.

2.3.3 Cross reactivity of vaccine-elicited EBV gH/gL plasma antibodies with rhLCV gH/gL

Given that neutralizing antibodies have been demonstrated to protect against oral challenge with rhLCV [30,44], it stands to reason that the partial protection observed in the SMNP group is attributed to the higher levels of neutralizing antibodies elicited by this adjuvant. However, despite all animals having comparable binding and neutralizing titers in the SMNP group, only one animal was protected. Although rhLCV and EBV gH/gL share 90% amino acid similarity, we hypothesized that antigenic dissimilarity between the two proteins may affect the ability of antibodies elicited by vaccination with EBV gH/gL to cross-protect against challenge with rhLCV gH/gL[45].

To investigate this further, we compared plasma antibody binding to rhLCV and EBV gH/gL by ELISA. In all immunized animals the average reciprocal endpoint binding titer to rhLCV gH/gL was 10-100-fold lower than the titer for EBV gH/gL at all time points tested (Fig. 3A). There was no significant difference in rhLCV gH/gL binding between the animal protected after oral rhLCV challenge (A21139) and the other vaccinated animals in the SMNP group (Fig. S4).

To assess the ability of antibodies to inhibit EBV and rhLCV gH/gL activity, we measured the ability of plasma from SMNP group animals collected at the time of challenge to inhibit fusion using a virus-free syncytia formation assay[28,30,46,47]. Plasma from SMNP group animals inhibited fusion driven by the EBV machinery in a dose-dependent manner (Fig. 3B). The same plasma samples could also inhibit fusion driven by the rhLCV gH/gL and gB (Fig. 3C), albeit less potently (Fig. 3D). Plasma from control animals had no activity in either assay (Fig. 3B and C).

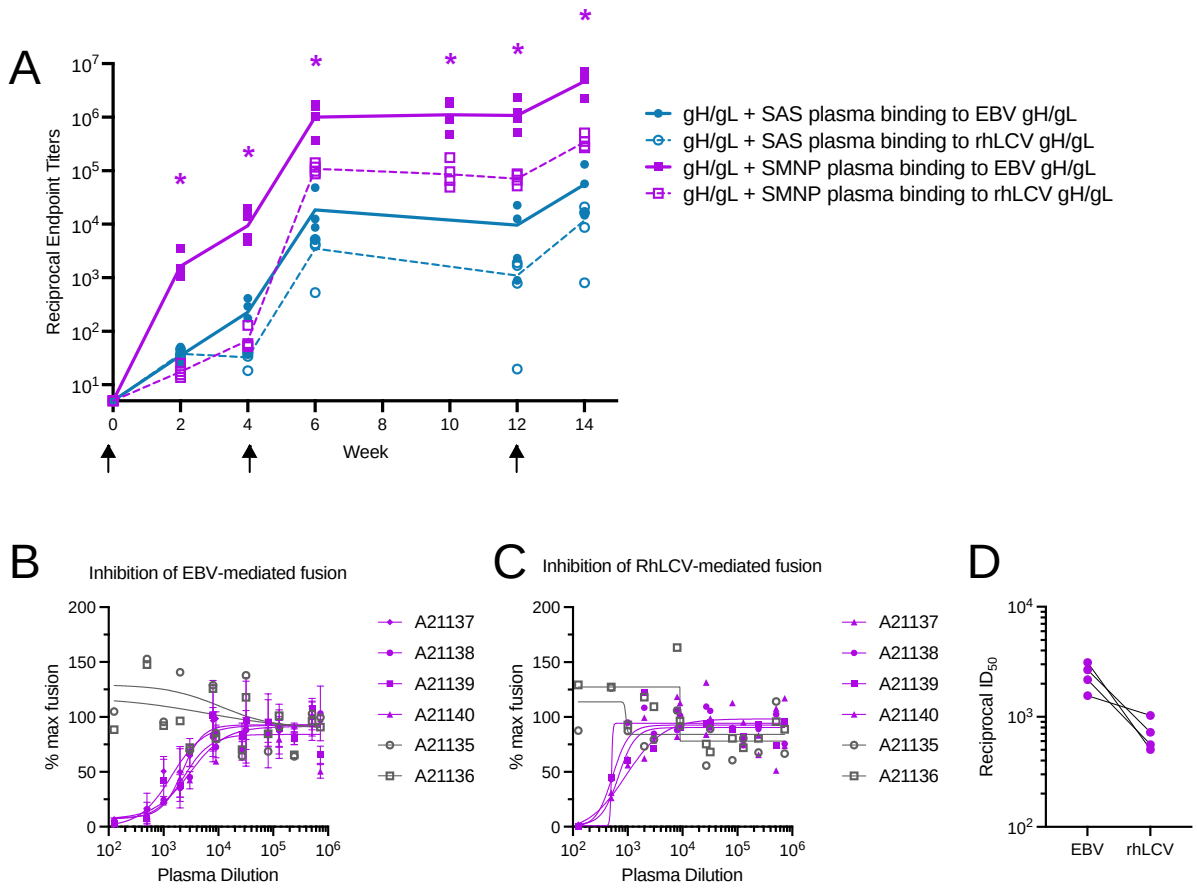

Figure 3: Serum cross-reactivity between EBV gH/gL and rhLCV gH/gL.

(**A**) Reciprocal endpoint binding titers against EBV gH/gL (solid lines) and rhLCV gH/gL (dashed lines) were measured by ELISA in plasma from animals immunized with gH/gL 60-mer formulated with SAS (blue) or SMNP (purple). Each point represents the endpoint binding titer of an individual animal, and the lines represent the geometric mean. Asterisk indicates significant difference of $p<0.05$ between EBV and rhLCV gH/gL endpoint titers determined using a Mann-Whitney U-test. (**B** and **C**) The ability of week 14 plasma from animals immunized with gH/gL 60-mer + SMNP to inhibit syncytia formation mediated by EBV (B) or rhLCV (C) gH/gL and gB. (**D**) The reciprocal dilution of plasma required to reduce EBV or rhLCV-mediated fusion by 50% (ID_{50}) was interpolated from the inhibition curves in (B) and (C).

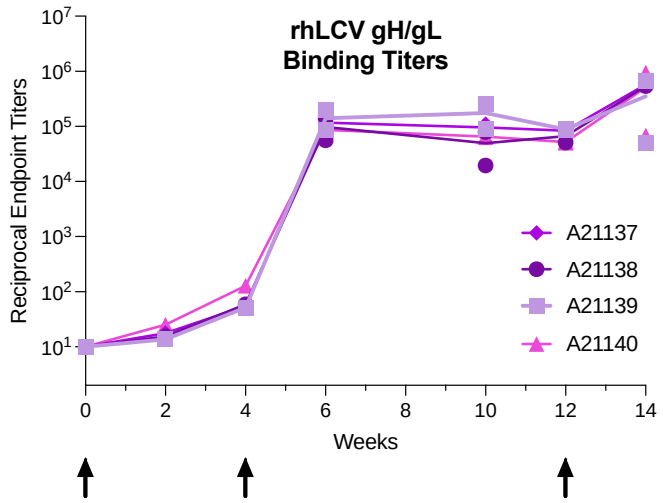

Figure S4: rhLCV gH/gL binding titers for gH/gL + SMNP immunized animals. Reciprocal endpoint titers from two replicates are shown for each animal at each timepoint with the mean values connected by a solid line.

2.3.4 Electron microscopy polyclonal epitope mapping of vaccinated animals

To gain a visual understanding of the differences between the vaccine-elicited antibodies to EBV and rhLCV, we employed electron microscopy polyclonal epitope mapping (EMPEM)[48]. Polyclonal IgG was purified from plasma of animals A21137, A21138 and A21139 from the SMNP group collected at the time of challenge, digested into antigen binding fragments (Fabs) and visualized in complex with EBV gH/gL or rhLCV gH/gL, by negative stain electron microscopy (nsEM). Single particles were broadly grouped into six distinct 2D nsEM classes based on the observed modes of Fab binding: 1) unbound gH/gL, 2) one Fab on the end in the plane of gH/gL, 3) one Fab on the end perpendicular to gH/gL, 4) one Fab in the middle of gH/gL, 5) two Fabs in middle of gH/gL and 6) one Fab on the end in the plane of gH/gL and one Fab in middle (Fig. 4 and S5).

In the sample from A21137, classes 3-5 were observed complex with EBV gH/gL. Classes 3 and 4 were also observed in complex with rhLCV gH/gL, but class 5 was absent. There was also a substantial portion of unbound rhLCV gH/gL and a small proportion of class 2, which was not observed in complex with EBV gH/gL.

In the sample from A21138, we observed classes 1, 4, and 5 in complex with EBV gH/gL, while class 5 was not observed in the rhLCV gH/gL sample prepared with the same plasma. In addition, there were fewer instances of class 4 and a greater proportion of unbound rhLCV gH/gL in the preparation. A very small proportion of class 3 particles was observed in the A21138 rhLCV gH/gL sample that was not observed in complex with EBV gH/gL.

The EMPEM profile of A21139 was notably different from A21137 and A21138. Classes 1, 2, and 4-6 were observed in the EBV gH/gL sample and all 6 classes were present in the rhLCV gH/gL sample. The proportions of classes 4-6 were comparable between EBV and rhLCV gH/gL. There were fewer class 2 Fabs in complex with rhLCV gH/gL sample compared to EBV gH/gL, and an obvious population of class 3 Fabs in complex with rhLCV gH/gL that were not observed in complex with EBV gH/gL.

Overall, EMPEM revealed qualitative differences between the EBV and rhLCV gH/gL complexes in all animals (Fig. 4 and S5), which support the observations that the plasma reactivity differs between the vaccine-matched EBV gH/gL and non-vaccine matched rhLCV gHgL (Fig. 3). The greater breadth of epitope recognition to both EBV and rhLCV gH/gL observed in A21139 as compared to A21137 and A21138 could be associated with the observed protection in this animal.

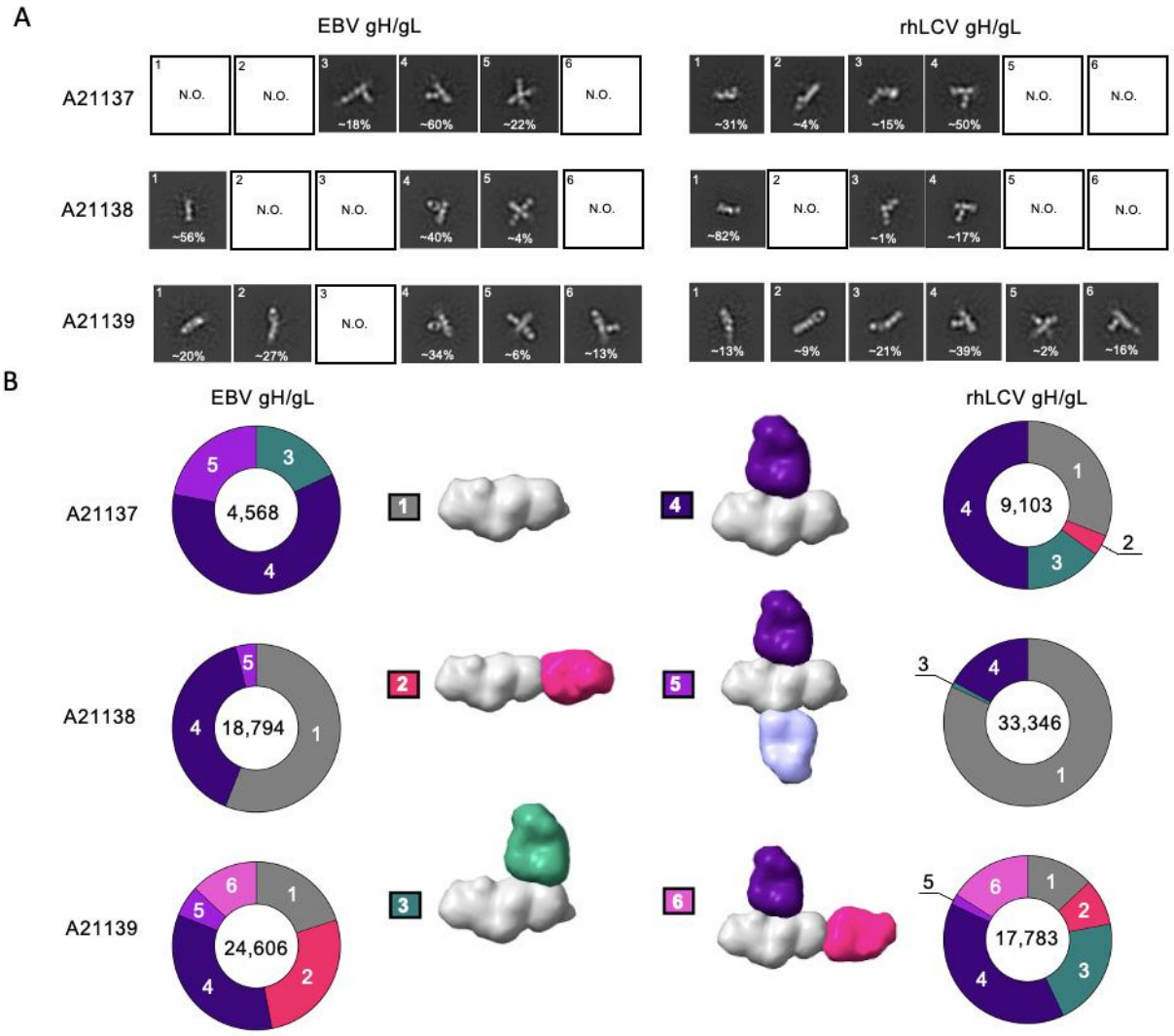

Figure 4: Electron microscopy polyclonal epitope mapping (EMPEM) analysis of polyclonal Fab fragments purified from animals A21137, A21138 and A21139 binding to EBV gH/gL and rhLCV gH/gL as indicated.

(A) 2D classes are shown representing the unique class observed defined as follows: 1) unbound gH/gL, 2) one pFab on end parallel to gH/gL, 3) one pFab on end perpendicular to gH/gL, 4) one pFab in middle 5) two pFabs in middle, 6) one pFab on end parallel to gH/gL and one pFab in middle. pFab specified as binding to the end of gH/gL could either be bound to the gH or gL domain. Number in the bottom of each panel corresponds to the percentage of particles in that class over the total number of particles in all classes for a given complex. N.O. =

not observed. (**B**) The frequencies of each class for every complex made are depicted in pie charts, with the total number of particles used in the center. Representative 20Å models corresponding to each class described in A) are shown in the key (gH/gL- grey, Fabs are colored based on the epitope – pink, green, dark purple, light purple).

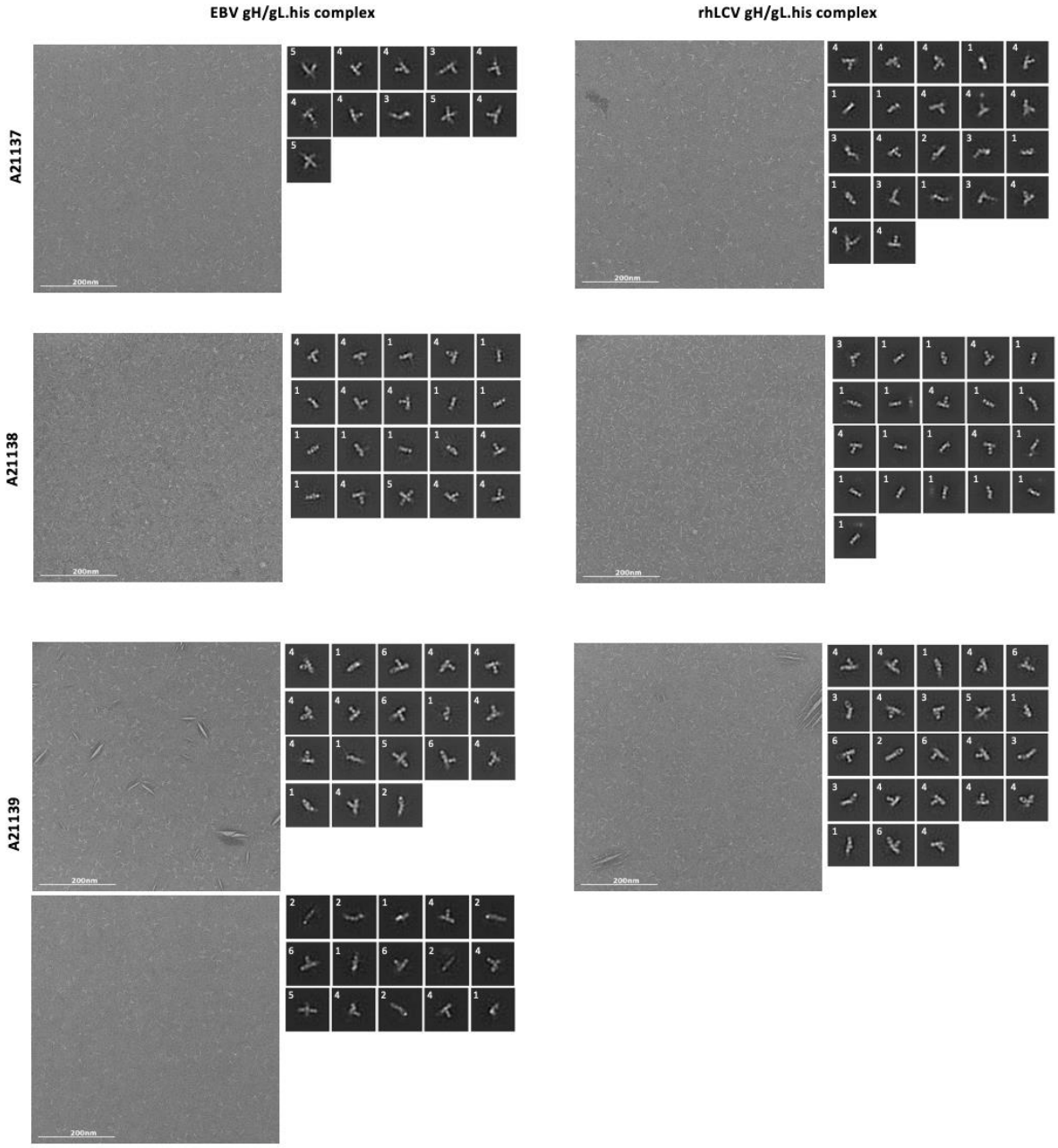

Figure S5: Representative views of electron microscopy polyclonal epitope mapping (EMPEM) analysis of polyclonal Fab fragments purified from animals A21137, A21138 and A21139 binding to EBV gH/gL and rhLCV gH/gL.

One representative micrograph from each complex is shown next to these views. Percentage of particles in each class were calculated using each of these datasets. Each view was assigned a number corresponding to one of the following classes: 1) unbound gH/gL, 2) one pFab on end

parallel to gH/gL) one pFab on end perpendicular to gH/gL, 4) one pFab in middle 5) two pFabs in middle, 6) one pFab on end parallel to gH/gL and one pFab in middle. From left to right, starting from the top, the total number of particles in each dataset were: 4,568; 9,103; 18,794; 33,346; 24,606; 17,783.

2.3.5 Neutralizing epitopes on EBV gH/gL are poorly conserved on rhLCV gH/gL

The lower binding titers to rhLCV gH/gL and different EMPEM profiles observed between polyclonal immune sera and EBV gH/gL versus rhLCV gH/gL indicate that the epitopes recognized by vaccine-elicited EBV gH/gL sera differ on rhLCV gH/gL. Moreover, the reduced ability of immune plasma to inhibit membrane fusion driven by the rhLCV fusion machinery (Fig. 3D) suggests that the neutralizing epitopes on EBV gH/gL are poorly conserved on rhLCV gH/gL. To investigate this further, we compared the binding of a panel of mAbs to gH/gL from both EBV and rhLCV using biolayer interferometry (BLI). AMMO1[28], CL40[49], CL59[49], E1D1[50], 770F7[27], 1D8[29] and 769B10[26] all bound to EBV gH/gL. In contrast, CL59, 769B10, and 1D8 did not bind rhLCV gH/gL (Fig. 5A). 770F7, E1D1 and CL40 bound to rhLCV gH/gL but the binding of these mAbs was weaker compared to EBV gH/gL, with notably faster off-rates. AMMO1 showed comparable binding to rhLCV gH/gL (Fig. 5A). Since the AMMO1 epitope is well conserved on gH/gL from rhLCV and EBV, and passive transfer of this mAb has been shown to protect against rhLCV infection[30], we sought to determine whether vaccinated animals elicited antibodies targeting this epitope by evaluating the ability of plasma to compete for binding to EBV gH/gL. Plasma from all SMNP group animals inhibited AMMO1 binding at a 1:50 dilution but the inhibition was reduced upon plasma dilution (Fig. 5B and C). In contrast, plasma from SMNP animals more potently inhibited binding of other gH/gL mAbs (Fig. 5B and C). Binding of E1D1 was readily inhibited by immunized plasma, while inhibition of CL40, 769B10 and 1D8 binding was intermediate between AMMO1 and E1D1 (Fig. 5C). None of the animals in the SAS

group inhibited binding of any the mAbs at the dilutions tested (Fig. 5B and C), consistent with the lower immunogenicity of this vaccine formulation (Fig. 1).

In the competition assays, antibodies that partially overlap with the AMMO1 epitope can lead to binding inhibition but not necessarily have the same binding and neutralizing properties as AMMO1. Given that the AMMO1 epitope is highly conserved on rhLCV gH/gL we evaluated the ability of the plasma from animals from the SMNP group to inhibit binding of this mAb to rhLCV gH/gL. In contrast to EBV gH/gL (Fig 5B), we did not observe any binding inhibition of AMMO1 to rhLCV gH/gL (Fig 5D) indicating that antibodies that bind the conserved AMMO1 epitope are not present in high titers in the SMNP immunized animals.

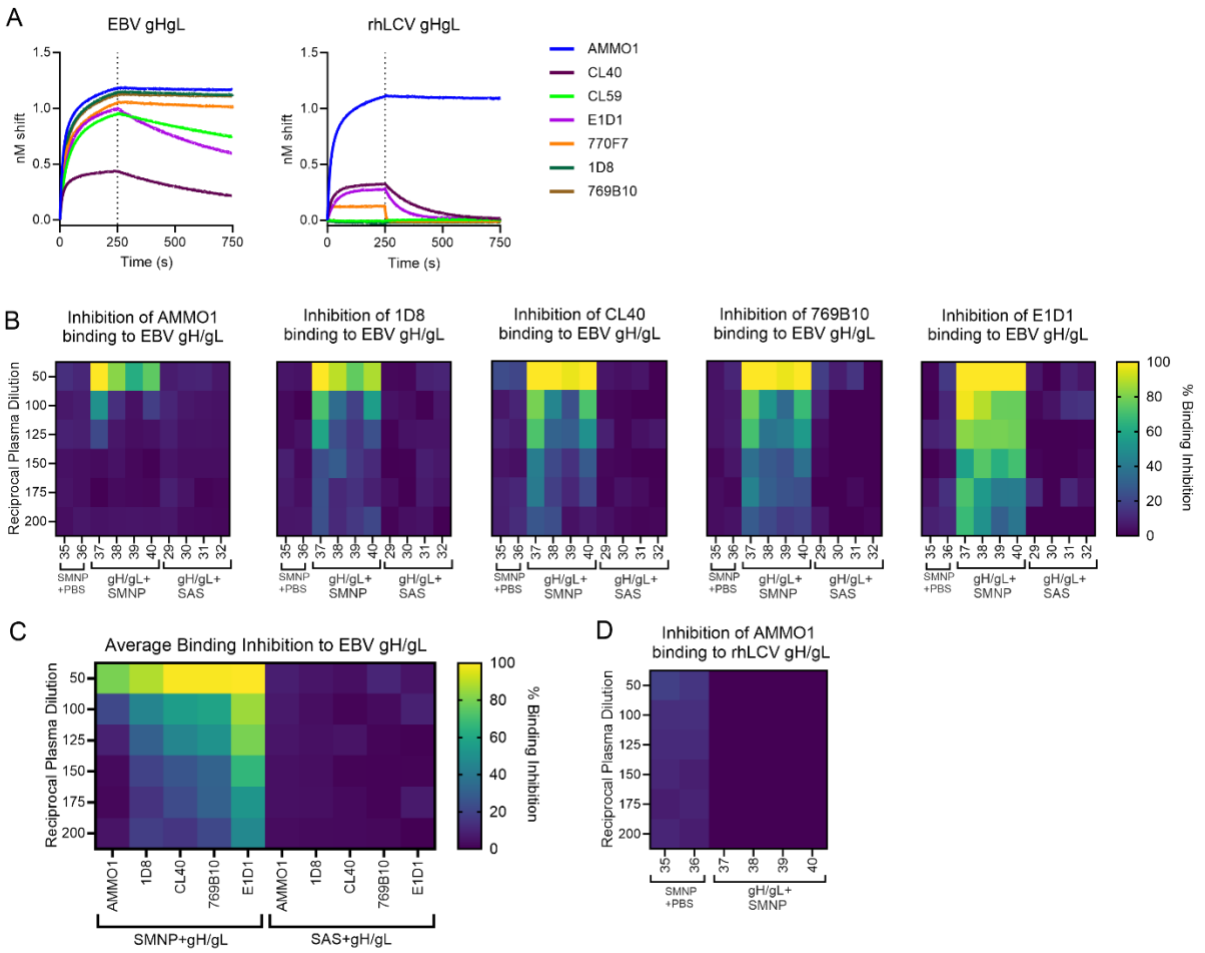

Figure 5: Neutralizing epitopes on EBV gH/gL are poorly conserved on rhLCV gH/gL. (**A**) Binding of a panel of anti-EBV gH/gL mAbs to a 50 nM solution of EBV gH/gL and rhLCV gH/gL as measured by BLI. (**B**) Ability of plasma collected 2 weeks after the final boost (week 14, Fig. 1A) from rhesus macaques immunized with gH/gL 60-mer formulated with SMNP or SAS to compete with the indicated mAbs for binding to EBV gH/gL as measured by BLI. (**C**) Average competition at indicated plasma dilutions from animals immunized with gH/gL 60-mer formulated with SMNP (left) or SAS (right) calculated from (B). (**D**) Ability of plasma from animals in (B) to compete with AMMO1 for binding to rhLCV gH/gL as measured by BLI. Heatmaps represent the average binding inhibition from two independent experiments in (B-D).

2.3.6 T cell responses in macaques immunized with gH/gL nanoparticles

Given that we were unable to unequivocally identify differences in the humoral response between A21139 and the other animals in the SMNP group, we examined the vaccine-elicited T cell responses. $CD4^+$ and $CD8^+$ T cells from PBMC collected 2 weeks after the second immunization were assayed for interleukin 2 (IL-2) and/or interferon gamma (IFN-γ) production as assessed by intercellular staining following a 6-hour stimulation with pools of overlapping peptides derived from EBV gH and gL (Genbank AFY97969.1 and AFY97944.1, respectively) (Fig. 6A and E, and S6).

Following peptide stimulation, the frequency of IL-2^+ IFN-γ^+ double positive $CD4^+$ T cells was low or undetectable in PBMC samples collected from the control and SAS groups before and after vaccination (Fig. 6B and C). In contrast, an increase in the frequency of cytokine producing $CD4^+$ T cells in all animals from the SMNP group was observed following immunization (Fig. 6D). In contrast to $CD4^+$ T cells, we were unable to detect any IL-2^+ IFN-γ^+ $CD8^+$ T cells in any group before or after immunization, except for animal A21140 in the SMNP group which had a very slight population at week 6 (Fig. 6E-H). We were unable to detect any changes in the frequency of TNF-α^+ $CD8^+$ T cells in peptide stimulated samples before or after immunization (Fig. S7).

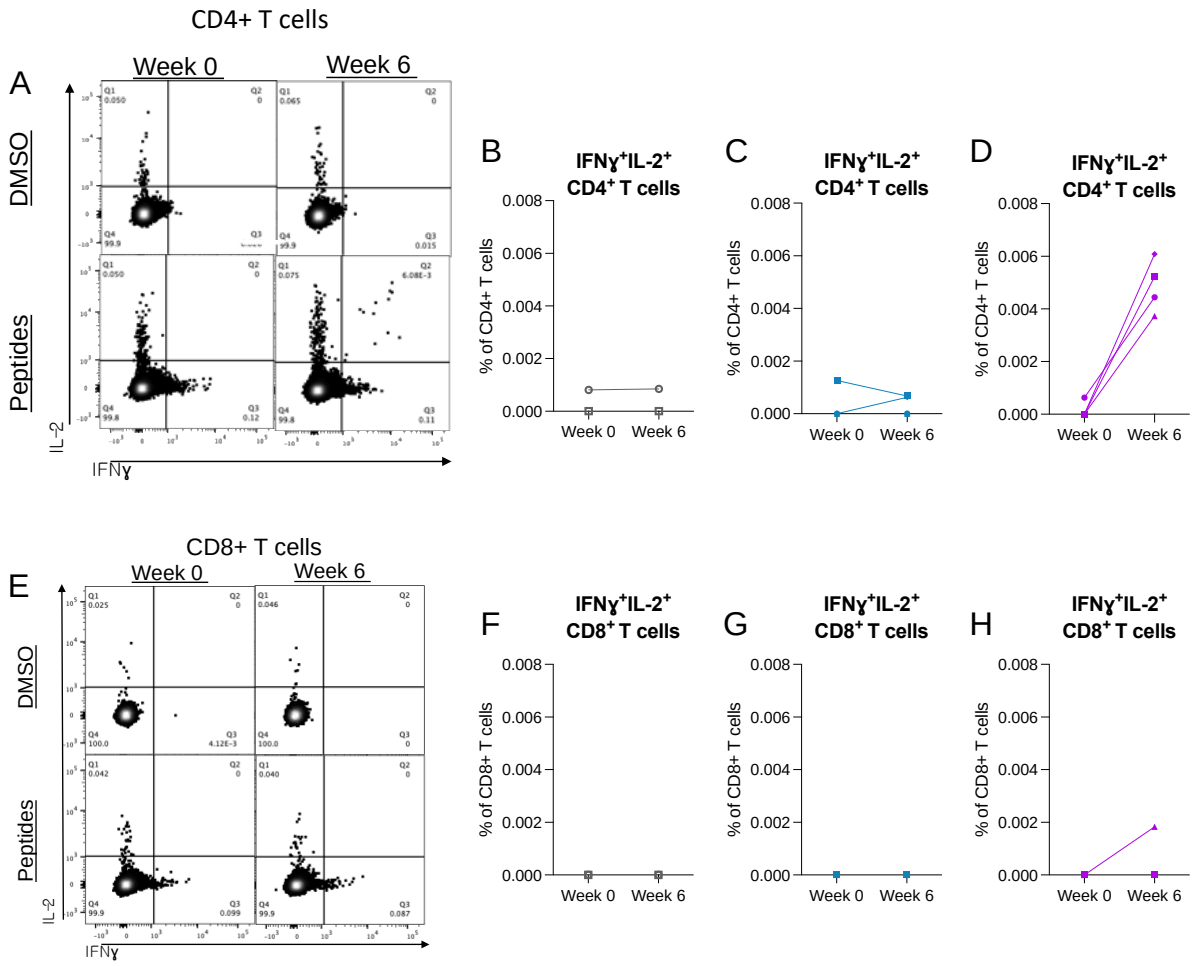

Figure 6: T cell responses elicited by gH/gL vaccination.

(A) Representative flow cytometry plots showing IFN-γ and IL-2 expression in $CD4^+$ T cells from PBMC collected prior to (week 0) and following 2 immunizations with gH/gL 60-mer (week 6), stimulated with either DMSO or overlapping gH/gL peptide pools. (**B**-**D**) Frequency of IFN-γ^+ IL-2^+ $CD4^+$ T cells after stimulation with gH/gL overlapping peptides from control animals (B), animals immunized with gH/gL 60-mer formulated with SAS (C), or animals immunized with gH/gL 60-mer formulated with SMNP (D). The frequencies of IFN-γ^+ IL-2^+ T cells are DMSO background subtracted. Wilcoxon matched-pairs signed rank test was performed for D. (**E**) Representative flow cytometry plots showing IFN-γ and IL-2 expression in $CD8^+$ T cells, following the same collection and stimulation conditions in (A**).** (**F**-**H**) Frequency of IFN-γ^+, IL-2^+, $CD8^+$ T cells after stimulation with gH/gL overlapping peptides from control animals (F), animals

immunized with gH/gL 60-mer formulated with SAS, (G) or animals immunized with gH/gL 60-mer formulated with SMNP (H).

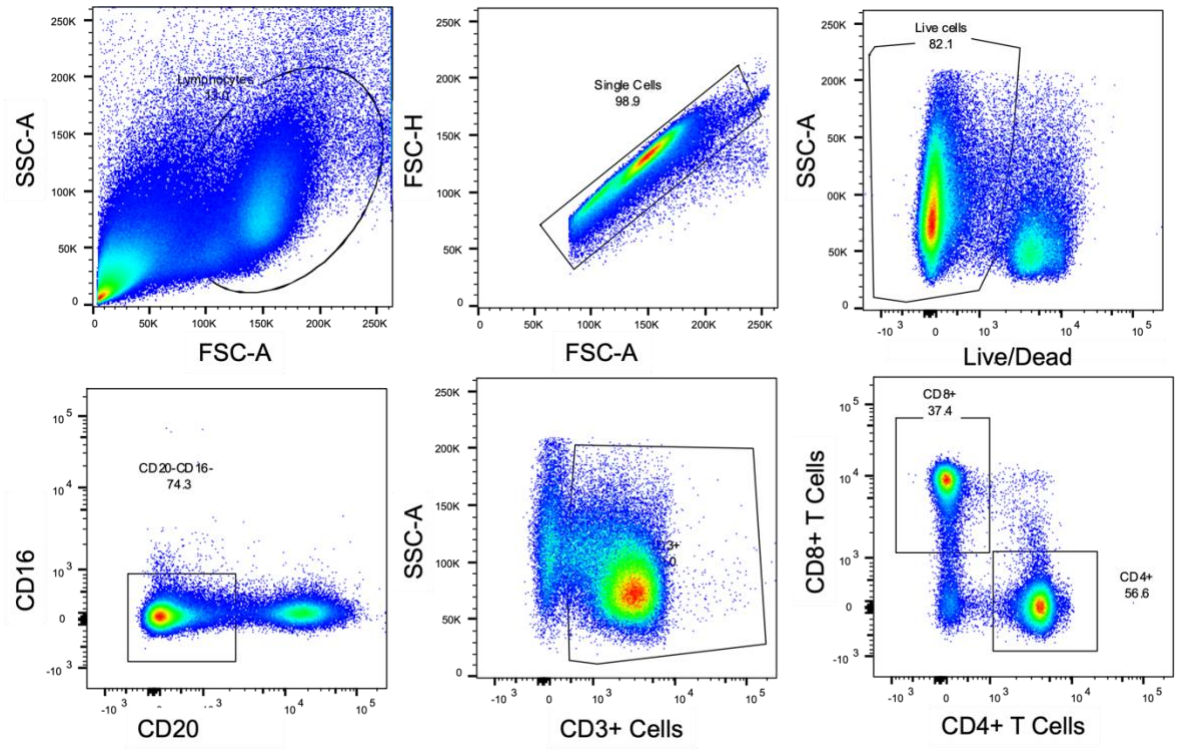

Figure S6: Gating strategy for T cells after peptide stimulation and ICS.

Single live lymphocytes that were $CD16^{-}$ $CD20^{-}$ $CD3^{+}$ and either $CD4^{+}$ or $CD8^{+}$ were analyzed for frequencies of IFNɣ and/or IL-2 positive cells.

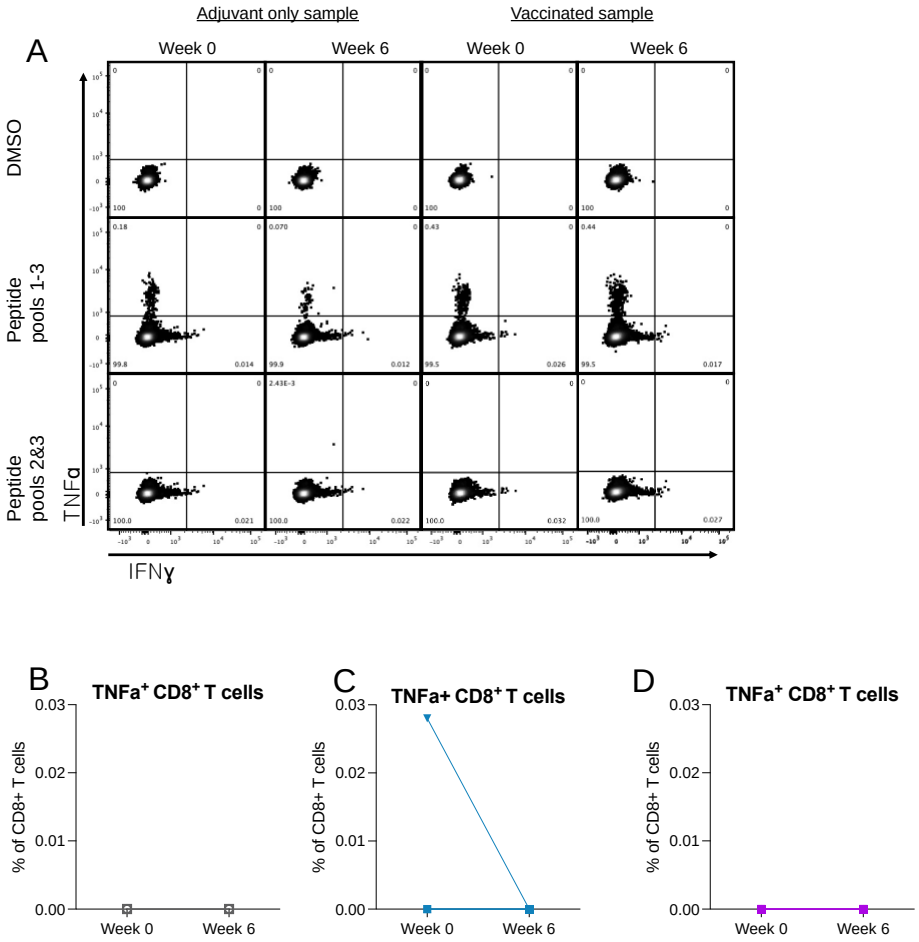

Figure S7: TNFα and IFNɣ production in CD8⁺ T cells in response to stimulation with peptide pools.

(**A**) Flow cytometry plots showing cytokine production in response to stimulation with DMSO (top), all 3 peptide pools (middle) and just pools 2 and 3 (bottom) for a representative sample from an adjuvant only control animal (left two columns) and a vaccinated animal (right two columns). (**B**-**D**) Frequency of TNFα⁺ CD8⁺ T cells among all CD8⁺ T cells in response to stimulation with pools 2 and 3 for (B) control macaques, (C) macaques immunized with gH/gL + SAS, and (D) macaques immunized with gH/gL + SMNP.

2.4 Discussion

Here we evaluated the immunogenicity of a gH/gL nanoparticle in rhesus macaques with two different adjuvants. When formulated with SMNP the gH/gL 60-mer elicited high titers of binding and EBV-neutralizing antibodies and higher frequency of antigen-specific B cell and $CD4^+$ T cell responses as compared to formulation with SAS. Vaccine-elicited plasma antibodies cross-reacted with gH/gL from the EBV orthologue rhLCV, but exhibited weaker binding, a reduced ability to inhibit cell fusion driven by rhLCV gH/gL, and different EMPEM profiles of the same sera binding to rhLCV gH/gL, as compared to EBV gH/gL. A panel of well-characterized anti-EBV gH/gL mAbs also showed substantially reduced binding to rhLCV gH/gL, highlighting a high degree of antigenic disparity between the two gH/gL proteins. These results demonstrate that the antigenic disparity between EBV and rhLCV poses a barrier to the evaluation of EBV vaccines in macaques.

Immunization of macaques with EBV vaccines is useful for assessing immunogenicity in a primate model that has an immune system more similar to humans than other small animals, which can support regulatory approval of vaccine candidates for clinical trials. However, challenge with the mismatched rhLCV may underestimate the ability of EBV subunit vaccines to protect against challenge with the matched human-tropic virus. As an alternative, proof of concept for gH/gL vaccines could be achieved by immunizing rhLCV negative macaques with the autologous rhLCV gH/gL immunogens and challenging with the strain matched rhLCV. A similar approach was used in a previous vaccine challenge study with rhLCV gp350[36].

In the current study, 1 of 4 animals was protected against experimental infection in the SMNP-adjuvanted group, which elicited higher binding and neutralizing titers than the SAS-adjuvanted group, supporting the notion that neutralizing antibodies will be an important component of an immune response elicited by an effective EBV vaccine. Within the SMNP

group there was no notable differences in the EBV or rhLCV gH/gL binding titers, EBV neutralizing titers, or ability to inhibit the activity of the rhLCV fusion machinery, in the protected animal compared to those that were infected. We did, however, observe broader epitope recognition among polyclonal Fab binding to rhLCV gH/gL as visualized by EMPEM in this animal. We did not observe any differences in the ability of plasma from this animal to outcompete mAbs that bind to known neutralizing epitopes on gH/gL, indicating that this plasma may be targeting novel epitopes conserved between EBV gH/gL and rhLCV gH/gL which may have contributed to protection.

Because of its ability to potently neutralize EBV infection of B cells and epithelial cells, the overlapping epitope targeted by AMMO1 and 769B10 represents a critical site of vulnerability on EBV[26–28]. Moreover, the observation that passive transfer of AMMO1 could protect rhesus macaques from rhLCV challenge highlights the importance of this epitope on rhLCV gH/gL as well[30]. Although the gH/gL 60-mer formulated with SMNP readily elicited antibodies that compete with several neutralizing epitopes on gH/gL, our binding-competition analysis indicates that the AMMO1 epitope is subdominant, and AMMO1-like antibodies that cross-react with rhLCV were not elicited by immunization with EBV gH/gL nanoparticles in macaques. A similar sub-dominance of the AMMO1 epitope was observed in mice immunized with several other gH/gL nanoparticles including the 60-mer used here[38]. Higher titers of antibodies that compete for the partially overlapping 769B10 epitope were elicited in SMNP group macaques, however it is unlikely that these antibodies contributed to the observed protection in the SMNP group animal since 769B10 does not cross-react with rhLCV gH/gL. Similarly, some vaccine elicited antibodies were able to compete with 1D8 for binding to EBV gH/gL, yet we do not expect them to contribute to protection due to the low cross-reactivity of 1D8 with rhLCV gH/gL.

Given that T cells play a critical role in controlling EBV infection[51] and have been shown to afford protection against viral challenge in humanized mice[52], we measured the frequency of cytokine-producing $CD4^+$ and $CD8^+$ T cells in the study animals. Following immunization, we observed an increase of $CD4^+$ T cells co-expressing IFNg and IL-2 in all animals in the SMNP group, while no animals mounted vaccine-specific $CD8^+$ T cell responses. The elevated frequency of cytokine producing $CD4^+$ T cells following immunization in the SMNP group is consistent with the higher binding and neutralizing titers in this group, since $CD4^+$ T cells play essential roles in coordinating immune responses by providing help to B cells, facilitating antibody production[53]. The lack of detectable vaccine-specific $CD8^+$ T cells suggests that humoral, rather than cellular immunity was responsible for the protection from challenge in the protected animal.

Consistent with another study, we demonstrate that multivalent gH/gL nanoparticle vaccines are immunogenic in non-human primates when formulated with SAS[26]. However, in a head-to-head comparison we observed that formulation with SMNP elicits stronger B- and $CD4^+$ T-cell responses in rhesus macaques, in line with the superior performance of SMNP over SAS in mice[40]. The enhanced immune responses and partial protection against challenge observed in the SMNP group underscores the importance of adjuvant selection in the development of EBV vaccines. Of note, SMNP is being evaluated in a first-in-human clinical trial (NCT06033209) and may therefore become available for subsequent immunogenicity studies of EBV vaccines in humans.

An alternative explanation for the lack of viremia, oral shedding or seroconversion in A21139 is that animal did not receive a sufficient viral inoculum. This is unlikely because i) a single dose of 50 transforming units was sufficient to infect all control animals in a previous study[30], although this is also limited by a small number (n=2) of animals, ii) 9 of 10 other animals

that also received two doses of 50 transforming units of rhLCV were infected in this study and iii) the animal was not inherently refractory to challenge because their PBMC were readily infectable *ex vivo*.

There are notable limitations to our study. The first is the small number of study animals. Although one of the immunized macaques remained uninfected after repeat challenge with rhLCV, and our results suggest that an expanded epitope recognition, as visualized by EMPEM, may have contributed to protection, a larger cohort of study animals will be required to unequivocally ascribe any particular vaccine-response responsible for this outcome. Because rhLCV-negative macaques from extended pathogen-specific colonies are not readily available, we obtained rhLCV-negative neonates and housed them until maternal antibodies, which could interfere with vaccine responses or serological assays, had waned. Obtaining animals in this manner is laborious, cumbersome and expensive. Therefore, we echo the calls of colleagues who work with the rhLCV infection model to expand support for the development of extended pathogen-specific colonies of rhLCV negative animals to enable further vaccine and pathogenesis studies[44]. A second limitation is that although gH/gL 60-mer formulated with SMNP elicited higher binding and neutralizing titers than SAS at all points we analyzed, we did not measure serum antibody or T cell levels beyond week 14. Understanding the durability of immune responses will be an important consideration for EBV vaccine development.

This study only evaluated an immunogen displaying gH/gL, future work including other proteins involved in fusion like gp42 and/or gB would be informative for optimizing vaccine design.

2.5 Materials and Methods

Study Design

All rhesus macaque work was carried out in accordance with all federal regulations and was approved by University of Washington and Fred Hutchinson Cancer Center IACUCs. Animal work was carried out at the Washington National Primate Research Center. Rhesus macaques were obtained from the Oregon National Primate Research Center within 24-72 hours of birth and hand-reared in a nursery to avoid natural transmission of rhLCV. After 2-3 weeks the animals were transported to the Washington National Primate Research Center and housed in pairs until 6 months of age. Sample size was determined by the availability of rhLCV-negative infant macaques and more animals were assigned to treatment (n=4 per group) than controls (n=2). Animals were randomly assigned to each group, while trying to ensure an equal mix of male and female animals as availability permitted. The group sizes used are comparable to similar studies published previously[30,36]. To ensure the animals remained rhLCV negative until the start of the study, starting at 2 months of age, blood and saliva from the animals were monitored monthly for the presence of rhLCV DNA by ddPCR using primers and probes specific for IR1. During this time the decay of maternal anti-VCA and anti-gB antibodies in the infant plasma were monitored by ELISA[30]. Study animals were acquired from two different birth cohorts and challenged with different viral stocks.

At approximately six months of age, two female and two male rhesus macaques were immunized with 50 µg EBV gH/gL 60-mer formulated with 50% (v/v) Sigma Adjuvant System (SAS) in 500 µl of PBS; one female and three male rhesus macaques were immunized with 50 µg EBV gH/gL 60-mer formulated with 400 µg of SMNP (prepared as previously described)[40] in 500 µl total volume of PBS; and one female and one male rhesus macaque were immunized with 400 µg SMNP in 500 µl total volume of PBS as a control group. Vaccinations were administered at weeks 0, 4, and 12. In all cases animals were immunized with a split dose

administered bilaterally in the quadriceps. Blood was drawn and oral swabs collected at weeks 0, 2, 4, 6, 10, 12, and 14 post immunization.

All animals were orally challenged with 50 transforming units of rhLCV once at week 14 and again at week 15 post immunization. Following challenge, blood and oral swabs were collected weekly until at least 2 serially collected samples tested positive for rhLCV in blood and saliva of all animals in a group, up to 12 weeks.

The primary endpoint was immunogenicity of the gH/gL nanoparticle vaccine as read out by binding titers and neutralizing titers. The secondary endpoint was protection from rhLCV challenge following vaccination. Initially we planned to collect blood and saliva for 10 weeks following challenge but extended to 12 weeks in the SMNP group to ensure that the protection observed in one animal was not a false-negative.

All binding and neutralization experiments were repeated at least once and ddPCR was used to detect rhLCV in DNA extracted from 2 separate aliquots of blood collected from each timepoint. gH/gL-specific B cell frequencies were measured from 2 separate aliquots of PBMC collected from each animal in the treatment groups and from one aliquot from each animal in the control group.

Rhesus macaque PBMC isolation

Blood was drawn by venipuncture and collected in EDTA-coated vacutainers. Whole blood was centrifuged at 1000 × *g* for 30 min and plasma was collected and made into 1 ml aliquots stored at -20 °C until use. Plasma was heat inactivated by incubating at 56 ºC for 30 minutes and then clarified by centrifugation prior to use. PBMC were further purified using a Ficoll cushion, and either subjected to DNA extraction using the QIAamp blood DNA kit (Qiagen) according to the manufacturer's instructions or frozen in liquid nitrogen in aliquots containing FBS with 10% DMSO.

Rhesus macaque oral swabs

A sterile polyester swab was rubbed on the buccal mucosa and along the upper and lower gum-lines outside of the teeth. Swabs were placed in 1 ml buffer containing 10 mM Tris, 25 mM EDTA, 50 mM potassium chloride, 1% Igepal CA 630 pH 8.0 (Sigma). 200 µl of buffer was extracted using the QIAamp blood DNA kit and eluted in 100 µl of buffer AE (Qiagen) following collection, and the remaining oral swab buffer was stored at -20 ºC.

Plasmids

cDNA encoding the C-terminal portion of rhLCV smallVCA (NCBI Genbank # YP_067949.1, amino acids #81-170) was cloned in frame with an N-terminal GST tag with a thrombin cleavage site in pGEX4.1 to create pGEX-rhLCV-VCA.

Amino acids 1-678 of rhLCV gH were amplified by PCR from pCAGGS-gH, and cloned in frame with a C-terminal His tag in pCVL-UCOE0.7-SFFV-IRES-GFP to create pCVL-UCOE0.7-SFFV-rhLCV-gH-HIS IRES GFP[46]. Amino acids 1-114 of rhLCV-gL were amplified by PCR from pCAGGS-rhLCV-gL and subcloned into pCVL-UCOE0.7-SFFV-gL-IRES-RFP to create pCVL-UCOE0.7-SFFV-rhLCV-gL-IRES-RFP.

rhLCV smallVCA protein expression and purification

BL21(DE3) *E. coli* (NEB, C2527H) cells were transformed with pGEX-rhLCV-VCA. A single colony was cultured in 2xYT media containing 100 µg/ml ampicillin to a final volume of 500 ml. When the OD reached 0.5 smallVCA, IPTG was added to a final concentration of 0.25 mM and incubated with shaking at 30 °C overnight.

The next day, cells were pelleted by centrifugation and resuspended in 20 ml bacterial cell lysis buffer (GoldBio, GB-177-100) with 30 mg of lysozyme (Sigma, 9001-63-2) and 2 protease

inhibitor tablets (Pierce Protease Inhibitor Mini Tablets, A32953). and incubated 1 hour at 37 °C with end over end rotation at 15 rpm.

Cell debris was pelleted by centrifugation at 20,000 × *g* for 20 minutes. Supernatant was incubated for 30 minutes with Glutathione Agarose Resin (GoldBio, G-250-5) pre-equilibrated with PBS followed by extensive washing with PBS, then protein was eluted with 50 mM Tris, 10 mM reduced glutathione, pH 8.0. The protein in the eluate was buffer exchanged into PBS, flash frozen in liquid nitrogen, and stored at -80 °C.

GST without the smallVCA fusion was produced by transforming BL21(DE3) with pGEX. Expression and purification was performed as described above.

EBV gH/gL 60mer expression and purification

Lentiviral Transduction

Lentivirus was produced as described previously[38] utilizing plasmids psPAX2, pMD2.G (both gifts from Didier Trono), and pCVL-UCOE0.7-SFFV-EBV-gH-C153T-60mer-IRES-GFP, pCVL-UCOE0.7-SFFV-EBV-gL-IRES-RFP, pCVL-UCOE0.7-SFFV-rhLCV-gH-IRES-GFP, or pCVL-UCOE0.7-SFFV-rhLCV-gL-IRES-RFP.

Polybrene was added to 10 ml of 293-6E cells at 1×10^6 cells/mL to a final concentration of 2 µg/ml, along with 2-3 ml lentiviral particles harboring the gH 60-mer and gL or rhLCV-gH-HIS and rhLCV gL expression constructs. Cultures were expanded until cell viability declined to ~80%. Cultures were centrifuged at 4000 × *g* for 10 minutes, and the supernatant passed through a 0.22 µm filter.

Purification of gH/gL 60-mer

gHgL 60-mer was purified using an affinity chromatography resin as described previously[38]. Supernatant containing gH/gL 60-mer was passed over an E1D1 affinity column, washed with

TBS, eluted with Pierce IgG elution buffer. The eluted protein was further purified by SEC using a Superose 6 Increase column with 50 mM Tris, 150 mM NaCl, 150 mM L-arginine, pH 8.0 as the mobile phase. Purified protein was flash frozen and stored at -80 ºC.

Purification of rhLCV gH/gL-HIS

Supernatant containing rhLCV-gH/gL-HIS was passed over Ni-NTA resin pre-equilibrated with Ni-NTA binding buffer (0.3 M NaCl, 20 mM Tris,10 mM imidazole, pH 8.0), followed by extensive washing with Ni-NTA binding buffer, and then eluted with 250 mM imidazole, 0.3 M NaCl, 20 mM Tris, pH 8.0 (Ni-NTA elution buffer). Ni-NTA-purified rhLCV-gH/gL-HIS was further purified by size exclusion chromatography (SEC) using a 10/300 Superdex 200 column (GE Healthcare) equilibrated into PBS. Purified protein was flash frozen and stored at -80 ºC until use.

Purification of untagged monomeric EBV gH/gL

Untagged EBV gH/gL was purified as previously described[38]. Briefly, clarified cell supernatant was adjusted to pH 5.5-6 using acetic acid and purified using CaptoMMC resin, followed by anion exchange chromatography using a HiTrap Q HP column and SEC with PBS as the mobile phase on the Superose 6 Increase 10/300 GL. The purified protein was aliquoted, flash frozen in liquid nitrogen and stored long term at -80 °C.

Biotinylation of recombinant proteins

Recombinant gH/gL proteins were biotinylated using the EZ-Link NHS-PEG4-Biotin Kit according to the manufacturer's instructions. Excess biotin was removed using a Zeba Spin Desalting Column.

rhLCV virus production

Rhesus LCV was isolated from LCL8664 cells by TPA/Butyrate induction as described previously[30]. LCL8664 cells were cultured 0.5-1×10^6 cells/ml. For induction, 2×10^7 cells were

stimulated with 50 ng/ml 12-O-Tetradecanoylphorbol 13-acetate (Sigma Cat. #P1585-1MG) and 3mM sodium butyrate (Sigma Cat. #303410-100G) in 10 ml. After an overnight 37 °C incubation, cells were pelleted by centrifugation, resuspended at 5×10^5 cells/ml, and cultured for 7 days at 37 °C. Supernatant was collected, passed through a 0.45 µM filter, then centrifuged at 10,000 × *g* for 2 hour at 4 °C. Supernatant was aspirated and the pellet was resuspended in the residual volume of the ultracentrifuge tube, ~2 ml of RPMI containing 10% FBS. Virus was dispensed into 250 µl aliquots and stored at -80 °C.

rhLCV titration

Titration of rhLCV was performed as previously described[30]. In short, serial dilutions of rhLCV were added to 96-well plates containing 1×10^5 rhesus PBMC in cRPMI containing 0.5 µg cyclosporin A. Each concentration of virus was tested against 20 PBMC-containing wells. Wells were visually inspected and scored as positive or negative for transformation. A transforming unit is defined the dilution that yields 62.5% positive wells[30,54]. Titration was performed using PBMC from 2 separate animals and the average transforming units/ml was used.

Preparation of EBV Reporter Viruses

GFP reporter viruses were produced as previously described[38]. Briefly B95-8/F was produced by transfecting 293–2089 cells with p509 and p2670 using GeneJuice transfection reagent[55,56]. Epithelial cell tropic virus was produced from Akata-GFP EBV treated with goat anti-human IgG (Southern Biotech Cat. #2040-01). 72 hours after induction, cell supernatant was clarified by centrifugation and passed through a 0.8 µm filter. Virions were concentrated 25-50-fold by centrifugation at 25,000 × *g* for 2 hours and re-suspended in PBS. Virus was stored at -80 °C and thawed immediately before use.

Digital droplet PCR

Digital droplet PCR (ddPCR) was performed as previously described[30]. In short, rhLCV DNA was quantified in DNA extracted from rhesus macaque PBMC and saliva using primers and FAM-labeled probe specific for internal repeat 1 (IR1). The amount of virus in blood was normalized to the number of PBMCs in a separate reaction using a primer/probe mix specific for the ribonuclease P/MRP subunit p30 (RPP30). For rhLCV load in saliva, concentration is expressed as copies/ml of swab buffer. Droplets were generated using a QX200 Droplet Generator (Bio-Rad). PCR was carried out on a C1000 Touch Thermal Cycler (Bio-Rad).

Following PCR, the droplets were read on aQX200 Droplet Reader (Bio-Rad). Droplets with fluorescence higher than the threshold (4000 for FAM, 3000 for HEX) were counted as positive. Data were analyzed and rhLCV copies per million PBMC were determined as previously described[30] using QuantaSoft Analysis Software (Bio-Rad) or QX Manager 1.1 Analysis software (Bio-Rad).

EBV neutralization assay in B cells

EBV neutralization assays were carried out as previously described[57]. In short, plasma was serially diluted in cRPMI in triplicate in 96-well round-bottom plates. B95-8/F virus diluted to achieve an infection frequency of approximately 5% was added and plates were incubated for 1 hour at 37 °C. Following the incubation, 5×10^4 Raji cells were added to each well and incubated for an hour at 37 °C. Cells were then washed once and re-suspended in fresh cRMPI at 37 °C. 72 hours later, cells were fixed in 10% formalin and the percentage of GFP+ Raji cells was determined using Luminex Guava HT.

To account for any false positive cells due to auto-fluorescence in the GFP channel, the average $\%GFP^+$ cells in negative control wells (n=5-10) was subtracted from each well. The infectivity ($\%GFP^+$) was plotted as a function of the $\log_{10}$ of the mAb concentration or plasma

dilution. The neutralization curve was fit using the log (inhibitor) vs response- variable slope (four parameters) analysis in Prism 7.03 (GraphPad Software).

EBV Neutralization Assay in Epithelial Cells:

SVKCR2 cells were seeded at 1.5×10^4 cells per well in a 96 well flat-bottom tissue culture plate. The next day, in a separate plate, plasma was serially diluted in a 96-well plate in duplicate wells, then Akata virus was added to each well and incubated for 15 min. The media was then aspirated from the SVKCR2 cells and replaced by the antibody-virus mixture. The plates were incubated at 37 °C for 48 hours, then cells were detached from the plate using 0.25% trypsin, transferred to a 96 well round bottom plate, washed twice with PBS, and fixed with 10% formalin. The $\%GFP^+$ cells were determined on a Luminex Guava HT and neutralization was determined as in the B cell neutralization assay.

gH/gL Neutravidin Capture ELISA

30 µl/well of a 0.3 µg/ml solution of NeutrAvidin (Thermofisher Cat. #31000) in ELISA coating buffer (0.1 M $NaHCO_3$ pH 9.4-9.6) was added to 384-well microplates (Thermofisher Cat.# 12565347) and incubated at 4 ºC for 16 hours. The next day, plates were washed 4 times with ELISA wash buffer (PBS with 0.02% Tween 20). Half the plate then received 30 µl/well of a 2 µg/ml solution of either biotinylated rhLCV or EBV gH/gL in PBS containing 3% bovine serum albumin (BSA) and 0.02% Tween 20, while the other half of the plate received only PBS containing 3% BSA and 0.02% Tween 20. Plates were incubated at 37 °C for 1 hour then washed 4 times with ELISA wash buffer and blocked with PBS containing 3% BSA, 10% non-fat milk, and 0.02% Tween 20 (neutravidin blocking buffer) for 1 hour. After 4 washes with ELISA wash buffer, plasma was diluted in neutravidin blocking buffer and three-fold serial dilutions were performed in duplicate, followed by a 1-hour incubation at 37 °C. 8-16 additional control wells were included that contained immobilized gH/gL but no plasma. Plates were washed with

ELISA wash buffer, and a 1:4000 dilution of goat anti-human IgG-HRP (SouthernBiotech Cat. #2010-05) in neutravidin blocking buffer was added to each well and incubated at 37 °C for 1 hour followed by 4 washes with ELISA wash buffer. 30 µl/well of SureBlue Reserve TMB Microwell Peroxidase substrate (SeraCare Cat. #5120-0081) was then added and incubated for 5 min, and then stopped with 30 µl/well of 1 N sulfuric acid. A_{450} of each well was read on a Molecular Devices SpectraMax M2 plate reader. A_{450} was plotted as a function of reciprocal plasma dilution and fit to sigmoidal dose response (variable slope) function using the Prism 9.3.0 package. The binding cutoff was defined as the average plus 10 times the standard deviation of the determined by calculating the average of A_{450} values of the control wells. Endpoint titers were interpolated from the point of the curve that intercepted the binding cutoff using the Prism 9.3.0 package.

rhLCV-smallVCA and EBV gB ELISAs

96-well flat-bottom plates (Thermofisher, Cat. #3455) were coated with 500 ng/well of GST-rhLCV smallVCA or 405 ng/well GST (for rhLCV smallVCA ELISAs) or 100 ng/well of EBV-gB EctoS (for EBV gB ELISAs) in ELISA coating buffer at 4 °C for 16 hours. The next day, plates were washed with ELISA wash buffer, blocked for 1 hour with 90 µl/well of PBS containing 10% nonfat milk and 0.03% Tween 20 (blocking buffer). After blocking, plasma was diluted 1:20 (for rhLCV smallVCA) or 1:50 (for EBV gB) in blocking buffer and added to wells in triplicate. Plates were incubated for 1 hour at 37 °C, washed and then treated with a 1:4000 dilution of goat anti-human IgG-HRP (SouthernBiotech) in blocking buffer at 37 °C for 1 hour. After washing, plates were developed and read with SureBlue Reserve TMB Microwell Peroxidase substrate, as described above. For rhLCV smallVCA ELISAs, the average absorbance of the triplicate GST wells was subtracted from the average absorbance of the triplicate GST-rhLCV smallVCA wells for each animal at each timepoint. If negative, this value was reported as zero. The average

absorbance of the triplicate gB EctoS coated wells with no plasma was subtracted from the absorbance of each gB EctoS well for each animal at each timepoint.

Virus-free fusion assay

CHO-K1 cells were seeded onto six-well tissue culture plates at a density of 3×10^5 cells/well. 24 hours later, cells were transfected with 0.5 µg each of pCAGGS-rhLCV-gH, pCAGGS-rhLCV-gL, pCAGGS-rhLCV-gB and 0.8 µg of pT7EMCLuc , using GeneJuice Transfection Reagent according to the manufacturer's instructions[58,59]. As a control for background luciferase activity, one well was transfected with the same mix as above, excluding the pCAGGS-rhLCV-gB plasmid.

24 hours later, macaque plasma was serially diluted in cF-12 in a white 96 well plate with clear bottom (Thermo Fisher Cat. #12-566-71). Both 293-T7 cells and the transfected CHO-K1 cells were trypsinized, washed once with cF-12, and re-suspended at a density of 3×10^5 cells/ml in cF-12 media. 50 µl/well of each cell suspension was added to the 96 well plate containing diluted plasma and incubated at 37 °C for 24 hours. Media was aspirated and the cells were lysed in 100 µl of Steady-Glo luciferase reagent. Luciferase activity was read on a Promega Glomax Navigator Microplate Luminometer. Values from control wells were subtracted, and data was normalized to fusion in absence of plasma. Normalized fusion was plotted against the reciprocal plasma dilution and fit to sigmoidal dose response (variable slope) function and the ID_{50} was interpolated using the Prism 9.3.0 package.

Staining of antigen specific B cells

Biotinylated EBV-gH/gL was conjugated to Totalseq allophycocyanin (APC)-streptavidin (BioLegend) or phycoerythrin (PE)- streptavidin (eBioscience). PBMC from macaques collected 14 weeks after the start of the immunization regimen were thawed and washed in cRPMI before resuspension in FACS buffer (1X PBS pH 7.4, 2% heat inactivated FBS, 1 mM EDTA). Cells

were resuspended in 50 µl of FACS buffer containing 300 ng of gH/gL-PE and gH/gL-APC, 1:500 eFluor 506 viability dye (eBioscience #65-0866-14) and the following antibodies at a 1:200 dilution: Rhesus Fc receptor inhibitor (eBioscience #14-9161-73), AF488 anti-human CD3 clone SP34-2 (BD Biosciences #557705), AF488 anti-human CD4 clone OKT4 (Biolegend # 317419), AF488 anti-human CD8 clone RPA-T8 (BD Biosciences #557704), AF488 anti-human CD14 clone M5E2 (BD Biosciences #561706), BV421 anti-human CD20 clone 2H7 (Biolegend #302329). Cells washed in FACS buffer and acquired on a BD FACSAria II cell sorter using FACSDiva software (BD Bioscience). After acquisition, the frequency of single live $CD3^-$ $CD4^-$ $CD8^-$ $CD14^-$ $CD20^+$ gH/gL-APC^+ gH/gL-PE^+ cells was analyzed using FlowJo Software.

T Cell Stimulation and ICS

PBMC from each animal/timepoint were thawed, washed in cRPMI, and rested overnight at 37 °C, 5% CO_2 then. split into 5 wells of a 96 well plate each with 1.2 million cells in 200 µl cRPMI. Three wells were stimulated with pools of peptides 15 amino acids in length, overlapping by 11 amino acids spanning gL (25 peptides), and two pools of 85 and 84 peptides spanning gH (1µg of total peptide per well) and anti-CD28/ anti-CD49d (BD Biosciences #347690) and Brefeldin A (Sigma-Aldrich #B-7651) at final concentrations of 1 µg/mL and 10 µg/ml, respectively. All peptides were synthesized by Mimitopes and were resuspended in DMSO. Two additional wells were incubated with 0.5% DMSO and 50 ng/ml PMA with 500 ng/ml ionomycin as a negative and positive controls.

Following a six-hour incubation at 37 °C 5%CO_2, 20 µl EDTA was added and cells were stored at 4 °C for up to 12 hours. Cells were then washed with PBS and stained with Live/Dead Fixable Blue Dead Cell Stain Kit (Invitrogen #L23105) according to the manufacturer's instructions, washed with FACS buffer and incubated with 1:25 dilution anti-CD16 (BioLegend #302036) and

1:50 anti-CD20 (BD #563126) antibodies per sample. Cells were then washed twice, and residual red blood cells were lysed and all cells fixed in 100 µl BD lysis buffer (BD #349202), washed, and incubated with 200 µl BD FACS Permeabilizing Solution 2 (BD #340973). Intracellular staining was done with 1:1000 dilution of anti-CD8 (BD #612889) and CD4 (BD #566148), 1:2500 anti- CD3 (BD #564117), 1:200 anti- TNFα (ThermoFisher #11-7349-82) and IFN-γ (BD #560371), and 1:50 anti- IL-2 (BioLegend #500310) antibodies. Cells were then washed and analyzed on a custom-built BD FACSymphony cytometer. Data were analyzed via FlowJo v10.9.0 Software (BD Life Sciences). Unless otherwise noted, the three samples stimulated with the different overlapping peptide pools were concatenated and analyzed together. To calculate the frequency of gH/gL specific responses, the frequency of IFN-γ and IL-2 double positive cells in the DMSO control wells was subtracted from the frequency in the concatenated peptide pool wells for each sample tested.

Biolayer Interferometry (BLI)

All BLI assays were performed on the Octet Red instrument at 30 °C with shaking at 1,000 RPM.

mAb binding to EBV and rhLCV gH/gL

Anti-human IgG Fc capture (AHC) biosensors (ForteBio) were loaded with anti-EBV gH/gL mAbs or kinetics buffer (KB: 1X PBS pH 7.4, 0.01% BSA, 0.02% Tween 20, and 0.005% NaN_3) alone at a concentration of 5 µg/ml in KB for 250 s. Biosensors were immersed in KB containing 250 nM of either rhLCV or EBV gH/gL for 250 s to measure association. Following this, sensors were immersed in KB and dissociation was measured for 500 s. Binding measurements were corrected by subtracting the binding signal of the 72A1 control mAb that does not react with gH/gL.

Competition BLI

Biotinylated anti-EBV gH/gL mAbs were diluted to 5 µg/ml in KB and were captured on streptavidin biosensors (ForteBio) for 250 s, baseline interference was then read for 60 s in KB, followed by immersion in a 50 nM solution of gH/gL alone, or gH/gL that was pre-incubated with diluted macaque plasma for 1 hour. Binding measurements were corrected by subtracting the binding signal of sensors immersed in KB. The maximum response (R_{max}) was determined to be the average binding signal measured from the last 5 seconds of the association phase. For each mAb-loaded sensor the R_{max} measured in the presence of serum, was plotted as a percentage of the R_{max} of the mAb binding to gH/gL alone. This pwas then subtracted from 100 to calculate the percent inhibition of binding. Negative values were adjusted to zero.

Polyclonal IgG purification from sera

1 ml of serum was heat-inactivated and purified over Protein A or Protein A/G resin to obtain polyclonal IgG (pIgG). pIgG eluted from the resin was incubated in small amounts with papain over several timepoints to identify the optimal condition for its digestion to a Fab. Once the proper conditions were determined (5 µg/ml papain 30 min digest for A21137, 20 µg/ml papain 1 hour digest for A21138 and 20 µg/ml papain 30 min digest for A21139), these reactions were scaled up to digest 1 ml of the serum at 37 ºC. Digested pIgG product purified via Protein A or A/G followed by SEC with a Superdex 200 10/300 column. Fractions corresponding to the polyclonal Fab (pFab) peak were pooled and used for complexing with gH/gL.

pFAb-gH/gL complex formation

Recombinant, monomeric, his-tagged EBV gH/gL or rhLCV gH/gL was incubated with a four-fold molar excess ratio of each pIgG for two hours at room temperature, and then purified via SEC using an S200 10/300 column. Fractions containing gH/gL/pFab complexes were isolated and subjected to negative stain electron microscopy.

Negative stain electron microscopy sample preparation, data processing and analysis

Each individual peak for every sample was stained separately on formvar/carbon Ted Pella 400 mesh copper grids at a concentration of ~0.01-0.02 mg/mL and stained with 2% (w/v) uranyl formate. Grids were imaged at 120 kV on a Talos L120C Transmission Electron Microscope. Data were collected using the Leginon software at 1.58 Å pixel size and 2 mm spherical aberration with a 40 e/Å^2 total exposure dose. For each complex, micrographs collected from the first peak of each trace, confirmed to elute before unliganded gH/gL, were loaded into separate Cryosparc[60] workspaces and processed. Particles were picked using a combination of Blob Picker and Template Picker. Particles that appeared to be unbound pFab or noise were filtered out during the 2D classification process. Each particle was then grouped into a specific class and approximate percentages were calculated by dividing the number of particles in each class by the total number of particles seen for the complex. In the case of A21139, two EBV gH/gL complexes were made that yielded comparable class distributions, and the percentages of Fab in each class were averaged across both experiments.

Statistical Analysis

A Mann-Whitney U test was used to compare the distribution of outcomes between the pairs of groups considered. Endpoint binding titer, Neutralization titer as inhibitory dilution to achieve 50% reduction in titer (ID_{50}) and frequency of gH/gL-specific B cells or T cells were compared across each adjuvant group.

2.6 Acknowledgments:

We would like to thank John McNevin for assistance with flow cytometry analysis in the BSL2+ facility, Steven Voght for assistance with technical editing, as well as Clayton Ferrier, Jesse

Day, and Charlotte Hotchkiss from the WANPRC for assistance with the rhesus macaque experiments. Graphics designed with BioRender were used to produce some figures in this manuscript. DJI is an investigator of the Howard Hughes Medical Institute.

2.7 Author Contributions

Conceptualization: ATM and KRE

Investigation: KRE, KS, LJH, GMK,

Formal analysis: KRE, KS, LJH, GmK, MPa and ATM

Visualization: KRE and GMK

Resources: JA, SCD, KAR, EB, DJI, MPr, GX, and EWN

Writing- original draft: ATM and KRE

Review and editing: all

Funding acquisition: AtM, MPa, SCD, and KRE

2.8 Chapter 2 Bibliography

1. Cohen, J. I. Epstein–Barr Virus Infection. *New England Journal of Medicine* **343**, 481–492 (2000).
2. Balfour, H. H. *et al.* Age-Specific Prevalence of Epstein–Barr Virus Infection Among Individuals Aged 6–19 Years in the United States and Factors Affecting Its Acquisition. *J Infect Dis* **208**, 1286–1293 (2013).
3. Henle, G., Henle, W. & Diehl, V. Relation of Burkitt's tumor-associated herpes-ytpe virus to infectious mononucleosis. *Proceedings of the National Academy of Sciences* **59**, 94–101 (1968).
4. Epstein, M. A., Achong, B. G. & Barr, Y. M. VIRUS PARTICLES IN CULTURED LYMPHOBLASTS FROM BURKITT'S LYMPHOMA. *The Lancet* **283**, 702–703 (1964).
5. HAUSEN, H. ZUR *et al.* Epstein–Barr Virus in Burkitt's Lymphoma and Nasopharyngeal Carcinoma: EBV DNA in Biopsies of Burkitt Tumours and Anaplastic Carcinomas of the Nasopharynx. *Nature* **228**, 1056–1058 (1970).
6. Weiss, L. M., Movahed, L. A., Warnke, R. A. & Sklar, J. Detection of Epstein–Barr Viral Genomes in Reed–Sternberg Cells of Hodgkin's Disease. *New England Journal of Medicine* **320**, 502–506 (1989).
7. Khan, G., Fitzmaurice, C., Naghavi, M. & Ahmed, L. A. Global and regional incidence, mortality and disability-adjusted life-years for Epstein-Barr virus-attributable malignancies, 1990-2017. *BMJ Open* **10**, e037505 (2020).

8. Shannon-Lowe, C. & Rickinson, A. The Global Landscape of EBV-Associated Tumors. *Frontiers in Oncology* vol. 9 Preprint at https://doi.org/10.3389/fonc.2019.00713 (2019).
9. Wong, Y., Meehan, M. T., Burrows, S. R., Doolan, D. L. & Miles, J. J. Estimating the global burden of Epstein-Barr virus-related cancers. *J Cancer Res Clin Oncol* **148**, 31–46 (2022).
10. Taylor, G. S., Long, H. M., Brooks, J. M., Rickinson, A. B. & Hislop, A. D. The immunology of Epstein-Barr virus-induced disease. *Annu Rev Immunol* **33**, 787–821 (2015).
11. Balandraud, N. & Roudier, J. Epstein-Barr virus and rheumatoid arthritis. *Joint Bone Spine* vol. 85 165–170 Preprint at https://doi.org/10.1016/j.jbspin.2017.04.011 (2018).
12. Bjornevik, K. *et al.* Longitudinal analysis reveals high prevalence of Epstein-Barr virus associated with multiple sclerosis. *Science (1979)* **375**, 296–301 (2022).
13. Cornillet, M., Verrouil, E., Cantagrel, A., Serre, G. & Nogueira, L. In ACPA-positive RA patients, antibodies to EBNA35-58Cit, a citrullinated peptide from the Epstein–Barr nuclear antigen-1, strongly cross-react with the peptide β60-74Cit which bears the immunodominant epitope of citrullinated fibrin. *Immunol Res* **61**, 117–125 (2015).
14. Handel, A. E. *et al.* An updated meta-analysis of risk of multiple sclerosis following infectious mononucleosis. *PLoS One* **5**, 1–5 (2010).
15. Lanz, T. V. *et al.* Clonally expanded B cells in multiple sclerosis bind EBV EBNA1 and GlialCAM. *Nature* **603**, 321–327 (2022).
16. Chen, T., Song, J., Liu, H., Zheng, H. & Chen, C. Positive Epstein-Barr virus detection in coronavirus disease 2019 (COVID-19) patients. *Sci Rep* **11**, 10902 (2021).
17. Paolucci, S. *et al.* EBV DNA increase in COVID-19 patients with impaired lymphocyte subpopulation count. *Int J Infect Dis* **104**, 315–319 (2021).
18. Simonnet, A. *et al.* High incidence of Epstein-Barr virus, cytomegalovirus, and human-herpes virus-6 reactivations in critically ill patients with COVID-19. *Infect Dis Now* **51**, 296–299 (2021).
19. Su, Y. *et al.* Multiple early factors anticipate post-acute COVID-19 sequelae. *Cell* **185**, 881-895.e20 (2022).
20. Gold, J. E., Okyay, R. A., Licht, W. E. & Hurley, D. J. Investigation of Long COVID Prevalence and Its Relationship to Epstein-Barr Virus Reactivation. *Pathogens* **10**, (2021).
21. Yao, Q. Y., Rickinson, A. B. & Epstein, M. A. A re-examination of75psteinstein-barr virus carrier state in healthy seropositive individuals. *Int J Cancer* **35**, 35–42 (1985).
22. Plotkin, S. A. Correlates of Protection Induced by Vaccination. *Clinical and Vaccine Immunology* **17**, 1055–1065 (2010).
23. Earle, K. A. *et al.* Evidence for antibody as a protective correlate for COVID-19 vaccines. *Vaccine* **39**, 4423–4428 (2021).
24. Haan, K. M., Kyeong Lee, S. & Longnecker, R. Different Functional Domains in the Cytoplasmic Tail of Glycoprotein B Are Involved in Epstein–Barr Virus-Induced Membrane Fusion. *Virology* **290**, 106–114 (2001).
25. Kirschner, A. N., Omerović, J., Popov, B., Longnecker, R. & Jardetzky, T. S. Soluble Epstein-Barr Virus Glycoproteins gH, gL, and gp42 Form a 1:1:1 Stable Complex That Acts Like Soluble gp42 in B-Cell Fusion but Not in Epithelial Cell Fusion. *J Virol* **80**, 9444–9454 (2006).
26. Bu, W. *et al.* Immunization with Components of the Viral Fusion Apparatus Elicits Antibodies That Neutralize Epstein-Barr Virus in B Cells and Epithelial Cells. *Immunity* **50**, 1305-1316.e6 (2019).
27. Chen, W.-H. *et al.* Epstein-Barr virus gH/gL has multiple sites of vulnerability for virus neutralization and fusion inhibition. *Immunity* **55**, 2135-2148.e6 (2022).

28. Snijder, J. *et al.* An Antibody Targeting the Fusion Machinery Neutralizes Dual-Tropic Infection and Defines a Site of Vulnerability on Epstein-Barr Virus. *Immunity* **48**, 799-811.e9 (2018).
29. Zhu, Q.-Y. *et al.* A potent and protective human neutralizing antibody targeting a novel vulnerable site of Epstein-Barr virus. *Nat Commun* **12**, 6624 (2021).
30. Singh, S. *et al.* Neutralizing Antibodies Protect against Oral Transmission of Lymphocryptovirus. *Cell Rep Med* **1**, 100033 (2020).
31. Moghaddam, A. *et al.* An Animal Model for Acute and Persistent Epstein-Barr Virus Infection. *Science (1979)* **276**, 2030–2033 (1997).
32. Carville, A. & Mansfield, K. G. Comparative pathobiology of macaque lymphocryptoviruses. *Comp Med* **58**, 57–67 (2008).
33. Rivailler, P., Jiang, H., Cho, Y., Quink, C. & Wang, F. Complete nucleotide sequence of the rhesus lymphocryptovirus: genetic validation for an Epstein-Barr virus animal model. *J Virol* **76**, 421–6 (2002).
34. Rivailler, P. *et al.* Experimental rhesus lymphocryptovirus infection in immunosuppressed macaques: an animal model for Epstein-Barr virus pathogenesis in the immunosuppressed host. *Blood* **104**, 1482–9 (2004).
35. Mühe, J. & Wang, F. Non-human Primate Lymphocryptoviruses: Past, Present, and Future. *Curr Top Microbiol Immunol* **391**, 385–405 (2015).
36. Sashihara, J. *et al.* Soluble Rhesus Lymphocryptovirus gp350 Protects against Infection and Reduces Viral Loads in Animals that Become Infected with Virus after Challenge. *PLoS Pathog* **7**, e1002308 (2011).
37. Cui, X. *et al.* Immunization with Epstein–Barr Virus Core Fusion Machinery Envelope Proteins Elicit High Titers of Neutralizing Activities and Protect Humanized Mice from Lethal Dose EBV Challenge. *Vaccines (Basel)* **9**, 285 (2021).
38. Malhi, H. *et al.* Immunization with a self-assembling nanoparticle vaccine displaying EBV gH/gL protects humanized mice against lethal viral challenge. *Cell Rep Med* **3**, 100658 (2022).
39. Wei, C.-J. *et al.* A bivalent Epstein-Barr virus vaccine induces neutralizing antibodies that block infection and confer immunity in humanized mice. *Sci Transl Med* **14**, eabf3685 (2022).
40. Silva, M. *et al.* A particulate saponin/TLR agonist vaccine adjuvant alters lymph flow and modulates adaptive immunity. *Sci Immunol* **6**, eabf1152 (2021).
41. Rao, P., Jiang, H. & Wang, F. Cloning of the rhesus lymphocryptovirus viral capsid antigen and Epstein-Barr virus-encoded small RNA homologues and use in diagnosis of acute and persistent infections. *J Clin Microbiol* **38**, 3219–25 (2000).
42. Kanekiyo, M. *et al.* Rational Design of an Epstein-Barr Virus Vaccine Targeting the Receptor-Binding Site. *Cell* **162**, 1090–100 (2015).
43. Silva, M. *et al.* A particulate saponin/TLR agonist vaccine adjuvant alters lymph flow and modulates adaptive immunity. *Sci Immunol* **6**, eabf1152 (2021).
44. Mühe, J. *et al.* Neutralizing antibodies against Epstein-Barr virus infection of B cells can protect from oral viral challenge in the rhesus macaque animal model. *Cell Rep Med* **2**, 100352 (2021).
45. Wu, L. & Hutt-Fletcher, L. M. Compatibility of the gH homologues of Epstein–Barr virus and related lymphocryptoviruses. *Journal of General Virology* **88**, 2129–2136 (2007).
46. Omerović, J. & Longnecker, R. Functional homology of gHs and gLs from EBV-related γ-herpesviruses for EBV-induced membrane fusion. *Virology* **365**, 157–165 (2007).
47. McShane, M. P. & Longnecker, R. Analysis of Fusion Using a Virus-Free Cell Fusion Assay. in *Methods in Molecular Biology* vol. 292 187–195 (Humana Press, New Jersey, 2005).

48. Bianchi, M. *et al.* Electron-Microscopy-Based Epitope Mapping Defines Specificities of Polyclonal Antibodies Elicited during HIV-1 BG505 Envelope Trimer Immunization. *Immunity* **49**, 288-300.e8 (2018).
49. Molesworth, S. J., Lake, C. M., Borza, C. M., Turk, S. M. & Hutt-Fletcher, L. M. Epstein-Barr virus gH is essential for penetration of B cells but also plays a role in attachment of virus to epithelial cells. *J Virol* **74**, 6324–32 (2000).
50. Oba, D. E. & Hutt-Fletcher, L. M. Induction of antibodies to the Epstein-Barr virus glycoprotein gp85 with a synthetic peptide corresponding to a sequence in the BXLF2 open reading frame. *J Virol* **62**, 1108–14 (1988).
51. Rickinson, A. B. & Moss, D. J. Human cytotoxic T lymphocyte responses to Epstein-Barr virus infection. *Annu Rev Immunol* **15**, 405–31 (1997).
52. van Zyl, D. G. *et al.* Immunogenic particles with a broad antigenic spectrum stimulate cytolytic T cells and offer increased protection against EBV infection ex vivo and in mice. *PLoS Pathog* **14**, e1007464 (2018).
53. Crotty, S. T Follicular Helper Cell Biology: A Decade of Discovery and Diseases. *Immunity* **50**, 1132–1148 (2019).
54. Nikitin, P. A. *et al.* An ATM/Chk2-Mediated DNA Damage-Responsive Signaling Pathway Suppresses Epstein-Barr Virus Transformation of Primary Human B Cells. *Cell Host Microbe* **8**, 510–522 (2010).
55. Delecluse, H.-J., Hilsendegen, T., Pich, D., Zeidler, R. & Hammerschmidt, W. Propagation and recovery of intact, infectious Epstein–Barr virus from prokaryotic to human cells. *Proceedings of the National Academy of Sciences* **95**, 8245–8250 (1998).
56. Neuhierl, B., Feederle, R., Hammerschmidt, W. & Delecluse, H. J. Glycoprotein gp110 of Epstein–Barr virus determines viral tropism and efficiency of infection. *Proceedings of the National Academy of Sciences* **99**, 15036–15041 (2002).
57. Sashihara, J., Burbelo, P. D., Savoldo, B., Pierson, T. C. & Cohen, J. I. Human antibody titers to Epstein–Barr Virus (EBV) gp350 correlate with neutralization of infectivity better than antibody titers to EBV gp42 using a rapid flow cytometry-based EBV neutralization assay. *Virology* **391**, 249–256 (2009).
58. Plate, A. E., Smajlović, J., Jardetzky, T. S. & Longnecker, R. Functional Analysis of Glycoprotein L (gL) from Rhesus Lymphocryptovirus in Epstein-Barr Virus-Mediated Cell Fusion Indicates a Direct Role of gL in gB-Induced Membrane Fusion. *J Virol* **83**, 7678–7689 (2009).
59. Okuma, K., Nakamura, M., Nakano, S., Niho, Y. & Matsuura, Y. Host Range of Human T-Cell Leukemia Virus Type I Analyzed by a Cell Fusion-Dependent Reporter Gene Activation Assay. *Virology* **254**, 235–244 (1999).
60. Punjani, A., Rubinstein, J. L., Fleet, D. J. & Brubaker, M. A. cryoSPARC: algorithms for rapid unsupervised cryo-EM structure determination. *Nat Methods* **14**, 290–296 (2017).

Chapter 3. An Alphavirus Replicon Vaccine Encoding gH/gL Elicits Neutralizing Antibodies That Protect Against EBV Challenge In Humanized Mice.

This work is under review at Science Translational Medicine as of Feb 01, 2024

Authors:
Kristina R. Edwards[1,2*], Harman Malhi[1,3*], Karina Schmidt[1], Leah J. Homad[1], Amelia R. Davis[1], Crystal B. Chhan[1,2], Samuel C. Scharffenberger[1,3], Karen Gaffney[4], Troy Hinkley[4], Nicole B. Potchen[1,2], Jing Yang Wang[5,6], Jason Price[7], James Olson[7], Neil P. King[5,6], Jennifer M. Lund[1,2], Zoe Moodie[1], Jesse H. Erasmus[4], Andrew T. McGuire[1,2,3#]

[1]Vaccine and Infectious Disease Division, Fred Hutchinson Cancer Center, Seattle WA, USA.
[2]Department of Global Health, University of Washington, Seattle, WA, USA.
[3]Department of Laboratory Medicine and Pathology, University of Washington, Seattle WA, USA.
[4]HDT Bio, Seattle WA, USA.
[5]Department of Biochemistry, University of Washington, Seattle, WA USA
[6]Institute for Protein Design, University of Washington, Seattle, WA USA
[7]Ben Towne Center for Childhood Cancer Research, Seattle Children's Research Institute, Seattle, WA, USA
[#]Corresponding author. Email: amcguire@fredhutch.org.

3.1 Abstract

Epstein-Barr virus (EBV) is associated with several malignancies, neurodegenerative disorders and is the causative agent of infectious mononucleosis. A vaccine that prevents EBV-driven morbidity and mortality remains an unmet need. EBV is orally transmitted, infecting both B cells and epithelial cells. The viral gH/gL glycoprotein complex is essential for infectivity irrespective of cell type. Neutralizing antibodies targeting gH/gL can prevent infection *in vitro* and *in vivo*, implicating gH/gL as a relevant immunogen for vaccine development. We developed and optimized the delivery of several alphavirus-derived replicon RNA (repRNA) vaccine candidates encoding gH/gL delivered by a cationic nanocarrier termed LION™. The lead candidate elicited high-titers of neutralizing antibodies that persisted for at least 8 months, and a vaccine-specific $CD8^+$ T cell response. Transfer of vaccine-elicited IgG protected humanized mice from EBV-driven tumor formation and death following high-dose viral challenge. These data demonstrate that LION/repRNA-gH/gL is an ideal candidate vaccine for preventing EBV infection and/or related malignancies in humans.

3.2 Introduction:

EBV is a ubiquitous gamma herpesvirus[1]. While primary infection typically is asymptomatic, it can result in infectious mononucleosis[2,3]. EBV was the first virus to be shown to be oncogenic in humans and is associated with approximately 358,000 new cases of cancer resulting in 209,000 deaths each year[4,5]. Beyond its contribution to the global cancer burden, EBV has been linked to autoimmune conditions such as rheumatoid arthritis and multiple sclerosis[6–10]. A successful vaccine against EBV that can prevent infection and/or reduce

disease remains an unmet need that would reduce global morbidity and mortality linked to these conditions.

Several vaccine candidates are in various stages of preclinical and clinical development, most of which target surface glycoproteins involved in attachment and entry[11]. EBV primarily infects B cells and epithelial cells and has distinct attachment and entry pathways for each[12]. The viral fusion machinery gH, gL, and gB are critical for infection irrespective of cell type[12,13]. gH and gL form a 1:1 heterodimeric complex that acts as a regulator of membrane fusion. Upon binding one or more host cell surface receptors gH/gL relays a triggering signal to the fusogen gB[13,14]. Multiple neutralizing monoclonal antibodies (mAbs) have been isolated against the gH/gL glycoprotein complex that can block viral entry into both epithelial cells and B cells *in vitro*[15–18]. The details of the interactions between gH/gL and cell surface receptors, and the molecular mechanisms by which it activates gB are poorly understood. Consequently, the mechanisms by which neutralizing mAbs against gH/gL prevent membrane fusion are not known. Nevertheless, passive transfer of gH/gL mAbs can protect against viral challenge in animal models of EBV infection[18,19]. Collectively these findings indicate that the gH/gL glycoprotein complex is a strong candidate for vaccine development that harbors several neutralizing epitopes[16–18]. To this end, our group and others have developed protein nanoparticles displaying EBV gH/gL that elicit high titers binding and neutralizing antibodies that protect against lethal EBV challenge in mice with humanized immune systems[15,20–22].

As an alternative to protein-based vaccines, we sought to leverage advances made in nucleic acid-based delivery to deliver gH/gL immunogens. An attenuated variant of the Venezuelan equine encephalitis virus, TC-83 strain, has been used to generate self-amplifying replicon RNA (repRNA) vaccines where the viral RNA replication complex is intact, but the structural genes are replaced with a gene of interest. Delivery of repRNA into cells promotes

synthesis of antigen-encoding RNA that self-adjuvants by triggering innate immune responses and promoting antigen cross-priming which enhances humoral and cellular immune responses compared to conventional mRNA. Delivery of repRNAs encoding diverse viral antigens with a cationic nanocarrier (termed LION) has been shown to elicit high titers of antibodies as well as T cell responses in several preclinical animal models[23–27]. Moreover, this platform has led to the development of an effective SARS-CoV-2 vaccine licensed for emergency clinical use[28,29]. LION formulated repRNA offers significant advantages over other RNA vaccine platforms, including limiting the dissemination of RNA to the injection site which induces antigen-specific adaptive immunity while avoiding systemic inflammation[23].

Here, we evaluated the ability of several LION/repRNA encoded gH/gL derivatives to elicit binding and neutralizing antibodies as well as T cell responses. After optimization of the construct and dosing regimen, polyclonal antibodies were evaluated for their ability to prevent EBV infection in a humanized mouse model. Passive transfer of antibodies elicited by vaccination with LION/repRNA encoding full-length gH/gL prior to challenge with a high dose of EBV provided protection from lethality. LION/repRNA-elicited antibodies also reduced viral load, prevented splenomegaly, and splenic tumor formation. In contrast, mice given IgG elicited by a more conventional gH/gL protein subunit vaccine became viremic, developed splenic tumors, and in some cases required euthanasia. In addition to eliciting superior humoral responses, the repRNA encoded gH/gL elicited a higher frequency of vaccine specific $CD8^+$ T cell responses. Collectively, these results demonstrate that LION/repRNA encoded gH/gL is an attractive alternative to recombinant subunit vaccines capable of eliciting high titers of protective antibodies that could be augmented by cellular immune responses.

3.3 Results:

3.3.1 Initial characterization:

To enable co-delivery of both gH and gL on a single repRNA, we designed two constructs. The first encodes gL and then full length gH (including the transmembrane and cytoplasmic domains) in tandem separated by a ribosomal skipping P2A peptide (Genbank MT559572.1) and the second encodes gH and then gL separated by P2A (Fig. 1A). Both constructs included the native signal peptide and a furin cleavage site upstream of P2A to facilitate removal of residual P2A residues on the N-terminal protein following translation. This tandem expression strategy ensures that both polypeptides are produced in each cell and promotes proper expression and co-folding of gH/gL. mRNA from each repRNA construct were transcribed and capped *in vitro* via T7 polymerase and vaccinia capping enzymes, respectively. repRNAs were formulated with LION and delivered to groups of 4 C57BL/6 mice at weeks 0 and 4. C57BL/6 mice were used for comparison with previous studies in the lab[20]. Blood was collected at the time of the first immunization and 2 weeks after each immunization for serological analyses (Fig. 1B). Both constructs were immunogenic and elicited reciprocal endpoint binding titers on the order of $1X10^4$ as soon as 2 weeks after the first immunization that reached $1X10^5$ by week 6 (Fig. 1C). Both constructs also elicited low, but detectable titers of antibodies that could neutralize EBV infection of B cells by week 2 that were not boosted by a second immunization at week 4 (Fig. 1D).

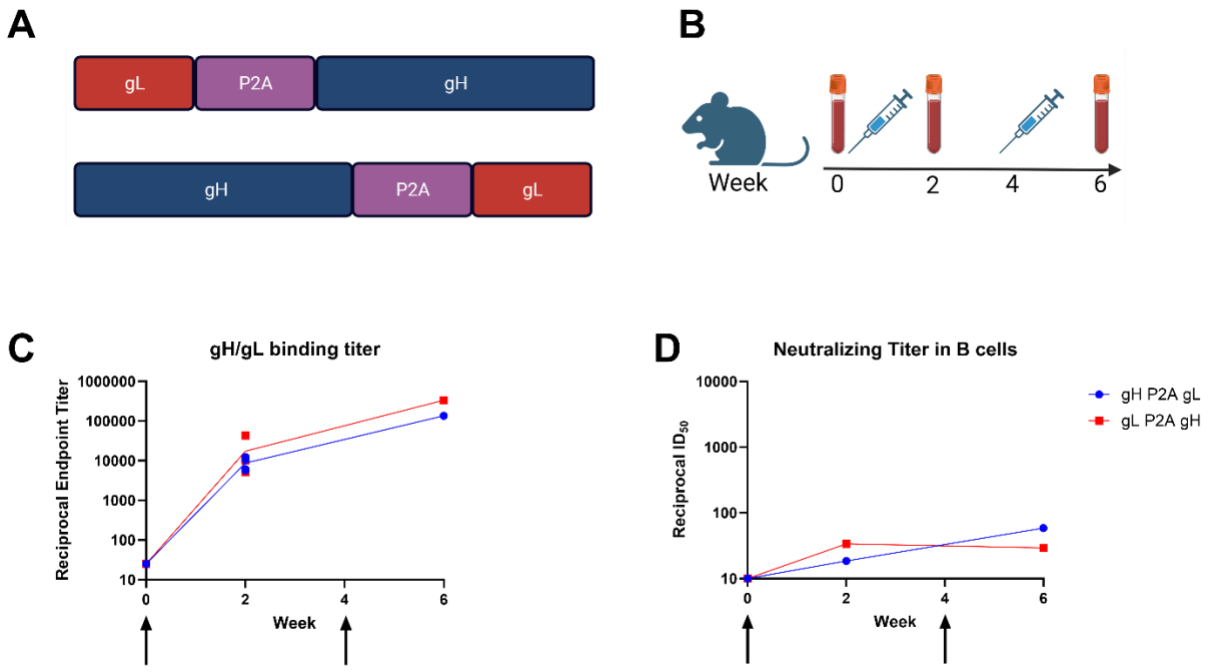

Figure 1: Development and immunogenicity studies of repRNAs encoding EBV gH/gL. (**A**) Schematic depicting the two repRNA inserts encoding gH and gL separated by a P2A peptide. (**B**) Immunization schedule in C57BL/6 mice. (**C**) Reciprocal endpoint gH/gL binding titers were measured in plasma by ELISA. Each dot represents an individual mouse (n=4) at weeks 0 and 2, or pooled plasma from the same 4 mice at week 6. The lines connect the mean (or value of pooled sera) across the tested timepoints. (**D**) The ability of plasma pooled from the 4 mice in (**C**) to neutralize EBV infection of B cells reported as the reciprocal dilution to reduce infectivity by 50% (ID_{50}). The lines connect the mean (or value of pooled sera) across the tested timepoints in **C** and **D**. Arrows indicate time of immunization.

3.3.2 *Dose optimization for LION/repRNA gH/gL vaccination*

Given that a second immunization did not boost the neutralizing titers in our pilot experiments, we sought to optimize time and dosing schedule. For this analysis we selected the gL-P2A-gH construct since it elicited slightly higher binding titers than the inverse construct (Fig. 1C).

Groups of 4 C57BL/6 mice received 0.1 μg, 1 μg, and 10 μg of LION/repRNA gH/gL at week 0. The animals were bled biweekly and the gH/gL-binding endpoint titers were monitored in near-real time. Following the priming immunization, we observed a dose-dependent increase in the binding titers until week 6 followed by a slight waning by week 8 (Fig. 2A and Table S1), at which point they received a second immunization with the same dose. The endpoint binding titers were boosted in the animals that received a second 10 μg dose. A slight boost was also observed in the animals that received a 1 μg dose, but not in the animals that received a 0.1 μg second dose (Fig. 2A).

We examined the ability of the immune plasma to neutralize EBV infection of epithelial and B cells *in vitro*. The trends observed in the endpoint binding titer kinetics were mirrored in the neutralizing titers against epithelial cell infection. Following the prime, there was a dose-dependent increase in epithelial-cell neutralizing titers until week 6 that waned slightly by week 8 and were boosted by a second dose in the 10 μg and 1 μg, but not the 0.1 μg, groups (Fig. 2B).

Only the 10 μg dose elicited antibodies capable of neutralizing B cell infection after a single immunization (Fig. 2C). Two weeks after a second immunization with a 10 μg dose, these titers were boosted over 10-fold to a reciprocal half-maximal inhibitory dilution (ID_{50}) near $1x10^3$. Weak transient neutralizing titers were observed 6 weeks after a second dose with 1 μg of

LION/repRNA gH/gL, while the 0.1 μg dose failed to elicit B-cell neutralizing antibodies at any timepoint (Fig. 2C).

In our initial experiments, all animals were euthanized at week 18. To measure durability of the antibody responses, a second cohort of animals (n=4) received 10 μg of LION/repRNA at weeks 0 and 8 and the antibody responses were monitored for a total of 32 weeks. We observed that the binding and neutralizing titers were maintained during this time (Fig. 2A-C). Varying the dose of the prime and boost can impact vaccine responses. For example, administration of a fractional dose boost in a malaria vaccine trial elicited superior antibody responses compared to a higher dose boost[30]. Conversely a low dose prime followed by a higher dose boost regimen of a SARS-CoV-2 vaccine showed greater immunogenicity and efficacy than a high dose prime/boost regimen[31,32]. To explore whether varying the prime and boost dose affected the immunogenicity of LION/repRNA gH/gL, we evaluated two de-escalating dose regimens, 10 μg/1 μg and 10 μg/0.1 μg, and one escalating dose 0.1 μg/10 μg regimen. Animals that received a 10 μg prime had comparable binding and B cell neutralizing titers as the original cohort of mice from the 10 μg/10 μg group at week 8 (Fig. 2A and D, C and F), while the epithelial cell neutralizing titers were lower in the mice in the 10 μg/1 μg and 10 μg/0.1 μg at week 8 (Fig. 2B and E and Table S1. None of the binding or neutralizing titers were boosted when the second dose was lower (Fig. 2D, E, F, dark and light purple curves). After the initial dose, the 0.1 μg/10 μg group had low gH/gL binding and epithelial cell neutralizing titers (Fig. 2D and E, light blue curve), but no measurable B cell neutralizing titers by week 8 (Fig. 2F, light blue curve). However, after the boost immunization of 10 μg at week 8, there were slightly higher gH/gL binding titers and epithelial cell neutralizing titers than the other mixed dose groups (Fig. 2D and E, light blue curve), but similar B cell neutralizing titers (Fig. 2F light blue curve and Table S1). Across all prime/boost regimens evaluated, a 10 μg prime followed by a 10 μg boost elicited superior binding and neutralizing titers (Table S1).

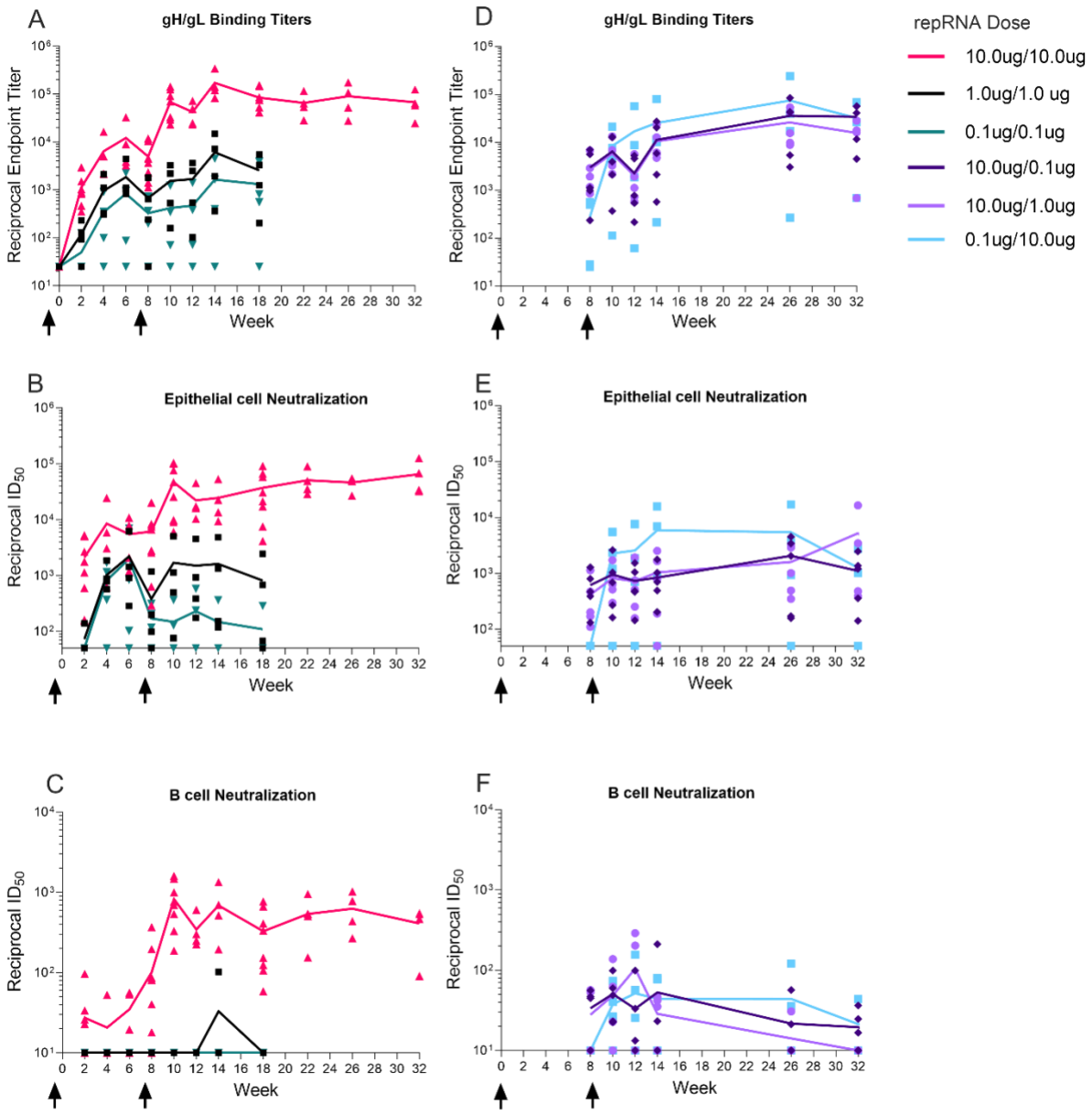

Figure 2: Dose optimization of gH/gL repRNA immunizations.

(**A**) Kinetics of reciprocal gH/gL endpoint binding titers. (**B**-**C**) half-maximal neutralizing titers against EBV infection of epithelial (**B**) or B cells (**C**) following equal doses of repRNA encoded gH/gL delivered at weeks 0 and 8 as indicated. The binding (**D**) and EBV neutralizing titers measured in epithelial (**E**) and B cell (**F**) infection assays following two unequal doses of repRNA encoded gH/gL delivered at weeks 0 and 8 as indicated. Each data point represents an

individual mouse at each timepoint (n=4 per group for equal 0.1 and 1ug prime/boost doses, n=8 for equal 10ug prime/boost doses, and n=5 per group for mixed dose prime/boost,) and lines connect the means. Arrows indicate the time of immunization. See Table S1 for statistical comparisons.

		0	2	4	6	8	10	12	14	18	26	32
ELISA	1ug/1ug	ND	**	*	n.s.	*	**	*	*	**	NA	NA
	0.1ug/ 0.1ug	ND	***	**	**	***	***	**	**	***	NA	NA
	10ug/ 0.1ug	ND	NA	NA	NA	n.s	**	*	*	NA	n.s.	n.s.
	10ug/ 1ug	ND	NA	NA	NA	n.s	**	*	*	NA	n.s.	n.s.
	0.1ug/ 10ug	ND	NA	NA	NA	**	**	n.s.	*	NA	n.s.	n.s.
		0	**2**	**4**	**6**	**8**	**10**	**12**	**14**	**18**	**26**	**32**
Epithelial Cell Neutralization	1ug/1ug	ND	**	n.s.	n.s.	*	**	*	*	**	NA	NA
	0.1ug/ 0.1ug	ND	**	n.s.	n.s.	**	**	*	*	**	NA	NA
	10ug/ 0.1ug	ND	NA	NA	NA	*	**	*	*	NA	*	*
	10ug/ 1ug	ND	NA	NA	NA	*	**	*	*	NA	*	*
	0.1ug/ 10ug	ND	NA	NA	NA	**	**	*	n.s.	NA	*	n.s.
		0	**2**	**4**	**6**	**8**	**10**	**12**	**14**	**18**	**26**	**32**
B Cell Neutralization	1ug/1ug	ND	n.s.	n.s.	n.s.	*	**	*	*	**	NA	NA
	0.1ug/ 0.1ug	ND	n.s.	n.s.	n.s.	*	**	*	*	**	NA	NA
	10ug/ 0.1ug	ND	NA	NA	NA	n.s.	**	n.s.	*	NA	*	*
	10ug/ 1ug	ND	NA	NA	NA	n.s.	**	n.s.	*	NA	*	*
	0.1ug/ 10ug	ND	NA	NA	NA	*	**	*	*	NA	*	n.s.

Table S1: Statistical differences from data shown in Figure 2.

Titers at individual timepoints were compared to the 10 ug/10 ug repRNA group and summarized above. Significance was calculated by Mann-Whitney test. ND – Not Done, NA – Not Applicable, n.s. – $p > 0.05$, * – $p \leq 0.05$, ** – $p \leq 0.01$, and *** – $p \leq 0.001$.

3.3.3 *repRNA encoding membrane anchored gH/gL monomer is more immunogenic than the gH/gL ectodomain*

After determining an optimal dose regimen for LION/repRNA gH/gL vaccination, we next compared the immunogenicity of a secreted gH/gL ectodomain with full-length gH/gL. To produce the ectodomain, gH was truncated at amino acid 679 in the gL-P2A-gH construct. 10 µg of LION/repRNA encoding the ectodomain was delivered at weeks 0 and 8, and plasma samples were collected through week 14. After the first immunization, the ectodomain elicited gH/gL binding titers that were nearly identical to full length gH/gL (Fig. 3A), however the epithelial cell neutralizing antibody titers were ~10-fold lower than full length gH/gL, and B cell neutralizing titers were not elicited by week 8 (Fig. 3B and C). A second immunization with the ectodomain boosted the epithelial cell neutralizing titers to similar levels achieved with full-length gH/gL, but the B cell neutralizing titers were ~5-fold lower and the neutralizing titers decayed more rapidly in both assays (Fig. 3A-C). We sought to discern whether the observed differences in neutralizing activity were due to differential epitope recognition between the plasma antibodies elicited by these two constructs. Week 12 plasma from both groups was pooled and evaluated for its ability to compete with the binding of mAbs with defined epitopes on gH/gL, including AMMO1[17], 769B10[15], E1D1[33] and CL40[34], CL59[34], 1D8[18], and 770F7[16]. With the exception of E1D1, which binds an epitope entirely on gL[35], plasma elicited by full length gH/gL competed the binding of all mAbs more potently than plasma elicited by the gH/gL ectodomain (Fig. 3D-J). Collectively, these data demonstrate that full length LION/repRNA gH/gL elicits a qualitatively different antibody response than the LION/repRNA gH/gL ectodomain resulting in higher neutralizing titers.

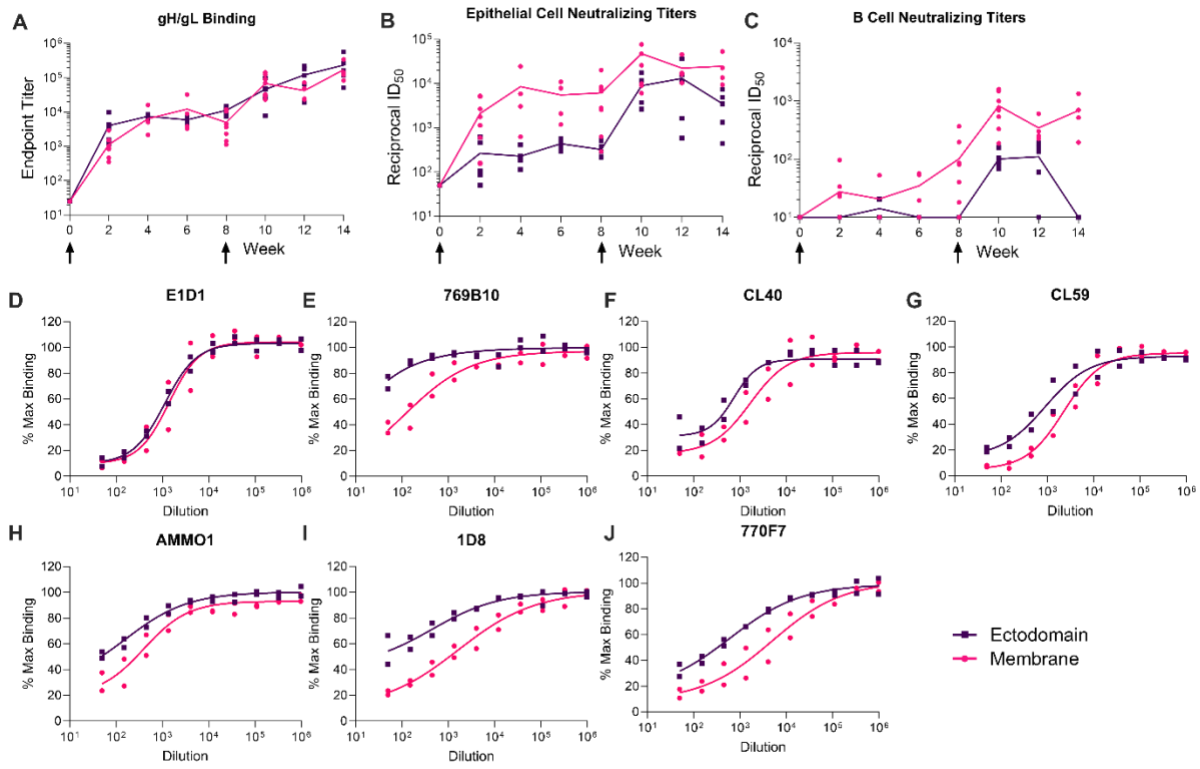

Figure 3: Full-length gH/gL delivered by LION/repRNA elicits higher neutralizing titers than the gH/gL ectodomain.

(**A**) Reciprocal gH/gL endpoint binding titers elicited by full length and gH/gL ectodomain measured by ELISA as indicated. (**B-C**) EBV neutralizing titers elicited by full length and gH/gL ectodomain repRNA immunization were measured in epithelial cell (**B**), or B cell (**C**) infection assays. Titers from two immunizations with 10ug full-length gH/gL (from Figure 2) are shown for comparison in **A**-**C**. Each dot represents an individual mouse at each timepoint (n=8 for full length gH/gL and n=5 for gH/gL ectodomain) and the lines connect the means. The arrows indicate the time of immunization. Asterisks denote a statistically significant difference between the two groups at a given time point determined using a Mann-Whitney test where * indicates $p \leq 0.05$ and ** indicates $p \leq 0.01$. (**D-J**) immune sera from mice vaccinated with full length and gH/gL ectodomain repRNA were evaluated for their ability to compete for binding to EBV gH/gL with the indicated monoclonal antibodies by competitive ELISA. Each dot represents a technical replicate with a line connecting the mean.

3.3.4. *Membrane retained gH/gL monomer repRNA immunization is more immunogenic than secreted gH/gL multimers*

We and others have previously showed that multimerization of gH/gL through genetic fusion to self-assembling nanoparticles substantially improves its immunogenicity when delivered as recombinant protein[15,20,21]. Therefore, we evaluated LION/repRNA delivery of multimeric gH/gL. Mice were immunized with 10 µg of LION/repRNA encoding the gH/gL ectodomain presented as different multimeric constructs, a 4-mer, 7-mer, and a 60-mer that we previously developed as protein subunit vaccines[20]. The 4-mer backbone is a computationally designed planar toroid, the 7-mer backbone is derived from the multimerization domain of C4b binding protein from *Gallus gallus*, and the 60-mer backbone is a computationally designed self assembling nanoparticle with icosahedral symmetry[20]. After the first immunization and through week similar gH/gL binding titers were elicited by all constructs (Fig. 4A and Table S2). After the second immunization, the binding titers elicited by the membrane-anchored monomer were comparable to the 4-mer and 7-mer, but higher than all the gH/gL 60-mer (Fig. 4A and Table S2). The differences in the neutralizing titers between the membrane-anchored gH/gL and multimeric constructs were starker. The membrane-anchored monomer elicited higher titers than the multimeric constructs in the B cell and epithelial cell neutralization assays at nearly every timepoint tested from weeks 8-34 (Figs. 4B and C and Table S2).

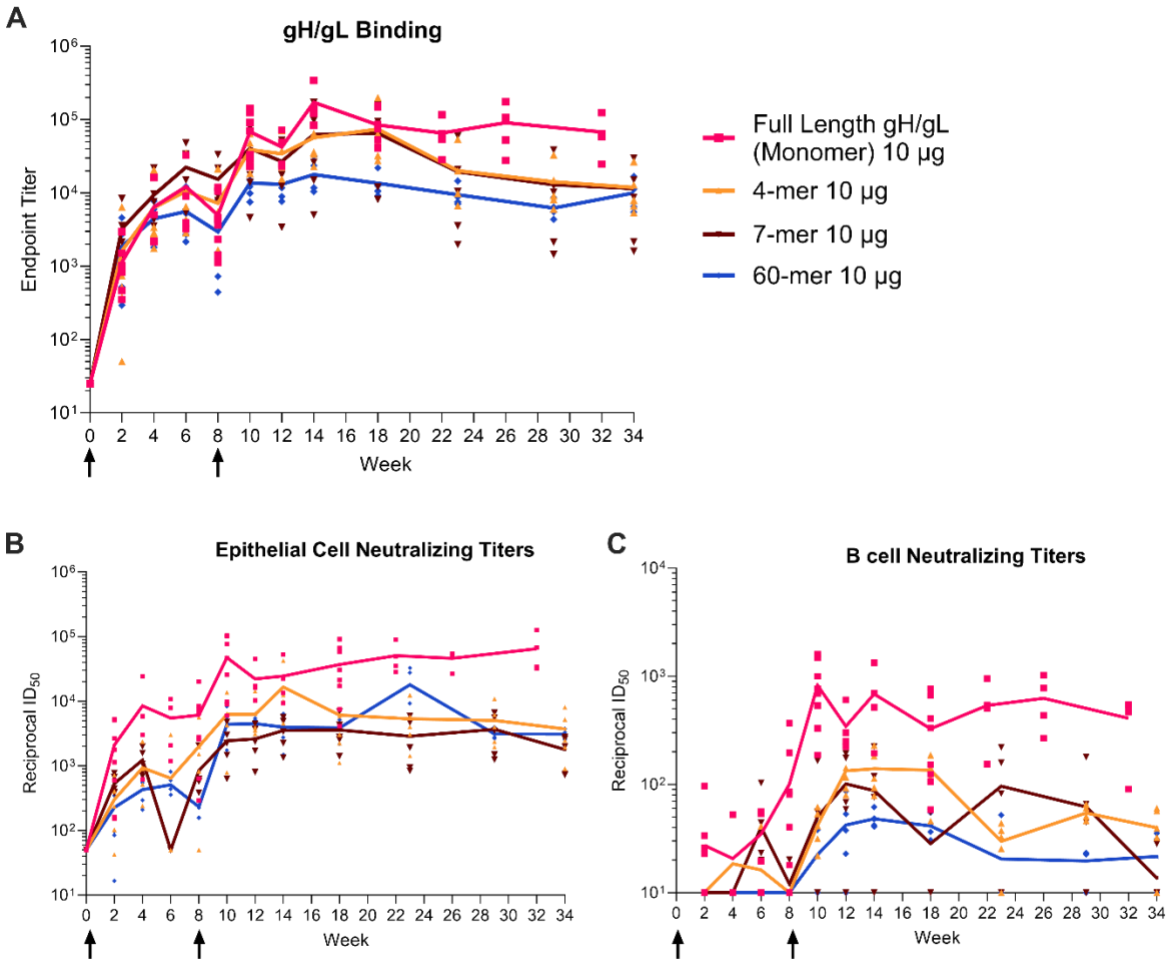

Figure 4: Full-length monomeric gH/gL elicits higher neutralizing titers than gH/gL multimers when delivered by LION/repRNA.

(**A**) Reciprocal endpoint gH/gL binding titers from mice immunized with full-length gH/gL, gH/gL 4-mer, gH/gL 7-mer and gH/gL 60-mer repRNAs were measured by ELISA. (**B**-**C**) EBV neutralizing titers in the serum from the mice in **A** were measured in epithelial (**B**) and B cell (**C**) infection assays. Titers from two immunizations with 10ug full-length gH/gL (from Figure 2) are included for comparison in **A**-**C**. Each dot represents an individual mouse at each timepoint (n=5 per group in multimer construct vaccinations, n=8 for full length gH/gL) and the lines connect the means. The arrows indicate the time of immunization. See Table S2 for statistical comparisons.

		0	2	4	6	8	10	12	14	18	22/23	32/34
ELISA	4-mer	ND	n.s.	n.s.	n.s.	n.s.	n.s.	n.s.	n.s.	n.s.	n.s.	*
	C4b (7-mer)	ND	n.s.	n.s.	n.s.	*	n.s.	n.s.	n.s.	n.s.	n.s.	*
	I3 (60-mer)	ND	n.s.	n.s.	n.s.	n.s.	*	*	*	**	*	*
		0	**2**	**4**	**6**	**8**	**10**	**12**	**14**	**18**	**22/23**	**32/34**
Epithelial Cell Neut.	4-mer 10ug	ND	n.s.	n.s.	*	n.s.	*	*	n.s.	*	*	*
	C4b (7-mer) 10ug	ND	n.s.	n.s.	**	*	**	*	*	**	*	*
	I3 (60-mer) 10ug	ND	*	n.s.	*	**	**	*	*	*	n.s.	*
		0	**2**	**4**	**6**	**8**	**10**	**12**	**14**	**18**	**22/23**	**32/34**
B Cell Neut.	4-mer	ND	n.s.	n.s.	n.s.	*	*	*	*	n.s.	*	*
	C4b (7-mer)	ND	n.s.	n.s.	n.s.	n.s.	*	*	*	**	n.s.	*
	I3 (60-mer)	ND	n.s.	n.s.	*	*	**	*	*	**	*	*

Table S2: Statistical differences from data shown in Figure 4.

Titers at individual timepoints were compared to the 10 ug/10 ug full-length monomer repRNA group and summarized above. Week 22 post-immunization of the 10 ug/10 ug full-length monomer was compared to weeks 23 of the multimer groups, and week 32 compared to week 34. Significance was calculated by Mann-Whitney test. ND – Not Done, n.s. – $p > 0.05$, * – $p \leq 0.05$, ** – $p \leq 0.01$, and *** – $p \leq 0.001$.

3.3.5 *Passive transfer of IgG elicited by LION/repRNA gH/gL protects humanized mice from lethal EBV challenge*

Having established that two 10 μg doses of LION/repRNA-encoded full length gH/gL delivered at weeks 0 and 8 showed favorable immunogenicity, we evaluated whether antibodies elicited by this regimen are protective *in vivo*. To do this, we undertook a passive transfer and challenge experiment in humanized mice. Use of humanized mice as a small animal model of EBV infection is well established[36–41]. In short, highly immunocompromised NOD *scid* gamma mice are irradiated and engrafted with human $CD34^+$ peripheral blood stem cells, which then reconstitute the human hematopoietic compartment in the mouse. This allows for EBV infection of human B cells *in vivo*. Humanized mice generate poor antibody responses[42], therefore it was necessary to passively transfer IgG from immunized C57BL/6 mice prior to EBV challenge. This approach has been previously used to evaluate the efficacy of anti-EBV mAbs and vaccine elicited antibodies[16,18–21].

Twenty-five mice were immunized with 10 μg of LION/repRNA encoding full-length monomeric gH/gL at weeks 0 and 8. To compare this to a more conventional recombinant vaccine with a known response, another group of 25 mice were given two doses of 5 μg of purified monomeric gH/gL ectodomain formulated with Sigma Adjuvant System at weeks 0 and 8 (Fig. 5A). At week 12, mice were euthanized and IgG was harvested from pooled plasma. IgG purified from mice immunized with repRNA showed stronger binding to gH/gL than IgG purified from protein vaccinated mice (Fig. S1).

After verifying successful engraftment of human $CD45^+$ cells and development of $CD19^+$ B cells in humanized mice (Fig. S2), 500 μg of purified total IgG from mice immunized with gH/gL encoded by LION/repRNA or protein was delivered to groups of 4 humanized mice. An additional 5 humanized mice received 500 μg of IgG purified from unimmunized C57BL/6 mice.

The next day, mice were bled to confirm IgG transfer and challenged via retro-orbital injection of 33,000 Raji infectious units of EBV. Five mice that did not receive IgG transfer remained unchallenged and served as an uninfected control group (Fig. 5A). No animals had plasma IgG prior to transfer, but all had similar levels at the time of challenge confirming transfer of equal amounts of IgG in all study animals (Fig. 5B). The LION/repRNA group had higher anti-gH/gL ELISA titers compared to the protein group (Fig. 5C) consistent with the higher activity of the purified IgG (Fig. S1). The gH/gL binding titers in humanized mice at the challenge were comparable, on the order of $1X10^5$, to those elicited by 2 doses of 10ug of LION/repRNA in C57BL/6 mice (compare Fig. 2A and Fig. 5C).

Starting 2 weeks post challenge and continuing weekly for 10 weeks, mice were weighed three times a week (Fig. S3) and bled weekly. To monitor for infection, DNA was extracted from whole blood and qPCR was used to measure viral DNA. At week 12, or sooner if humane endpoints were met, mice were euthanized and spleens were examined for splenomegaly, the presence of viral DNA and splenomegaly (Figs. 5I-J and S4).

Following challenge, 100% of the mice in the uninfected control group survived (Fig. 5D) and lacked detectable viral DNA in the blood (Fig. 5E) and the spleen (Fig. 5I). In contrast, none of the mice in the group that received control IgG survived beyond 8 weeks (Fig. 5D). All control IgG receiving mice were viremic (Fig. 5F) and had high levels of viral DNA in the spleen (Fig. 5I). These mice also developed splenomegaly (Fig. 5J) and had splenic tumors (Fig. S4). Three of the mice in the protein group developed viremia by week 8 (Fig. 5G) and two required euthanasia at weeks 8 and 9 (Fig. 5D), and the other three survived until week 12 (60% survival). Four of five mice in the protein group had elevated levels of viral DNA in the spleen (Fig. 5I), three developed splenomegaly (Fig. 5J), and two developed splenic tumors (Fig. S4). In the repRNA group, only one mouse exhibited transient low-level viremia (Fig. 5H) and 100%

of the mice survived for 12 weeks following challenge (Fig. 5D). At week 12, the spleen weights were comparable to the uninfected controls (Fig. 5J) and free of viral DNA (Fig. 5I) and tumors (Fig. S4).

In sum, immunization with gH/gL repRNA elicited higher gH/gL IgG titers that provided superior protection from lethal EBV challenge, as compared to a conventional protein-based vaccine formulation in a humanized mouse model.

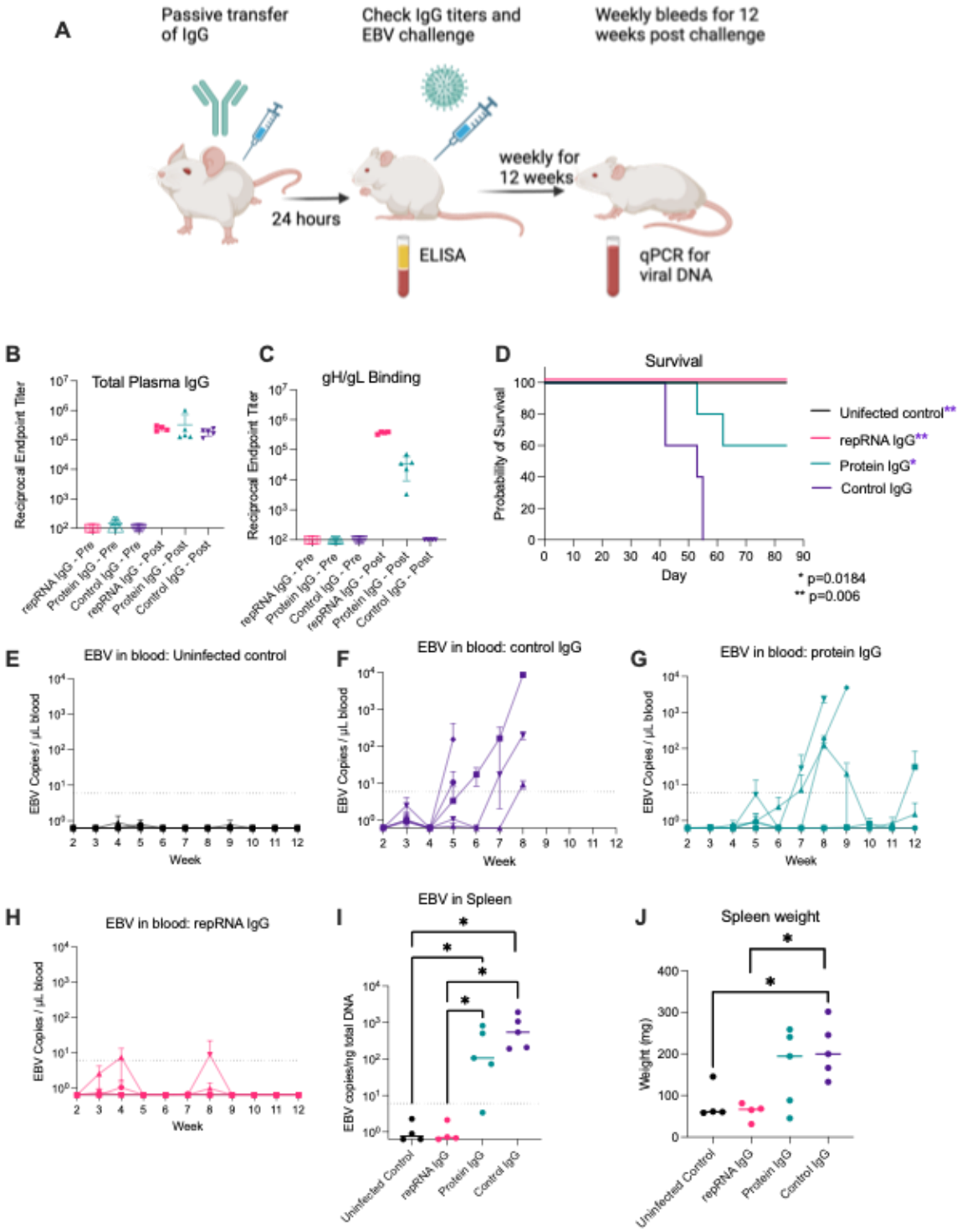

Figure 5: IgG elicited by LION/repRNA- gH/gL protects humanized mice from lethal EBV challenge.

(**A**) 0.5 mg IgG harvested from pooled plasma from gH/gL protein immunized mice, LION/repRNA-gH/gL immunized mice, control IgG from naïve animals, or PBS was delivered to humanized mice via intraperitoneal injection. 24 hr after transfer, mice were bled to ensure antibody transfer and infected with 33,000 Raji-infectious units of EBV. Mice were then bled weekly starting at week 2 post challenge to monitor for signs of infection, all mice were euthanized at week 12 or earlier if humane endpoints were met. (**B**-**C**) Reciprocal endpoint titers of total IgG (**B**) and gH/gL binding (**C**) were measured 1 day post-transfer by ELISA. (**D**) Survival of mice after challenge. Significant differences between each group and the control IgG were determined using a log-rank Mantel-Cox test. (**E**-**H**) Viral DNA in the peripheral blood of negative control mice as well as mice that received IgG from repRNA immunized, protein immunized, and control IgG groups was measured by qPCR as indicated. (**I**) Viral DNA copy number was quantified in splenic DNA extracts at necropsy. Each dot represents an individual mouse, the bar represents the median copy number, and the dashed line indicates the limit of detection. (**J**) Spleen weights at necropsy, each dot represents an individual mouse, and bar represents the median weight. Significant differences between spleen EBV (**I**) and spleen weights (**J**) between all pairs of groups were assessed using Mann-Whitney tests with $*$ denoting $p \leq 0.05$.

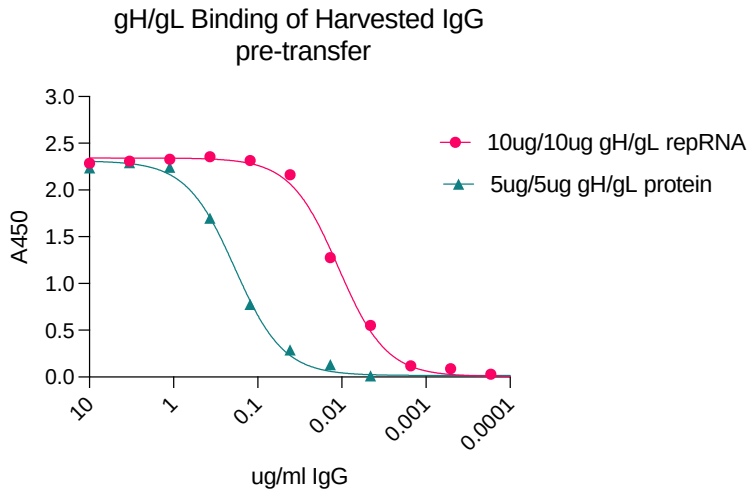

Figure S1: gH/gL binding of purified IgG after two immunizations with full length gH/gL encoded by repRNA or the recombinant gH/gL ectodomain as indicated.

The purified IgG was used for transfer experiments in Figure 5.

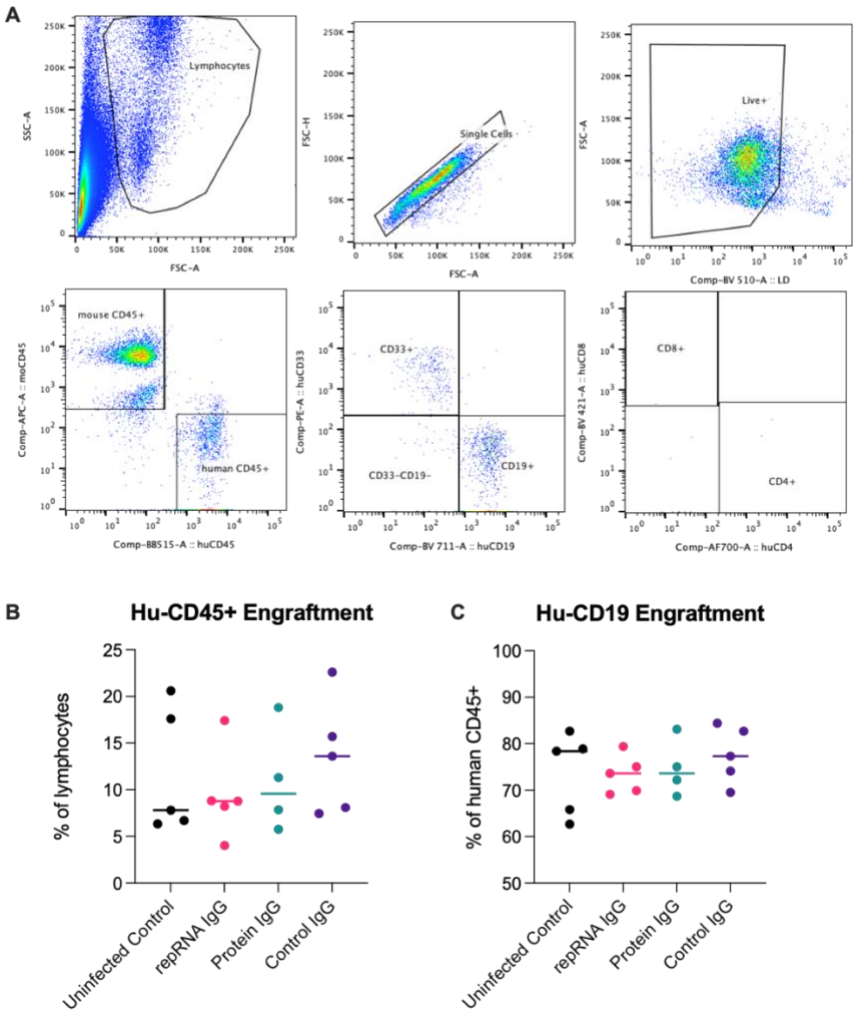

Figure S2: Cell engraftment in humanized mice.

(**A**) Gating strategy to determine human CD45^{+} cells within live single cell lymphocyte population as well as CD19^{+} B cells within huCD45^{+} cells. (**B**-**C**) Frequency of human CD45+ lymphocytes (**B**) and human CD19+ B cells (**C**) in the mice assigned to the various treatment groups.

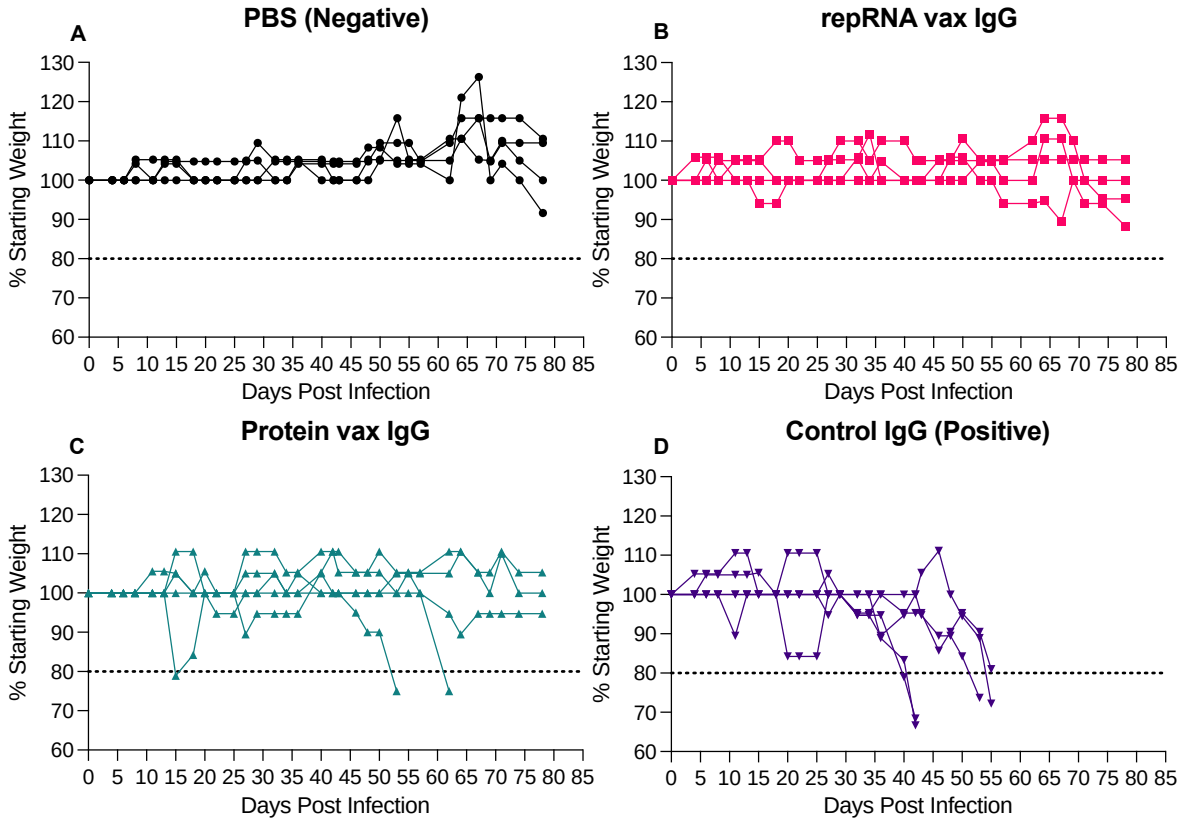

Figure S3: Weight of mice from Figure 5 after EBV challenge.

The percent of the starting weight over time for (**A**) uninfected control mice treated with PBS, (**B**) mice given IgG elicited by LION/repRNA-gH/gL prior to EBV challenge, (**C**) mice given IgG elicited by protein vaccination prior to challenge, and (**D**) mice given control IgG prior to challenge (infection control). Dashed line indicates threshold for humane endpoint.

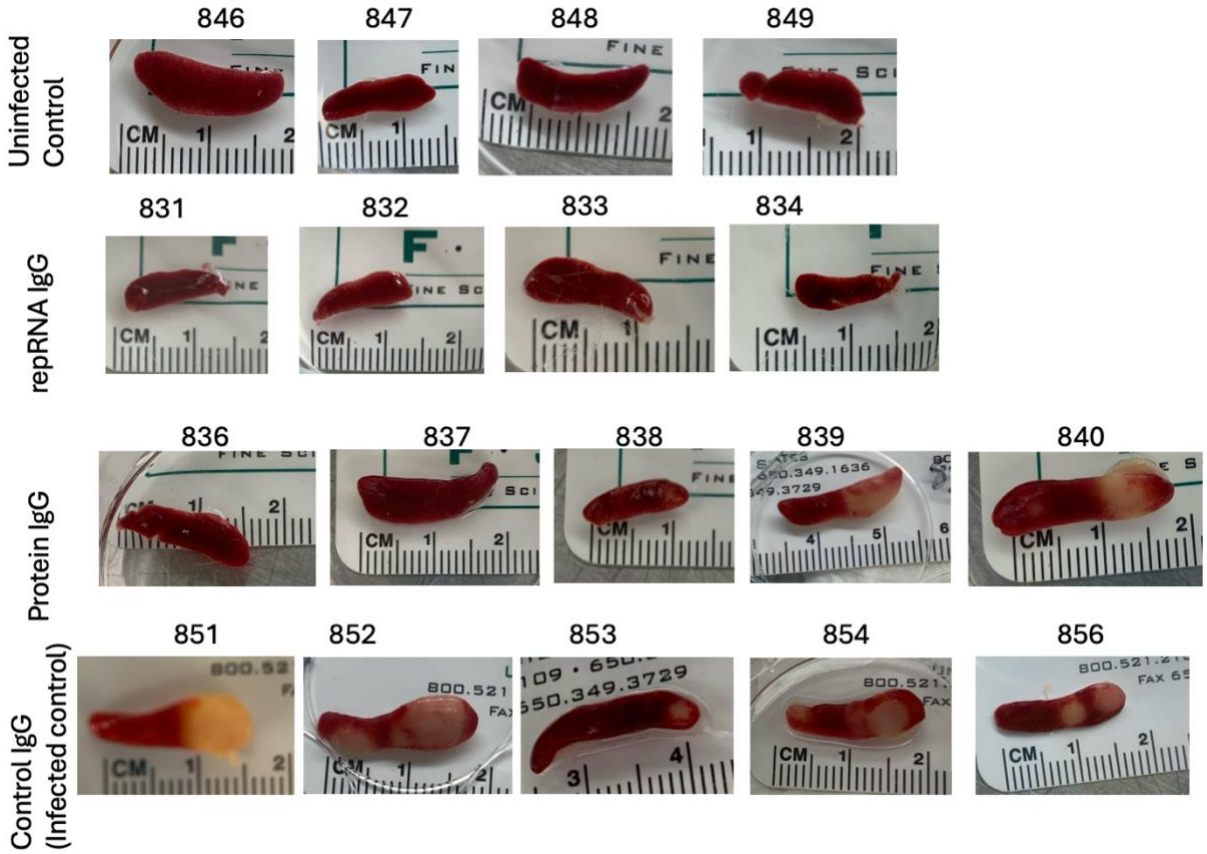

Figure S4: Spleens from individual animals from Figure 5 collected at time of euthanasia.

3.3.6 *LION/repRNA gH/gL elicits higher cellular responses than immunization with adjuvanted recombinant gH/gL*

The challenge experiments demonstrated that antibodies elicited by repRNA immunization conferred superior antibody-mediated protection compared to antibodies elicited by protein. To compare cellular immunity elicited by both vaccines, we collected splenocytes from ten animals used to generate IgG for transfer experiments, stimulated them with the recombinant gH/gL ectodomain *ex vivo*, and analyzed $CD4^+$ and $CD8^+$ T cells for production of IFNɣ (Fig S5). Mice vaccinated with repRNA had higher amounts of vaccine-elicited $CD8^+$ T cells, as defined by the frequency of $IFN\gamma^+$ $CD8^+$ T cells after splenocyte exposure to gH/gL (Fig. 6A). No significant difference in $IFN\gamma^+$ $CD4^+$ T cell vaccine responses were observed (Fig. 6B).

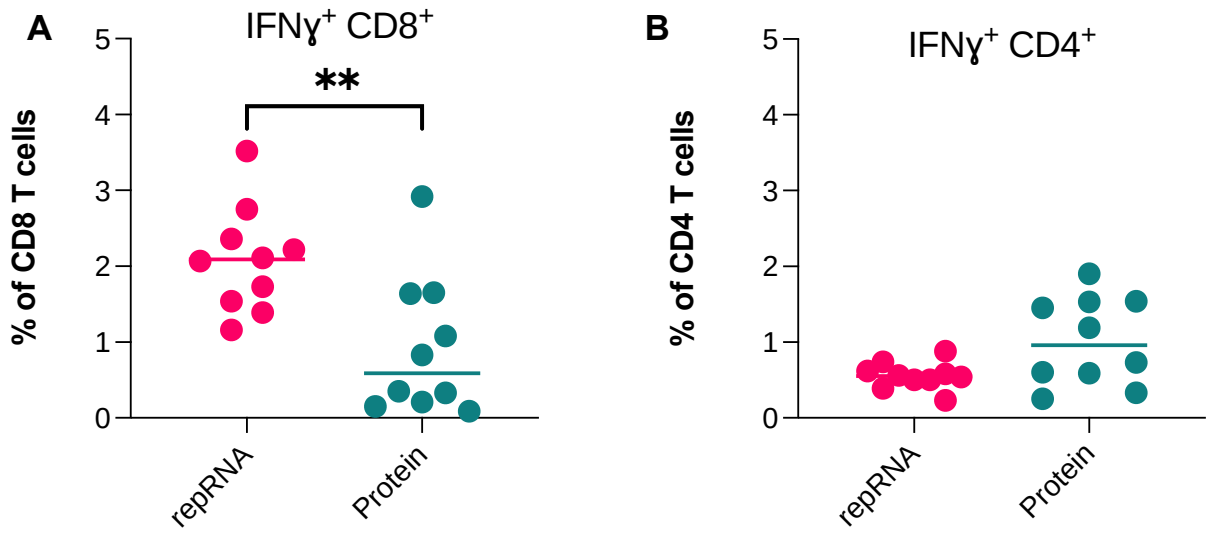

Figure 6: LION/repRNA-gH/gL immunization elicits stronger vaccine-specific CD8+ T cell responses than protein monomer immunization.

(**A**-**B**) $IFN\gamma^+$ $CD8^+$ (**A)** and $IFN\gamma^+$ $CD4^+$ (**B**) T cell responses were quantified in gH/gL stimulated splenocytes using an intercellular staining assay. Each dot represents an individual mouse,

where the frequency of IFNɣ$^+$ T cells in splenocytes mock simulated with media alone (negative control) has been subtracted from the frequency of IFNɣ$^+$ T cells after gH/gL stimulation. The gating strategy is shown in Figure S5. The bars represent the mean, ** $p \leq 0.01$, and significant differences between groups in the % of CD4+ (**A**) and CD8+ (**B**) cells were determined using a Mann-Whitney test.

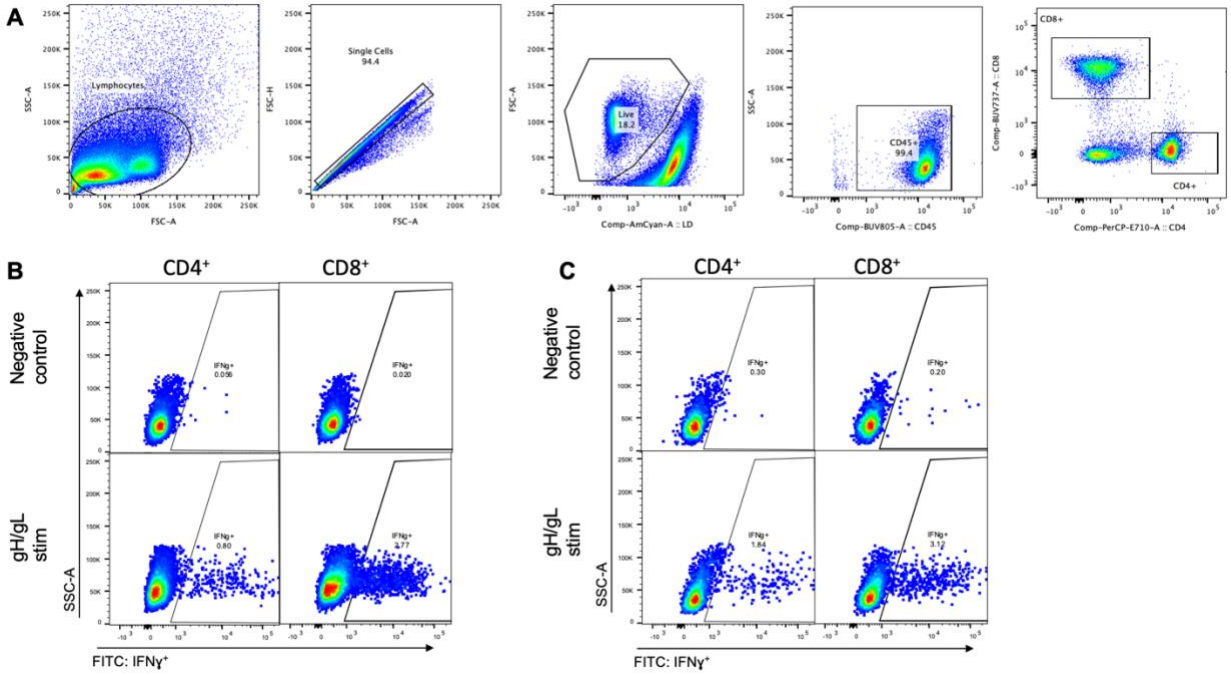

Figure S5: Gating strategy for evaluating IFNɣ$^+$ CD4$^+$ and CD8$^+$ T cells.
(**A**) Gating strategy for CD4$^+$ and CD8$^+$ T cell populations. (**B**) IFNɣ$^+$ staining within CD4$^+$ and CD8$^+$ T cell populations for a representative repRNA immunized animal after media only stimulation (negative control) and gH/gL stimulation of splenocytes as indicated. (**C**) IFNɣ$^+$ staining within CD4$^+$ and CD8$^+$ T cell populations for a representative protein immunized animal after media only negative control and gH/gL stimulation of splenocytes.

3.4 Discussion

EBV is an important human oncovirus for which there is no vaccine. High titers of neutralizing antibodies against the gH/gL glycoprotein complex protect against experimental EBV infection in animal models, suggesting that eliciting these responses will be an important goal of an effective EBV vaccine. Here we report the development and optimization of a LION/repRNA vaccine encoding the EBV gH/gL glycoprotein complex. Optimization included testing the effect of the order of the two glycoproteins gH and gL in tandem expression constructs, varying the timing and dosing of repRNA delivery, evaluating the effect of soluble versus membrane-anchored antigen, and comparing the immunogenicity of different multimeric constructs encoded by repRNA.

Favorable immunogenicity of repRNA encoded gH/gL was achieved when the glycoprotein complex was membrane anchored, and the highest dose of repRNA was delivered 8 weeks apart in a prime/boost regimen. This resulted in high titers of binding and neutralizing antibodies that were maintained for up to 32 weeks following immunization.

LION/repRNA delivery of either the full-length membrane-anchored, or soluble gH/gL ectodomain elicited similar gH/gL binding titers. However, the soluble version elicited less potent neutralizing titers against EBV infection of both B- and epithelial cells demonstrating a qualitative difference in antibody response to the two antigens. This was further supported by the observation that plasma from mice immunized with full-length gH/gL more readily competed the binding of previously described neutralizing mAbs. These differences in the antibody responses could be due to several non-exclusive possibilities. Membrane anchoring may restrict access to immunodominant, non-neutralizing epitopes that are more exposed to the immune system on the secreted ectodomain. Similarly, membrane anchoring may lead to epitope exposure in a repetitive array that is optimal for engagement of B cell receptors targeting

neutralizing epitopes. Although the precise mechanisms that underlie the observed differences between the neutralizing titers elicited by membrane anchored gH/gL are not clear, we note that a similar phenomenon was observed when comparing mRNA delivery of membrane anchored and secreted MERS Spike protein[43], and that mRNA-based SARS-CoV-2 vaccines are based on full length rather than secreted spike proteins[43–46]. Collectively these observations underscore the importance of evaluating membrane anchoring in nucleic acid delivery of viral glycoprotein vaccine antigens.

We and others previously demonstrated that the immunogenicity of recombinant gH/gL was substantially enhanced by multimeric display on self-assembling nanoparticles[15,20–22]. When delivered by repRNA/LION, gH/gL 4-mers, 7-mers, and 60-mers were less immunogenic than membrane bound monomeric gH/gL. The reduced antigenicity is likely related to low levels of expression since the yields of these multimeric antigens were inversely correlated with valency when expressed from plasmid DNA *in vitro*[20]. Consistent with this observation, the binding and neutralizing titers were the lowest in mice immunized with the highest valency repRNA encoded gH/gL nanoparticle. As noted above, expression of membrane anchored monomeric gH/gL antigens on the surface of the cell most-likely resulted in the display of gH/gL as an array on the cell-surface, which effectively achieved a multimerization effect without compromising the level of gH/gL expression.

Evaluating the efficacy of EBV vaccines *in vivo* is difficult since the virus has near-obligate tropism for humans, which are the only natural host. NSG mice engrafted with $CD34^+$ hematopoietic progenitor cells have been used as small animal to evaluate the ability of monoclonal[16,18,19,47,48] or vaccine elicited antibodies[20–22,49] to protect against EBV challenge. Here we showed that IgG elicited by repRNA-delivered gH/gL was able to prevent lethality from high-dose EBV challenge, reduce viral load in the blood and spleen, and prevent splenic tumors

and splenomegaly. This protection was superior to that achieved by passive transfer of IgG elicited by immunization with a more conventional recombinant gH/gL protein delivered with adjuvant. We previously showed that two immunizations with recombinant multimeric gH/gL nanoparticles elicited similar levels of neutralizing antibodies to repRNA encoded (monomeric) gH/gL and that passive transfer of the same amount of gH/gL nanoparticle-elicited IgG could also achieve a comparable level of protection in humanized mice. These results demonstrate that repRNA delivery of gH/gL is a viable strategy to elicit high titers of neutralizing antibodies necessary for protection in humanized mice that obviates the challenges of expressing and purifying gH/gL nanoparticles.

The immune incompetence of huCD34 engrafted NSG mice limits the utility of direct immunization, however the protection afforded by transfer or repRNA elicited IgG clearly highlights a key role of antibodies in anti-EBV immunity. Given that $CD8^+$ T cells play a critical role in controlling EBV infection in humans[50], it stands to reason that antibody-mediated protection elicited by repRNA could be augmented by cellular immune responses[51,52]. In this regard, we note that repRNA elicited higher frequencies of $IFN\gamma^+$ producing $CD8^+$ T cell responses in immune competent B6 mice.

Humanized mice are not a perfect model for EBV infection as only human-origin B cells support infection and the natural route of oral transmission is not possible [36,38]. Oral challenge of rhesus macaques with the EBV ortholog, rhesus lymphocryptovirus provides an orthogonal challenge model to evaluate immunogenicity of repRNA vaccines, however the antigenic disparity between EBV and rhLCV may belie the predictive efficacy of EBV vaccines in the rhesus macaque model (Chapter 2).

Passive transfer of total IgG elicited by recombinant monomeric gH/gL with lower anti-gH/gL activity was less protective than IgG elicited by repRNA in humanized mice. A similar

phenomenon was observed comparing recombinant monomeric vs multimeric gH/gL vaccines[20], suggesting that protection correlates with neutralizing titer. In support of this notion, passive transfer of a neutralizing gH/gL mAb was protective against oral challenge with rhesus LCV provided that the antibody was present at adequate levels[19]. Collectively these observations indicate that a neutralizing threshold is required for protection against EBV infection. This implies that a vaccine that induces sterilizing immunity will need to elicit durable high-titer antibodies. We note that the antibody titers elicited by repRNA delivery of gH/gL remained stable for at least 8 months following immunization suggesting that this platform may be capable of conferring long-term immunity to EBV. Extended durability studies that examine titer longevity and underlying antigen-specific B cells responses are warranted.

In sum, we demonstrate that repRNA/LION delivery of gH/gL elicited high titers of neutralizing antibodies that protected against lethal challenge in a humanized mouse infection model. In addition to eliciting durable neutralizing antibody responses repRNA/LION delivery of gH/gL elicited higher levels of vaccine specific $CD8^+$ T cell responses as compared to a recombinant gH/gL protein. The robust immunogenicity of repRNA encoded gH/gL, relative ease of manufacturing, and favorable safety and reactogenicity profile of the delivery platform warrants the development of repRNA EBV vaccines for human clinical trials[23].

3.6 Methods:

Cell lines

All cell lines were incubated at 37°C in the presence of 5% CO_2 and were not tested for mycoplasma contamination. 293-T and 293-6E (human female) were maintained in Freestyle 293 media with gentle shaking. Raji cells (human male) were maintained in RPMI + 10% FBS, 2

mM L-glutamine, 100 U/ml penicillin, and 100 µg/ml streptomycin (cRPMI). 293-2089 cells (human female) were grown in cRPMI containing 100 µg/ml hygromycin[53]. AKATA (human female) B cells harboring EBV in which the thymidine kinase gene has been replaced with a neomycin and GFP cassette virus (AKATA-GFP) were grown in cRPMI containing 350 µg/ml G418 [34]. SVKCR2 cells (human male) were grown in DMEM containing 10% cosmic calf serum, 2 mM L-glutamine, 100 U/ml penicillin, 100 µg/ml streptomycin, 10 ng/ml cholera toxin and 400 µg/ml G418[54].

Mice

NOD-scid Il2rgnull (NSG) and C57BL/6 mice were housed in a specific pathogen-free facility at FHCC. The facility is accredited by the Association for Assessment and Accreditation of Laboratory Animal Care. Mice were handled in accordance with the NIH Guide for the Care and Use of Laboratory Animals, and experiments were approved by the FH Institutional Animal Care and Use Committee and Institutional Review Board. All C57BL/6 and NSG mice used in this study were female and 6 weeks old when experiments were initiated.

Plasmids

Codon optimized cDNA encoding EBV gH (GenBank AFY97969.1) and gL (GenBank: AFY97944.1) separated by a furin cleavage site and a porcine teschovirus-1 (P2A) ribosomal skipping peptide in both orientations (gH-furin-P2A-gL or gL-furin-P2A-gH) with a 5' Kozak consensus sequence were synthesized by Twist Biosciences and cloned into pVEE-rep encoding the 5′ and 3′ untranslated regions and the nonstructural open reading frame of Venezuelan equine encephalitis virus, strain TC-83, between PflFI and Sac II sites[28,55], creating pVEE-gH-gL and pVEE-gL-gH. pVEE-gL-gH-Ecto was created by introducing a stop codon at AA 170 in gH using the QuikChange II Site-directed mutagenesis kit. pVEE-gL-gH-MDT1100, pVEE-gL-gH-C4b, and pVEE-gL-gH-I3 were produced by amplifying the entire pVEE-gL-gH-Ectodomain plasmid using gene-specific primers and Platinum SuperFi II DNA Polymerase

according to the manufacturer's instructions. Separate sets of gene specific primers with overlapping homology to the 5' and 3' ends of the amplified linear pVEE-gL-gH-Ecto fragment were used to amplify the MDT1100, C4b and I3 multimerization domains from pTT3-gH-IMX313, pCVL-UCOE0.7-SFFV-gH-C153T-cTRP(6)ss-IRES-GFP, and pCVL-UCOE0.7-SFFV-gH--C153T-I3-IRES-GFP plasmids[20], respectively. The linear pVEE-gL-gH-Ecto fragment was fused to each multimerization domain fragment using the In-Fusion® Snap Assembly Master Mix (Takara) according to the manufacturer's instructions.

The variable regions corresponding to 769B10[15], 1D8[18], and 770F7[16] heavy and light chains were synthesized by Integrated DNA Technologies and cloned into pTT3-AMMO1-HC and pTT3-AMMO1LC (for lambda) or pTT3-E1D1LC (for Kappa)[17,19]. All plasmids were confirmed by Sanger sequencing.

repRNA production

Template pVEE DNAs were linearized by enzymatic digestion with Not I followed by phenol-chloroform treatment and ethanol precipitation. Linearized template was transcribed using the MEGAscript T7 Transcription Kit (Invitrogen) followed by capping with New England Biolabs Vaccinia Capping System as previously described[55]. Capped transcripts were then precipitated in lithium chloride and resuspended in nuclease-free water to a final concentration of 1 mg/ml and analyzed by agarose-gel electrophoresis. All RNA was aliquoted and stored at −80°C.

Recombinant Proteins

The recombinant gH/gL ectodomain was produced by transfecting pTT3-gH-HIS-AVI and pTT3-gL in 293 6E cells using PEI Max according to the manufacturer's instructions and purified using NiNTA affinity chromatography followed by size exclusion chromatography as previously described[17,20]. Recombinant monoclonal antibodies were produced by co-transfecting heavy and light chain plasmids into 293 6E cells using PEI Max according to the manufacturer's instructions and purified using Protein A Agarose (Gold Bio Cat. #P-400-5).

Preparation of EBV Reporter Viruses

To produce B-cell tropic GFP reporter viruses (B95-8/F), 5×10^6 293–2089 cells were seeded on a 100mm tissue culture dish in cRPMI containing 100 µg/ml hygromycin. 48 hr later the cells were washed with PBS, the media was replaced with cRPMI without hygromycin, and cells were transfected with 6 µg each of p509 and p2670 expressing BZLF1 and BALF4, respectively, using GeneJuice transfection reagent (SigmaAldrich Cat. #70967)[53,56]. 72 hr post transfection, the cell supernatant was collected and centrifuged at 500 × *g* for 3 min to pellet any cell debris, and passed through a 0.8 µm filter. Virions were concentrated 25-50-fold by centrifugation at 25,000 × *g* for 2 hr and re-suspended in PBS. Virus was stored at -80°C and thawed immediately before use.

Epithelial cell tropic virus was produced from Akata-GFP EBV cells suspended at 4×10^6 cells/ml in RPMI containing 1% FBS by adding goat anti-human IgG (Southern Biotech Cat. #2040-01) to a final concentration of 100 µg/ml, and the culture was incubated at 37°C for 4 hr. Cells were then diluted to 2×10^6 cells/ml in RPMI containing 1% FBS and cultured for 72 hr. Cultures were centrifuged at 300 × *g* for 10 min to pellet cells and supernatant was passed through a 0.8 µm filter. Bacitracin was added to a final concentration of 100 µg/ml. Virions were concentrated 25× by centrifugation at 25,000 × *g* for 2 hr and re-suspended in RPMI containing 100 µg/ml bacitracin. Virus was stored at -80°C and thawed immediately before use.

EBV neutralization assay in B cells

EBV neutralization assays were carried out in Raji cells as previously described [57]. In short, plasma from mice was serially diluted in 25 µl cRPMI in triplicate in 96-well round-bottom plates. 12.5 µl of diluted of B95-8/F virus diluted to achieve an infection frequency of approximately 1-5% was added and plates were incubated for 1hr at 37°C. Following the incubation, 12.5 µl of Raji cells at 4×10^6 cells/ml was added to each well and incubated for an hour at 37°C. Cells

were then washed once in cRPMI, re-suspended in fresh cRPMI at 37˚C. 72 hr later, cells were fixed in 10% formalin and the percentage of GFP+ Raji cells was determined using a Luminex Guava HT or BDFACS Celesta.

To account for any false positive cells due to auto-fluorescence in the GFP channel, the average %GFP^+ cells in negative control wells (n=5-10) was subtracted from each well. The infectivity (%GFP^+) for each well was plotted as a function of the log_{10} of the plasma dilution. Plasma dilution is reported relative to the final assay volume (50 µl). The neutralization curve was fit using the log (inhibitor) vs response-variable slope (four parameters) analysis in GraphPad Prism 10.0.2 (GraphPad Software). The half maximal inhibitory plasma dilution ID_{50} was interpolated from the curve in GraphPad GraphPad Prism 10.0.2. Statistical differences between ID_{50} values for different cohorts were tested at each timepoint by Mann-Whitney test in GraphPad Prism 10.0.2 with no correction for multiplicity.

EBV Neutralization Assay in Epithelial Cells

SVKCR2 cells were seeded at a density of 1.5×10^4 cells per well in a 96 well flat-bottom tissue culture plate. The next day plasma was serially diluted in duplicate wells of a 96 well plate, then Akata-GFP virus was added to each well and incubated for 15 min. The media was then aspirated from the SVKCR2 cells and replaced by the antibody-virus mixture. The plates were incubated at 37°C for 48 hr, then cells were detached from the plate using 0.25% trypsin, transferred to a 96 well round bottom plate, washed twice with PBS, and fixed with 10% formalin. The percentage of GFP+ cells were determined on a BDFACS Celesta and percent neutralization, ID_{50}, and statistical differences were determined as in the B cell neutralization assay.

Immunizations in C57BL/6 mice

Comparative immunogenicity studies were performed in groups of 4 or 5 C57BL/6 mice between 7 and 10 weeks of age. Each group included both male and female mice. Blood was collected retro-orbitally before immunization for a baseline measurement. Mice were immunized at weeks 0 and 8. Injections of repRNA were formulated by diluting RNA to the desired concentration in PBS and sterile filtering. Sterile RNA was then mixed as a 1:1 volumetric ratio with sterile LION[28], 40% sucrose, 100 mM citrate, and RNAse free water. Final repRNA concentrations were 1 µg/ml, 10 µg/ml, 100 µg/ml. Immunizations were delivered via split dose intramuscular injection consisting of two 50 µL doses delivered to each rear leg. Blood was collected retro-orbitally every 2 weeks after the first and second immunizations or via cardiac puncture at indicated timepoints. Blood was collected in citrate coated tubes. Plasma was separated from whole blood via centrifugation, then heat inactivated at 56°C for 30 min.
To generate IgG for passive transfer experiments, immunizations were performed in groups of 25 C57BL/6 mice (12 or 13 male and female, varied per group) between 7 and 10 weeks of age. After collecting a pre-bleed, mice were immunized at weeks 0 and 8 with 5 µg of gH/gL monomer in PBS with 50% (v/v) Sigma Adjuvant System (SAS) (Sigma Cat. #S6322) for a total volume of 100 µL per immunization. Mice were immunized with 10 µg repRNA via intramuscular injection as above. Blood was collected retro-orbitally at week 8 and via cardiac puncture at week 12. Plasma was separated from whole blood via centrifugation and collected plasma was heat inactivated at 56˚ C for 30 min.

IgG purification from murine plasma

Terminal plasma from each group was pooled, diluted in protein G binding buffer (ThermoFisher Cat# 21019), and passed over a column containing 1ml of protein A/G agarose (ThermoFisher Cat# 20422) . The column was then washed 3 times with five column volumes of binding buffer.

Finally, IgG was eluted from the resin in 1 ml fractions using IgG elution buffer (ThermoFisher Cat# 21004) into 0.1ml of 1M Tris-HCl, pH 8.0. Fractions were buffer exchanged into PBS, concentrated, passed through a 0.2 µm filter, and quantified by measuring the absorbance at 280nm using a Nanodrop One (ThermoFisher Cat. #13-400-519).

Measurement of plasma antibody endpoint binding titers by anti-His capture ELISA

30 µl/well of rabbit anti-His tag antibody (SigmaAldrich Cat. #SAB5600227) was adsorbed at a concentration of 0.5 µg/ml on to 384 well microplates at 4 ˚ C for 16 hr in a solution of 0.1 M NaHCO3 pH 9.4–9.6 (coating buffer). The following day, plates were washed 4 times with 1x PBS and 0.02% Tween 20 (ELISA wash buffer) prior to blocking for 1 hr with 90 µl/well of PBS containing 10% non-fat milk and 0.02% Tween 20 (blocking buffer). After blocking, plates were washed 4 times and 30 µl/well of 2 µg/ml monomeric His-tagged gH/gL diluted in blocking buffer was added to the plate and incubated for 1 hr. Plates were washed and plasma diluted in blocking buffer was added to the top row of the plate. Three-fold serial dilutions were performed in duplicate followed by a 1 hr incubation at 37 ˚ C. Additional control wells containing immobilized gH/gL but no immune plasma were included. After washing, a 1:4,000 dilution of goat anti-mouse IgG-HRP (SouthernBiotech Cat. #2010-05) in blocking buffer was added to each well and incubated at 37 ˚ C for 1 hr. After four washes, 30 µl/well of SureBlue Reserve TMB Microwell Peroxidase substrate (SeraCare Cat. #5120-0081) was added. After 5 min, 30 µl/well of 1N sulfuric acid was added and the A_{450} of each well was read on a Molecular Devices SpectraMax M2 plate reader. The binding threshold was defined as the average plus 10 times the SD of the determined by calculating the average of A_{450} values of the control wells. Endpoint titers were interpolated from the point of the curve that intercepted the binding threshold using the GraphPad Prism 10.0.2 package. Statistical differences between different cohorts were

tested at each timepoint by Mann-Whitney test using the GraphPad Prism 10.0.2 package with no correction for multiplicity.

Measure of competitive binding titers by ELISA

Coating, blocking, and gH/gL immobilization steps were performed as described under ‘‘Measurement of plasma antibody endpoint binding titers by anti-His capture ELISA.’’ Following capture of monomeric gH/gL, equal amounts of plasma from each mouse in a group were pooled and diluted in blocking buffer and 2-fold serial dilutions were performed, followed by a 1 hr incubation at 37ºC. After washing, monoclonal antibodies AMMO1, CL40, CL59, E1D1, 769B10, 770F7, and 1D8 were added at a concentration that achieves half-maximal binding (EC_{50}; pre-determined in the same assay in the absence of competing plasma) to each well containing serially diluted pooled plasma from each group, followed by a 1 hr incubation at 37ºC. After four washes with ELISA washing buffer, a 1:20,000 dilution of goat anti-human IgG-HRP (Jackson ImmunoResearch Cat. # 109-035-088) in blocking buffer was added to each well and incubated at 37ºC for 1 h followed by four washes with ELISA wash buffer. Addition of SureBlue Reserve TMB Microwell Peroxidase substrate, addition of 1N sulfuric acid, and reading of plates was performed as described above. The average A_{450} values of buffer only control wells were subtracted from each mAb containing well and plotted in GraphPad Prism 10.0.2. A_{450} values were plotted as a function of the $\log_{10}$ of the plasma dilution. A binding curve was fit using the Sigmoidal, 4PL, X is log(concentration) least squares fit function. Maximum binding was defined as the best-fit value for the top of each curve computed in Prism. A_{450} values at each dilution on the curve were divided by the maximum binding and multiplied by 100 to calculate the % of max binding ([A_{450} at each dilution/ max binding] x100). The titer at which half-maximal binding was observed was interpolated from the binding curve using the GraphPad Prism 10.0.2 package.

Stimulation of splenocytes

Spleens were harvested from 5 male and 5 female mice immunized with repRNA gHgL or protein monomer gHgL at week 12 post immunization. Splenocytes were isolated by mechanical dissociation in RBC lysis buffer (ThermoFisher Cat. #A1049201) using a 100 µm filter. After dissociation and lysis, cells were washed in FACS buffer once and resuspended in 5 ml FACS buffer. In 96-well plates, splenocytes were plated at a concentration of $2x10^6$ cells/well in cRPMI. Cells were stimulated with either cRPMI alone (negative control), 50 µg/ml gH/gL in cRPMI, or 0.5 µg/ml anti-CD3 (ThermoFisher Cat. #14-0037-82**)** and 0.25 µg/ml anti-CD28 (ThermoFisher Cat. #14-0281-82) (positive control). Cells were incubated at 37ºC, 5% CO_2 for 72 hr prior to start of intracellular staining. Five hours before the end of restimulation 20 µl of brefeldin A (eBioscience Cat. #00-4506-51) at 10 ng/ml and 20 µl 1000x monensin (eBioscience Cat. #00-4505-51) was added to each well.

Intracellular staining (ICS)

After stimulation, plates were centrifuged at 400 x g for 5 min at 8ºC and supernatants were transferred to a new plate and frozen at -20ºC. Cell pellets were resuspended in 200 µl FACS buffer, centrifuged at 400 x g for 5 min, and resuspended in 50 µl viability staining mix: 1:500 BV510 live-dead dye (eBioscience Cat. #65-0866-14) and 1:500 Fc Block (Biolegend Cat. #101302) in PBS. Cells were stained on ice in dark for 15 min. 150 µl FACS buffer was added to each well, plates were centrifuged 400 x g 5 min, and supernatant removed. Cell pellets were then resuspended in surface staining mix: a 1:200 dilution of the following anti- mouse CD45 BUV805 (BD Bioscience Cat. #568336), CD3 BUV395 (BD Bioscience Cat. #740268), CD8 BUV737 (BD Bioscience Cat. #612759), and CD4 PerCPCy5.5 (Thermofisher Cat. #45-0042-80) antibodies in FACS buffer. Cells were stained on ice in dark 30 min. After staining, cells were resuspended in 150 µl FACS buffer and washed once in 200 µl FACS buffer. Cells were

then fixed and permeabilized for 20 min on ice using 100 µl 1X CytoFix solution (BD Bioscience Cat. #554714). Plates then washed twice in 1X CytoPerm Wash Buffer (BD Bioscience Cat. #554714). ICS was then done by resuspension in 50 µl/well ICS mix: in CytoPerm wash buffer, a 1:200 dilution anti-mouse IFN-ɣ AF488 (Biolegend Cat. #505815). Cells were stained on ice in dark 30 min. Cells washed twice in CytoPerm wash buffer and resuspended in FACS buffer for acquisition. Samples were acquired on BD Fortessa X50 cytometer. The frequency of IFNɣ$^+$ cells in the Lymphocyte/Singlet/Live/CD45$^+$/CD4$^+$ or CD8$^+$ population was determined for each sample. The frequency of CD4$^+$ or CD8$^+$ T cells expressing IFNɣ from baseline cRPMI stimulation was subtracted from the final reported values.

EBV infection in humanized mice

Twenty-five six week old NSG mice were irradiated (275R of total body irradiation) and received 1x10^6 CD34$^+$ huPBSC in 200 µl PBS through i.v. injection. Eight weeks later, successful human cell engraftment was confirmed by the presence of human CD45$^+$ cells in peripheral blood by flow cytometry. Using 50 µl blood, RBCs were lysed and cells were stained using a BV510 viability dye, and the following antibodies at a 1:100 dilution unless otherwise noted: hCD45 FITC (eBioscience Cat. #5010066), mCD45 APC (eBioscience Cat. #17-0451-82) (1:500 dilution), hCD33 PE (BD Bioscience Cat. #555450), hCD19 BV711 (Biolegend Cat.# 302246), hCD4 AF700 (eBioscience Cat. #56-0048-82) and hCD8 BV421 (BD Bioscience Cat. #562429). Cells were stained for 30 min on ice, washed twice in FACS buffer, fixed in 200 µl of 10% formalin 15 min on ice, washed and resuspended in 200 µl FACS buffer for acquisition and analyzed on a BDFACS Celesta. 10 weeks post-engraftment, 500 µg of experimental or control antibodies were injected per humanized NSG mouse via intraperitoneal injection (i.p.). 24 hr later, mice were bled in the left eye to confirm passive transfer of IgG, and received a dose of EBV B95.8/F67 equivalent to 33,000 Raji infectious units as determined by infection of Raji cells

via retro-orbital injection in the right eye. Each group of mice receiving the same IgG preparation and/or EBV were housed separately from each other. Mice were weighed three times weekly. Beginning at two weeks post-infection, peripheral blood samples were collected to measure the presence of EBV DNA in whole blood. Twelve weeks post-challenge, or until mice lost 20% of their starting weight, mice were euthanized. Spleens were photographed and weighed, then DNA was extracted from splenocytes utilizing the DNeasy Blood & Tissue Kit (QIAGEN) and according to the manufacturer's instructions for subsequent viral load analysis.

Measurement of total plasma IgG in huCD34+ engrafted NSG mice

Plasma was serially diluted in ELISA coating buffer in duplicate and incubated on 384-well microplates at 4ºC for 16 hr. At least 10 additional control wells were included that contained only coating buffer and no plasma. The next day, plates were washed 4x with ELISA wash buffer prior to blocking for 1 hr with 100 µl/well of ELISA blocking buffer. After blocking, plates were washed and a 1:4000 dilution of goat anti-mouse IgG Human ads-HRP in ELISA blocking buffer was added to each well and incubated 1hr at 37ºC. Plates were washed and addition of SureBlue Reserve TMB Microwell Peroxidase substrate, addition of 1N sulfuric acid, and reading of plates was performed as described above. The average A450 values of buffer only control wells were subtracted from each plasma containing well and plotted in GraphPad Prism 10.0.2. A450 values were plotted as a function of the log10 of the plasma dilution. A binding curve was fit using the Sigmoidal, 4PL, X is log(concentration) least squares fit function. The binding threshold was determined as in "Measurement of plasma antibody endpoint binding titers by anti-His capture ELISA".

Quantitative PCR analysis EBV DNA in huCD34 engrafted mice

A primer-probe mix specific for the EBV BALF5 gene [58] was used to quantify EBV in DNA extracted from blood or spleen in hCD34 engrafted NSG recipient mice at the time points

described. Each 25 µl qPCR reaction contained 12.5 µl QuantiTect Probe PCR Master Mix (QIAGEN), 600 nM of each primer and 300 nM of FAM-labeled probe (IDT), 1.25 µl of a TaqMan VIC-labeled RNase-P primer probe mix (Fisher Sci Cat. #4316844). For analysis of splenocytes, reactions contained 1 µg DNA extracted from splenocytes as template. To analyze EBV in peripheral blood, 50 µl of blood collected via cardiac puncture or retro-orbital bleed DNA extracted using the DNeasy Blood and Tissue Kit (QIAGEN) and eluted in 50 µl of Buffer AE (QIAGEN). 10 µl of extracted DNA was used as template in qPCR. Reactions were heated to 95ºC for 15 minutes to activate DNA polymerase followed by 50 cycles of 95ºC for 15 s 60ºC for 60 s, on an Applied Biosystems QuantStudio 7 Flex Real Time PCR System. Synthetic DNA fragments containing the BALF5 target gene as well as flanking genomic regions were synthesized as double stranded DNA gBlocks (IDT), and were used to generate a standard curve with known gene copy numbers ranging from 10^7-10^0 copies/µl. The copy number in extracted DNA was determined by interpolating from the standard curve. Serial dilutions of reference standard were used to experimentally determine a limit of detection of 6.25 copies, which corresponds to the amount of template that can be detected in > 95% of reactions. For graphical purposes, samples with no amplification or those yielding values below the limit of detection were assigned a value of 0.625 copies.

3.7 Chapter 3 Bibliography

1. Cohen, J. I. Epstein–Barr Virus Infection. *New England Journal of Medicine* **343**, 481–492 (2000).
2. Henle, G., Henle, W. & Diehl, V. Relation of Burkitt's tumor-associated herpes-ytpe virus to infectious mononucleosis. *Proceedings of the National Academy of Sciences* **59**, 94–101 (1968).
3. Dunmire, S. K., Hogquist, K. A. & Balfour, H. H. Infectious Mononucleosis. in 211–240 (2015). doi:10.1007/978-3-319-22822-8_9.
4. Wong, Y., Meehan, M. T., Burrows, S. R., Doolan, D. L. & Miles, J. J. Estimating the global burden of Epstein-Barr virus-related cancers. *J Cancer Res Clin Oncol* **148**, 31–46 (2022).
5. Khan, G., Fitzmaurice, C., Naghavi, M. & Ahmed, L. A. Global and regional incidence, mortality and disability-adjusted life-years for Epstein-Barr virus-attributable malignancies, 1990-2017. *BMJ Open* **10**, e037505 (2020).
6. Balandraud, N. & Roudier, J. Epstein-Barr virus and rheumatoid arthritis. *Joint Bone Spine* vol. 85 165–170 Preprint at https://doi.org/10.1016/j.jbspin.2017.04.011 (2018).

7. Bjornevik, K. *et al.* Longitudinal analysis reveals high prevalence of Epstein-Barr virus associated with multiple sclerosis. *Science (1979)* **375**, 296–301 (2022).
8. Cornillet, M., Verrouil, E., Cantagrel, A., Serre, G. & Nogueira, L. In ACPA-positive RA patients, antibodies to EBNA35-58Cit, a citrullinated peptide from the Epstein–Barr nuclear antigen-1, strongly cross-react with the peptide β60-74Cit which bears the immunodominant epitope of citrullinated fibrin. *Immunol Res* **61**, 117–125 (2015).
9. Handel, A. E. *et al.* An updated meta-analysis of risk of multiple sclerosis following infectious mononucleosis. *PLoS One* **5**, 1–5 (2010).
10. Lanz, T. V. *et al.* Clonally expanded B cells in multiple sclerosis bind EBV EBNA1 and GlialCAM. *Nature* **603**, 321–327 (2022).
11. Zhong, L. *et al.* Urgency and necessity of Epstein-Barr virus prophylactic vaccines. *NPJ Vaccines* **7**, 159 (2022).
12. Bu, G.-L., Xie, C., Kang, Y.-F., Zeng, M.-S. & Sun, C. How EBV Infects: The Tropism and Underlying Molecular Mechanism for Viral Infection. *Viruses* **14**, (2022).
13. Connolly, S. A., Jardetzky, T. S. & Longnecker, R. The structural basis of herpesvirus entry. *Nat Rev Microbiol* **19**, 110–121 (2021).
14. Gonzalez-Del Pino, G. L. & Heldwein, E. E. Well Put Together-A Guide to Accessorizing with the Herpesvirus gH/gL Complexes. *Viruses* **14**, (2022).
15. Bu, W. *et al.* Immunization with Components of the Viral Fusion Apparatus Elicits Antibodies That Neutralize Epstein-Barr Virus in B Cells and Epithelial Cells. *Immunity* **50**, 1305-1316.e6 (2019).
16. Chen, W.-H. *et al.* Epstein-Barr virus gH/gL has multiple sites of vulnerability for virus neutralization and fusion inhibition. *Immunity* **55**, 2135-2148.e6 (2022).
17. Snijder, J. *et al.* An Antibody Targeting the Fusion Machinery Neutralizes Dual-Tropic Infection and Defines a Site of Vulnerability on Epstein-Barr Virus. *Immunity* **48**, 799-811.e9 (2018).
18. Zhu, Q.-Y. *et al.* A potent and protective human neutralizing antibody targeting a novel vulnerable site of Epstein-Barr virus. *Nat Commun* **12**, 6624 (2021).
19. Singh, S. *et al.* Neutralizing Antibodies Protect against Oral Transmission of Lymphocryptovirus. *Cell Rep Med* **1**, 100033 (2020).
20. Malhi, H. *et al.* Immunization with a self-assembling nanoparticle vaccine displaying EBV gH/gL protects humanized mice against lethal viral challenge. *Cell Rep Med* **3**, 100658 (2022).
21. Cui, X. *et al.* Immunization with Epstein–Barr Virus Core Fusion Machinery Envelope Proteins Elicit High Titers of Neutralizing Activities and Protect Humanized Mice from Lethal Dose EBV Challenge. *Vaccines (Basel)* **9**, 285 (2021).
22. Wei, C.-J. *et al.* A bivalent Epstein-Barr virus vaccine induces neutralizing antibodies that block infection and confer immunity in humanized mice. *Sci Transl Med* **14**, eabf3685 (2022).
23. Kimura, T. *et al.* A localizing nanocarrier formulation enables multi-target immune responses to multivalent replicating RNA with limited systemic inflammation. *Mol Ther* **31**, 2360–2375 (2023).
24. O'Connor, M. A. *et al.* A replicon RNA vaccine can induce durable protective immunity from SARS-CoV-2 in nonhuman primates after neutralizing antibodies have waned. *PLoS Pathog* **19**, e1011298 (2023).
25. Khandhar, A. P. *et al.* Evaluation of repRNA vaccine for induction and in utero transfer of maternal antibodies in a pregnant rabbit model. *Mol Ther* **31**, 1046–1058 (2023).
26. Hawman, D. W. *et al.* Replicating RNA platform enables rapid response to the SARS-CoV-2 Omicron variant and elicits enhanced protection in naïve hamsters compared to ancestral vaccine. *EBioMedicine* **83**, 104196 (2022).
27. Leventhal, S. S. *et al.* Replicating RNA vaccination elicits an unexpected immune response that efficiently protects mice against lethal Crimean-Congo hemorrhagic fever virus challenge. *EBioMedicine* **82**, 104188 (2022).
28. Erasmus, J. H. *et al.* An Alphavirus-derived replicon RNA vaccine induces SARS-CoV-2 neutralizing antibody and T cell responses in mice and nonhuman primates. *Sci Transl Med* **12**, (2020).
29. HDT Bio. HDT Bio's COVID-19 Vaccine Wins Regulatory Approval in India. *https://www.hdt.bio/news-blog/hdt-bios-covid-19-vaccine-wins-regulatory-approval-in-india* (2022).

30. Regules, J. A. *et al.* Fractional Third and Fourth Dose of RTS,S/AS01 Malaria Candidate Vaccine: A Phase 2a Controlled Human Malaria Parasite Infection and Immunogenicity Study. *Journal of Infectious Diseases* **214**, 762–771 (2016).
31. Voysey, M. *et al.* Single-dose administration and the influence of the timing of the booster dose on immunogenicity and efficacy of ChAdOx1 nCoV-19 (AZD1222) vaccine: a pooled analysis of four randomised trials. *Lancet* **397**, 881–891 (2021).
32. Voysey, M. *et al.* Safety and efficacy of the ChAdOx1 nCoV-19 vaccine (AZD1222) against SARS-CoV-2: an interim analysis of four randomised controlled trials in Brazil, South Africa, and the UK. *Lancet* **397**, 99–111 (2021).
33. Oba, D. E. & Hutt-Fletcher, L. M. Induction of antibodies to the Epstein-Barr virus glycoprotein gp85 with a synthetic peptide corresponding to a sequence in the BXLF2 open reading frame. *J Virol* **62**, 1108–14 (1988).
34. Molesworth, S. J., Lake, C. M., Borza, C. M., Turk, S. M. & Hutt-Fletcher, L. M. Epstein-Barr Virus gH Is Essential for Penetration of B Cells but Also Plays a Role in Attachment of Virus to Epithelial Cells. *J Virol* **74**, 6324–6332 (2000).
35. Sathiyamoorthy, K. *et al.* Structural basis for Epstein-Barr virus host cell tropism mediated by gp42 and gHgL entry glycoproteins. *Nat Commun* **7**, 13557 (2016).
36. Fujiwara, S. & Nakamura, H. Animal Models for Gammaherpesvirus Infections: Recent Development in the Analysis of Virus-Induced Pathogenesis. *Pathogens* **9**, 116 (2020).
37. Fujiwara, S., Matsuda, G. & Imadome, K.-I. Humanized mouse models of epstein-barr virus infection and associated diseases. *Pathogens* **2**, 153–76 (2013).
38. Fujiwara, S., Imadome, K.-I. & Takei, M. Modeling EBV infection and pathogenesis in new-generation humanized mice. *Exp Mol Med* **47**, e135–e135 (2015).
39. Yajima, M. *et al.* A New Humanized Mouse Model of Epstein-Barr Virus Infection That Reproduces Persistent Infection, Lymphoproliferative Disorder, and Cell-Mediated and Humoral Immune Responses. *J Infect Dis* **198**, 673–682 (2008).
40. Münz, C. Humanized mouse models for Epstein Barr virus infection. *Curr Opin Virol* **25**, 113–118 (2017).
41. Münz, C. EBV Infection of Mice with Reconstituted Human Immune System Components. *Curr Top Microbiol Immunol* **391**, 407–23 (2015).
42. Yu, H. *et al.* A novel humanized mouse model with significant improvement of class-switched, antigen-specific antibody production. *Blood* **129**, 959–969 (2017).
43. Corbett, K. S. *et al.* SARS-CoV-2 mRNA vaccine design enabled by prototype pathogen preparedness. *Nature* **586**, 567–571 (2020).
44. Polack, F. P. *et al.* Safety and Efficacy of the BNT162b2 mRNA Covid-19 Vaccine. *N Engl J Med* **383**, 2603–2615 (2020).
45. Baden, L. R. *et al.* Efficacy and Safety of the mRNA-1273 SARS-CoV-2 Vaccine. *N Engl J Med* **384**, 403–416 (2021).
46. Walsh, E. E. *et al.* Safety and Immunogenicity of Two RNA-Based Covid-19 Vaccine Candidates. *N Engl J Med* **383**, 2439–2450 (2020).
47. Zhang, X. *et al.* Protective anti-gB neutralizing antibodies targeting two vulnerable sites for EBV-cell membrane fusion. *Proc Natl Acad Sci U S A* **119**, e2202371119 (2022).
48. Wu, Q. *et al.* Neutralizing antibodies against EBV gp42 show potent in vivo protection and define novel epitopes. *Emerg Microbes Infect* **12**, 2245920 (2023).
49. Sun, C. *et al.* A gB nanoparticle vaccine elicits a protective neutralizing antibody response against EBV. *Cell Host Microbe* **31**, 1882-1897.e10 (2023).
50. Taylor, G. S., Long, H. M., Brooks, J. M., Rickinson, A. B. & Hislop, A. D. The immunology of Epstein-Barr virus-induced disease. *Annu Rev Immunol* **33**, 787–821 (2015).
51. Cui, X. & Snapper, C. M. Epstein Barr Virus: Development of Vaccines and Immune Cell Therapy for EBV-Associated Diseases. *Front Immunol* **12**, 734471 (2021).
52. Cohen, J. I. Vaccine Development for Epstein-Barr Virus. *Adv Exp Med Biol* **1045**, 477–493 (2018).
53. Delecluse, H.-J., Hilsendegen, T., Pich, D., Zeidler, R. & Hammerschmidt, W. Propagation and recovery of intact, infectious Epstein–Barr virus from prokaryotic to human cells. *Proceedings of the National Academy of Sciences* **95**, 8245–8250 (1998).

54. Li, Q. X. *et al.* Epstein–Barr virus infection and replication in a human epithelial cell system. *Nature* **356**, 347–350 (1992).
55. Erasmus, J. H. *et al.* A Nanostructured Lipid Carrier for Delivery of a Replicating Viral RNA Provides Single, Low-Dose Protection against Zika. *Mol Ther* **26**, 2507–2522 (2018).
56. Neuhierl, B., Feederle, R., Hammerschmidt, W. & Delecluse, H. J. Glycoprotein gp110 of Epstein–Barr virus determines viral tropism and efficiency of infection. *Proceedings of the National Academy of Sciences* **99**, 15036–15041 (2002).
57. Sashihara, J., Burbelo, P. D., Savoldo, B., Pierson, T. C. & Cohen, J. I. Human antibody titers to Epstein–Barr Virus (EBV) gp350 correlate with neutralization of infectivity better than antibody titers to EBV gp42 using a rapid flow cytometry-based EBV neutralization assay. *Virology* **391**, 249–256 (2009).
58. Kimura, H. *et al.* Quantitative Analysis of Epstein-Barr Virus Load by Using a Real-Time PCR Assay. *J Clin Microbiol* **37**, 132–136 (1999).

Chapter 4. Defining a Novel Pathway of Epstein-Barr Virus Infection With Implications for Vaccine Development

This work is still in progress as of Feb 01, 2024

Authors: Kristina Edwards[1,2], Leah Homad[1], Karina Schmidt[1], Yu-Hsin Wan[1], Andrew McGuire[1,2,3]

[1]Vaccine and Infectious Disease Division, Fred Hutchinson Cancer Center, Seattle WA, USA.
[2]Department of Global Health, University of Washington, Seattle, WA, USA.
[3]Department of Laboratory Medicine and Pathology, University of Washington, Seattle WA, USA.

4.1 Abstract:

Epstein-Barr Virus (EBV) is an orally transmitted, γ-herpesvirus associated with development of a multitude of cancers and autoimmune conditions like multiple sclerosis. A vaccine to prevent infection and/or EBV-associated disease is urgently needed. An understanding of the neutralizing antibody response elicited by natural infection can help to inform promising vaccine targets. The viral attachment protein for B cell infection is gp350, and it has been a major target for vaccine design. The 72A1 mAb, previously isolated from a murine hybridoma, targets the EBV glycoprotein gp350, and potently neutralizes infection *in vitro.* Using a 'humanized' version of the 72A1 mAb in a humanized mouse model for EBV infection, we observed paradoxical behavior of 72A1, resulting in enhanced disease in humanized mice when delivered prior to viral challenge. Previous work by other groups has shown that murine 72A1 isolated from hybridoma cell lines is protective against EBV infection and disease, implying that the enhanced disease phenotype observed in experiments with humanized 72A1 involved the Fc region of this antibody. Here we show that mice given 0.5 mg of 72A1 prior to viral challenge displayed worsened disease outcomes compared to an irrelevant control, and that mutating the Fc region of this mAb to prevent FcɣR binding (72A1 silent Fc) leads to improved outcomes after

challenge compared to wild type. Accompanying *in vitro* work has shown that 72A1, but not the 72A1 silent Fc, is able to mediate attachment and infection to an otherwise resistant B cell line lacking the gp350 attachment ligands. However, this infection pathway appears to be less efficient than canonical gp350 mediated attachment and is perhaps not the sole explanation for the phenotype observed in the humanized mice. Further work in humanized mice is underway to better characterize immunological changes after infection in the presence of 72A1, as well as the effect of Fc affinity for FcɣR on this disease phenotype.

4.2 Introduction

Epstein Barr Virus (EBV) is a ubiquitous virus, infecting over 90% of adults globally[1]. Most people acquire EBV during early childhood, and primary infection is typically asymptomatic[2], yet can occasionally lead to the development of infectious mononucleosis (IM)[3,4]. EBV was also the first virus to be linked to the development of cancer[5]. EBV associated malignancies have been estimated to be responsible for 137,900–208,700 deaths per year[6]. EBV has also been linked to the development of auto immune conditions such as multiple sclerosis (MS)[7–9] and rheumatoid arthritis[10–12]. A vaccine against EBV would have the potential to lessen the morbidity and mortality caused by EBV associated disorders and confer significant benefit for global health[13].

Antibodies are the major correlate of protection for most successful vaccines[14], and all of the viral glycoproteins that mediate entry are targeted by neutralizing antibodies during infection[15–17]. It remains unclear which of these are the best to include in a potential vaccine. Most EBV vaccines to date target the viral protein gp350[18–22]. During B cell infection, gp350 mediates attachment by binding to CD21 or CD35 on the B cell surface[23–26]. Additionally, gp350 is the most abundant protein on the surface of the virus and it is the main target of antibodies

that neutralize EBV infection of B cells[18,27,28] . However, anti-gp350 antibodies do not prevent infection of epithelial cells[23,24,29–32] and in fact have been reported to enhance epithelial cell infection *in vitro*[33]. Moreover, mutated EBV lacking gp350 remains infectious *in vitro* and *in vivo*, although less efficiently than wild type virus[34]. In a phase two clinical trial testing a gp350-based vaccine, vaccination was able to prevent the development of IM after infection, but showed no efficacy in preventing infection[21].

Due to the failure of gp350-based vaccines to prevent infection, other EBV glycoproteins may make more appropriate vaccine targets. Among these, the glycoproteins involved in viral fusion with both cell types, gH/gL and gB are potential vaccine targets [27,35–37]. gB is the fusion protein that mediates the merger of the host and viral membranes. Its activity is dependent on gH and gL, which form a heterodimeric complex that trigger gB activity following a conformational change resulting from the engagement of one or more cellular receptors[38–41].

One way to identify promising targets for vaccine design is to isolate and characterize antibodies that are able to neutralize infection. Determining if and how antibodies against EBV can prevent infection *in vitro* and in animal models can inform vaccine design. A difficulty of evaluating EBV in animal models is that EBV, like other gamma-herpesvirus, is very specific for its host[42,43]. However, there are animal models that facilitate study of the virus. For a small animal model of EBV, humanized mice are often used. These are sublethally irradiated NOD-*scid* IL2Rg^{null} (NSG) mice that have been engrafted with human peripheral blood stem cells[44,45]. This reconstitutes most components of the human hematopoietic system in the mice[45–48]. Humanized mice can then be infected with EBV and used to model B cell infection, but not epithelial cell infection as the murine epithelial cells do not support viral infection[49]. EBV infected humanized mice recapitulate some aspects of human disease. Viral DNA can be detected in the blood and in certain organs including the spleen, lymph nodes, and kidneys of infected mice, and immunophenotyping of these mice shows a characteristic decrease in B cells and a

corresponding rise in cytotoxic CD8+ T cells specific for EBV infected B cells[44,45,49]. Additionally, depending on viral challenge dose, mice may also develop fatal lymphoproliferative disorders[44,45,49].

The humanized mouse model can be used to evaluate the efficacy of potential interventions against infection *in vivo*. For example, passive transfer of neutralizing mAbs into humanized mice before EBV challenge can be performed to evaluate *in vivo* antibody-mediated protection[37,50–53]. Here we show that passive delivery of the anti-gp350 mAb 72A1 in the humanized mouse model enhanced disease *in vivo* despite being potently neutralizing *in vitro*. Further work has determined that this effect is related to the Fc portion of this mAb. We generated a 72A1 mAb that has impaired binding to FcɣR (72A1 silent Fc)[54]. Passive delivery of 72A1 silent Fc to humanized mice prior to EBV challenge led to improved survival compared to WT 72A1. Additional *in vitro* work has shown a potential for WT 72A1, but no other tested mAbs, to mediate infection in an otherwise resistant B cell line in an Fc-dependent manner. There's an established precedent for antibodies mediating viral infection through Fc-receptor binding to the Fc region of antibodies bound to virus. For example, in Dengue virus, cross reactive non-neutralizing antibodies allow for enhanced pathology via uptake of virus through FcɣR, rather than canonical viral entry receptors[55]. In addition to cross-reactive non neutralizing antibodies, antibody dependent enhancement of infection can also occur with sub-neutralizing concentrations of neutralizing antibodies[55]. The specific mechanism of 72A1 mediated enhancement of disease observed in the humanized mouse model is still under investigation, but has potential implications for the design of EBV vaccines and decisions of what viral antigens to target.

4.3 Results and Discussion:

4.3.1 'Humanized' 72A1 mediates worsened disease in humanized mice

We previously compared the protection mediated by two antibodies, AMMO1 and 72A1, that can potently neutralize EBV infection of B cells *in vitro*. AMMO1 was isolated from PBMC of an asymptomatic EBV carrier[56], whereas 72A1 was purified from a mouse hybridoma cell line[23,57]. In order to make these antibodies more comparable, 72A1 was expressed in plasmids encoding the human IgG1 heavy chain and human lambda light chain[50] as to mitigate any kinetic or effector function differences that might have arisen due to the species of origin. Mice received 0.5 mg antibody via IP injection, then 48 hours post antibody transfer, mice were challenged with a sublethal dose of EBV (Fig. 1A). Following challenge, mice were monitored for signs of infection including viremia and weight loss (Fig. 1A). These data are combined from two independent experiments, one experiment was previously published in Singh *et al*. 2020[50], and the second experiment an unpublished repeat to confirm the observed disease enhancement. After viral challenge, all negative control mice had no detectable virus in the spleen and survived the study period, while all positive infected control mice had viral titers in the spleen, slight splenomegaly, and all mice survived EBV challenge (Fig. 1B-D). Mice treated with AMMO1 were similar to negative controls, barring one mouse with low level virus in the spleen (Fig. 1B-D). However, mice receiving 72A1 had increased viremia, splenomegaly, and 40% mortality (Fig. 1B-D).

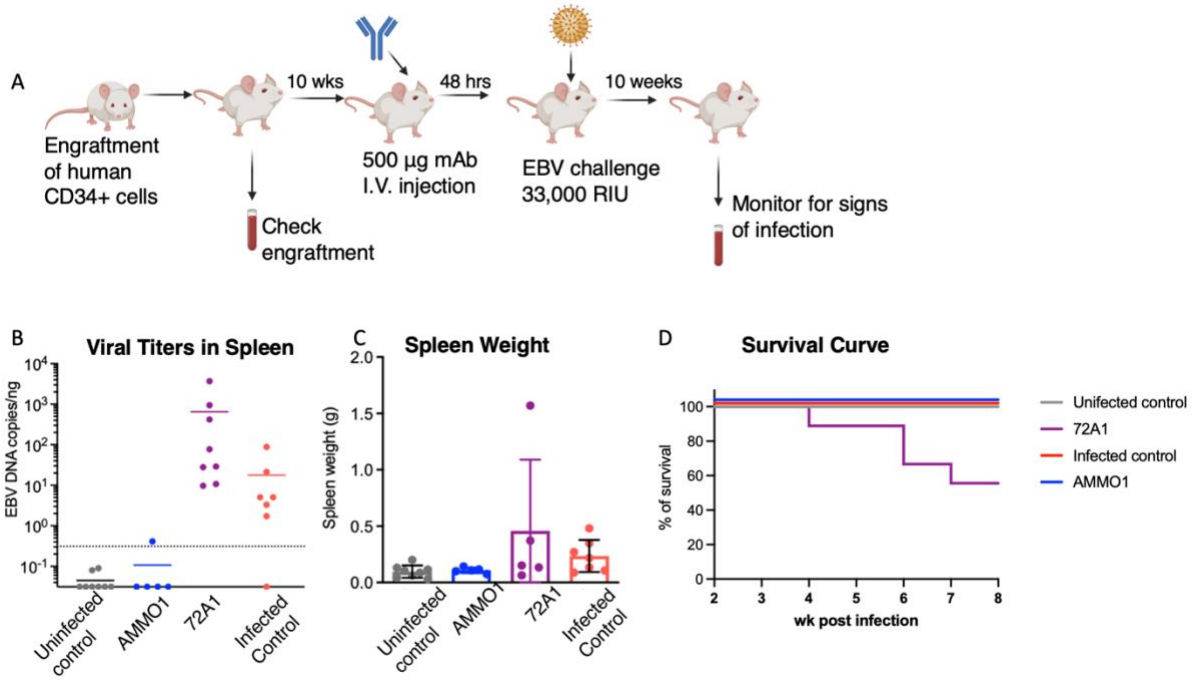

Figure 1 Transfer of 72A1 leads to enhanced disease in humanized mouse challenge model.

(**A**) Experimental design: Groups of humanized mice were given intraperitoneal injections of 500 ug 72A1 (n=8), AMMO1 (n=5), or PBS (infected control n=7 and uninfected control n=8) 48 hours prior to EBV challenge. Infected control, 72A1, and AMMO1 groups received 33,000 RIU EBV while the uninfected control group received PBS via r.o. injection. Mice were monitored for signs of infection. (**B**) Viral DNA copy number was quantified in splenic DNA extracts at necropsy. Each dot represents an individual mouse, the bar represents the median copy number, and the dashed line indicates the limit of detection. (**C**) Spleen weights at necropsy, each dot represents an individual mouse, and bar represents the median weight. (**D**) Kaplan-Meier curve showing survival after challenge.

4.3.2 72A1 mediates worsened disease in Fc-dependent manner

The lack of protection and enhanced mortality, splenic viral load and splenomegaly in the 72A1 group was surprising given, the mAb's potent B cell neutralization *in vitro* [23,57] . Additionally, a prior study by Haque et al showed passive delivery of 72A1 in a similar humanized mouse model was protective against EBV driven tumor formation[52]. The 72A1 antibody in the Haque et al study was isolated directly from the murine hybridoma cell line[52]. The disparate outcomes between the two studies led us to the hypothesis that the Fc region of this mAb was involved in mediating worsened outcomes after challenge.

To investigate this further, we made a mutant 72A1 mAb with Fc mutations E233P/L234V/L235A/G236del/S267K to abrogate binding to Fc gamma receptor[54] (72A1 Silent Fc). We gave mice 0.5 mg of WT (humanized) 72A1, 72A1 silent Fc, AMMO1, or an irrelevant mAb (VRC01) 24 hours prior to challenge (Fig. 2A). In this study mice were given a lethal dose (50,000 RIU) EBV (Fig. 2A). After challenge, mice given AMMO1 did not have detectable virus in blood at any timepoint tested (Fig. 2B), while all other groups had detectable virus prior to the end of the study. All mice given AMMO1 survived until the end of the study (Fig. 2C). As a infection control, mice were given VRC01 prior to challenge, and all mice in this group became viremic (Fig. 2B) and succumbed to infection during the study (Fig. 2C). The enhanced infection phenotype observed after treatment with WT 72A1 in Fig. 1 was replicated, with mice having detectable virus and earlier mortality compared to the infection control (VRC01) group (Fig. 2B and C). All mice in the WT 72A1 group had met study endpoints by week 7 post infection, compared to week 9 for the VRC01positive control group. Mice that received silent Fc 72A1 all became viremic, but these mice had increased survival compared to both the WT 72A1 and the positive control groups, with 60% survival by the end of study (Fig. 2B and C).

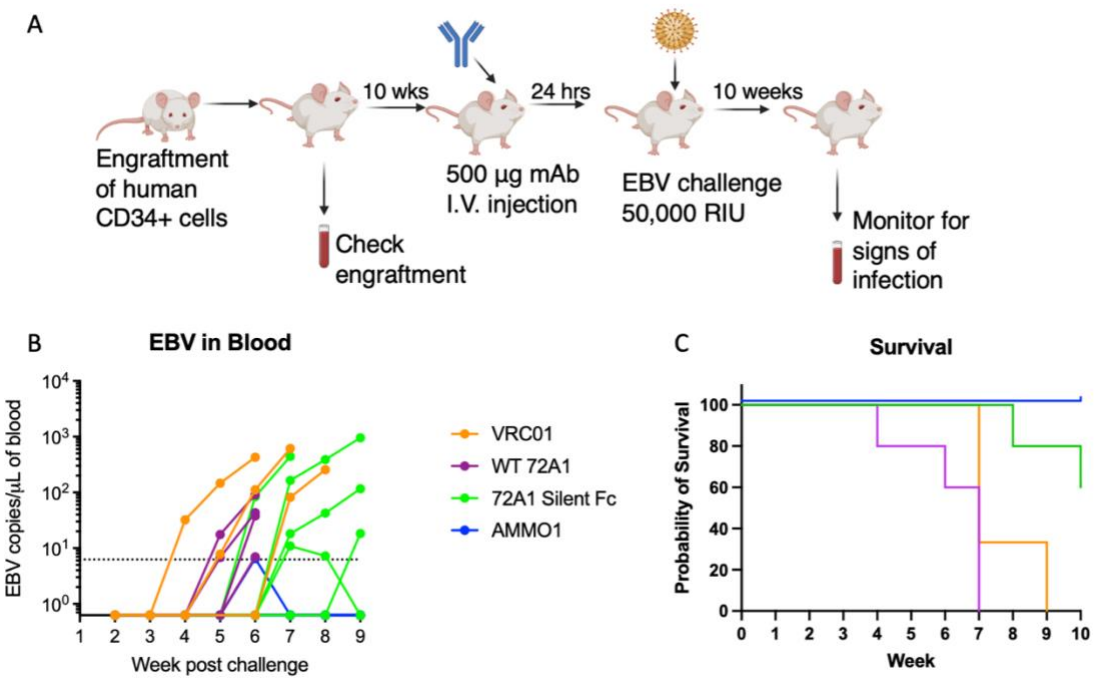

Figure 2: Humanized mouse challenge after treatment with 72A1 or 72A1 silent Fc mAb.

(**A**) Experimental design: Groups of humanized mice were given intraperitoneal injections of 500 ug WT 72A1 (n=5), Silent Fc 72A1 (n=4), VRC01 (n=3) or AMMO1 (n=5) 24 hours prior to EBV challenge. At challenge all mice received 50,000 RIU EBV via r.o. injection. Mice weighed 3x weekly and bled 1x per week to monitor for signs of infection. (**B**) Viral DNA in the peripheral blood of VRC01 mice, WT 72A1 mice, 72A1 silent Fc mice, and AMMO1 mice was measured by qPCR as indicated. (**C**) Kaplan-Meier curve showing survival after challenge.

4.3.3 Otherwise resistant B cells become susceptible to 72A1-mediated EBV attachment in an Fc-dependent manner

The observed *in vivo* data suggests a role for the Fc portion of the mAb playing a role in the observed disease enhancement. This led us to a model where typically attachment is mediated by the viral protein gp350 binding to either CD21 or CD35 on the B cell (Fig. 3A). However, an antibody against gp350 can disrupt this canonical attachment but still mediate attachment via binding of the antibody both to the viral antigen and to FcɣR on the cell (Fig. 3B).

To further investigate a potential mechanism behind what we observed in the humanized mice, transgenic cell lines were created to assess the ability of 72A1 to mediate attachment in an Fc-dependent manner. NALM6 cells are a pre-B cell line that do not express CD21 or CD35[26], the two canonical B cell attachment receptors for EBV[25,26], making them resistant to EBV infection. Using these cells we generated a transgenic cell line expressing the human FcɣRiib, NALM6-FcɣRiib. These cells were then used to see if WT 72A1, silent Fc 72A1, and AMMO1 were capable of mediating attachment of fluorescently labelled gp350 or gH/gL. We saw no fluorescent labelling of parental NALM6 cells with gH/gL or gp350 in the presence or absence of antibody (Fig. 3C). However the NALM6-FcɣRiib cells stained positive for gH/gL or gp350 when a mAb that can bind the fluorescent antigen and had an intact Fc region was present (Fig. 3C), demonstrating attachment of the antigen to the cells in an Fc-dependent manner.

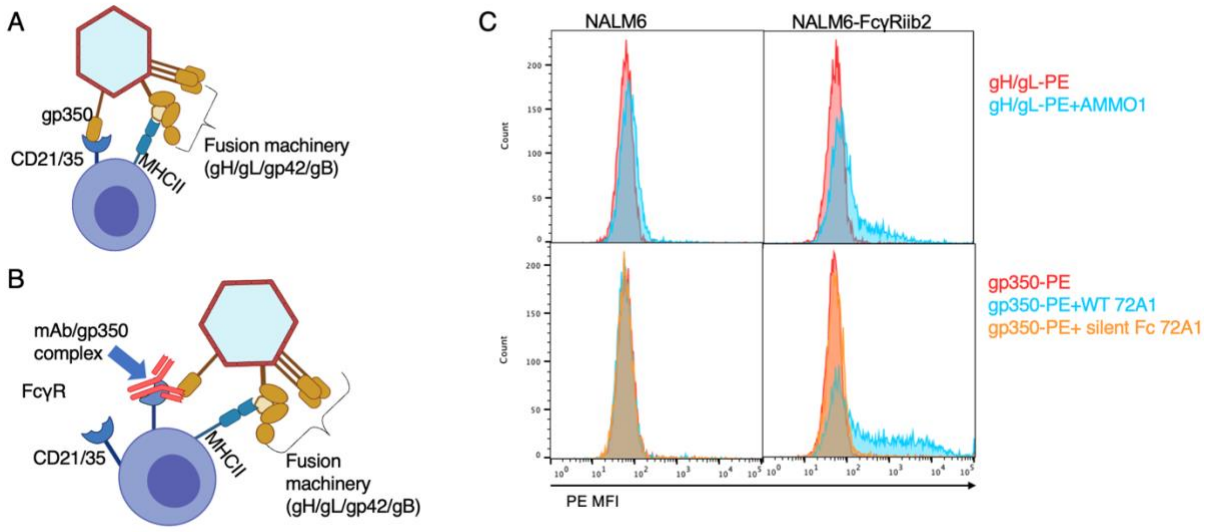

Figure 3: Fc-dependent attachment of EBV glycoproteins.

(**A**) Canonical method of EBV attachment to B cells, utilizing EBV gp350 binding to CD21 or CD35 on the B cell surface. (**B**) Alternative (proposed) method of Fc-mediated EBV attachment, where antibodies against gp350 can block canonical binding but facilitate Fc-mediated attachment via antibody/virus complex binding to FcɣRiib on the B cell surface. (**C**) Attachment staining of NALM6 and NALM6-FcɣRiib cells with fluorescently labelled gH/gL with and without AMMO1, and gp350, with and without WT 72A1 and silent Fc 72A1.

4.3.4 Fc mediated infection is limited to 72A1

We next wanted to determine if Fc-mediated attachment could promote downstream infection. To do this, EBV was incubated with mAb or media alone prior to infection of NALM6 or NALM6-FcɣRiib. We also included NALM6 cells transduced with CD21 (NALM6-CD21) to act as a point of reference for the normal attachment and infection process for EBV. NALM6-FcɣRiib cells, where only infected when virus was pre-incubated with WT 72A1, but not virus alone, silent Fc 72A1, or AMMO1 (Fig. 4A). AMMO1 is a neutralizing antibody that inhibits fusion, step downstream of the initial attachment step, so while this antibody may be capable of mediating attachment, it is not able to mediate infection as it still prevents viral fusion. We next tested a panel of mAbs against EBV gH/gL with varying neutralizing capabilities against B cell infection (Fig. 4B). We found no antibody mediated infection in the parental NALM6 cell line (Fig. 4B). Interestingly, we saw that antibody mediated infection in NALM6-FcɣRiib cells was limited to WT 72A1 (Fig. 4B). Other mAbs included in the panel, like E1D1, bind to gH/gL with high affinity but are poorly neutralizing against B cell infection. This indicates that the viral antigen bound by an antibody may influence whether or not Fc-mediated infection can take place. Using our transgenic NALM6 infection assay, Fc-mediated infection is noticeably less efficient than infection via canonical attachment through gp350 binding to CD21 (Fig. 4C). In this cell type mAbs retained their expected neutralization against B cell infection, with 72A1 and AMMO1 displaying potent neutralization while E1D1 and CL40 showed intermediate neutralization (Fig. 4C).

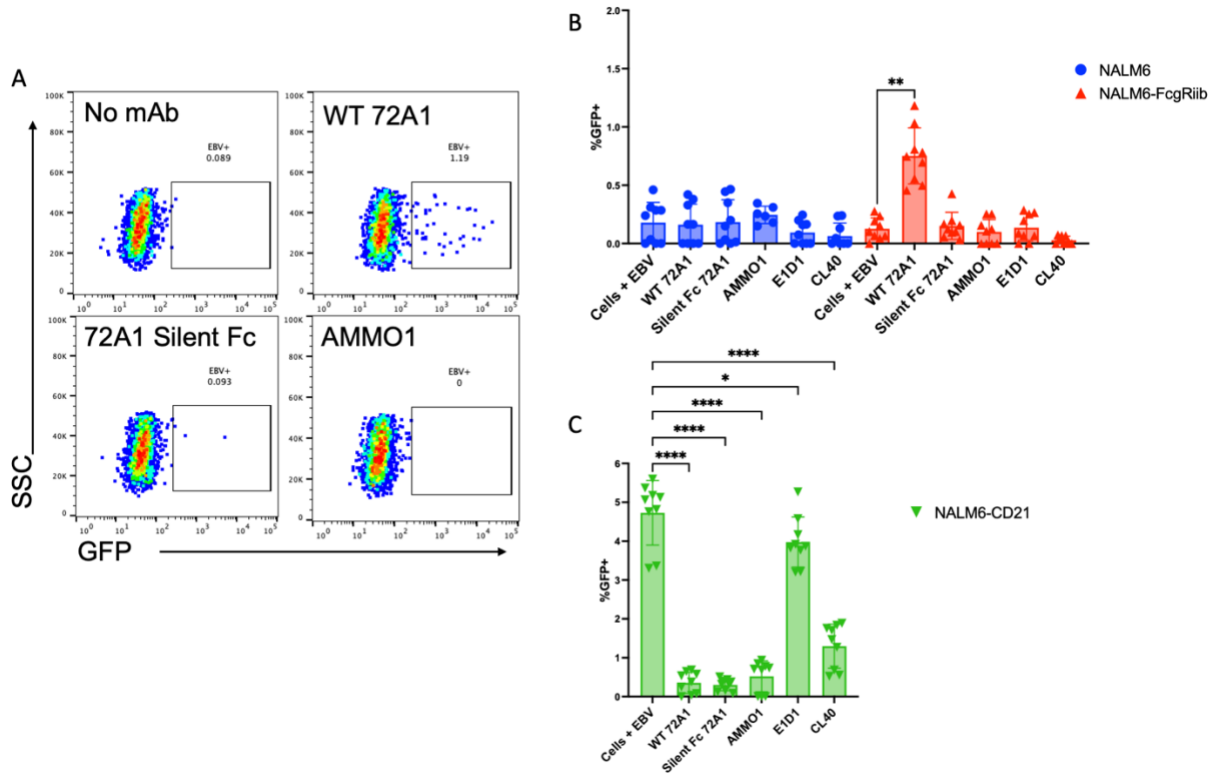

Figure 4: Fc-mediated attachment facilitates EBV infection in vitro.

(**A**) Infection of NALM6-FcɣRiib with EBV incubated with cRPMI, WT 72A1, Silent Fc 72A1, and AMMO1 as indicated. Representative wells are shown. (**B**) Infection of NALM6 or NALM6-FcɣRiib cells with indicated conditions. Each condition ran in triplicate, with three replicates. For each cell type, each infection condition was compared to the cells + EBV condition and significance determined by Dunn's multiple comparisons test. ** indicates a significance below 0.01. No comparison was shown on the plot for P values above 0.05. (C) NALM6-CD21 cells with indicated conditions. Each condition ran in triplicate, with three replicates. Each infection condition was compared to the cells + EBV condition and significance determined by Dunn's multiple comparisons test. * indicates a significance below 0.05, **** indicates significance below 0.0001.

4.4 Conclusions and future directions:

Using the humanized mouse model for EBV infection, we are able to repeatably show that the WT 72A1 mAb, while neutralizing *in vitro*, seems to mediate worsened disease in an Fc dependent mechanism. However, this work is still ongoing. As noted in Fig. 4B, 72A1 can mediate infection of otherwise resistant B cell lines in an Fc-dependent manner, which could potentially explain the lack of protection observed with 72A1 in the humanized mouse model. Yet *in vitro*, the level of infection via Fc-mediated attachment is still much lower than infection using the canonical attachment receptor. The low-level infection we've modeled *in vitro* does not explain the worsened disease outcomes observed *in vivo*. In addition, our Fc-mediated infection assay uses transgenic NALM6-FcɣRiib cells. These cells have been transduced to express FcɣR at a high level, and express FcɣR higher than another B cell line, Raji B cells, that are commonly used in infection assays with EBV (data not shown). To date, I have been unable to demonstrate Fc-mediated attachment using the Raji cell line (not shown). While we have been able to demonstrate that Fc-mediated attachment and infection can occur *in vitro*, the relevance of this towards explaining the WT 72A1 mediated enhanced disease phenotype in the humanized mouse model remains to be determined. However it appears the Fc portion of the antibody is involved, as passive transfer of 72A1 silent Fc led to better survival in humanized mice compared to WT 72A1.

We hypothesize that in the enhanced disease seen in humanized mice, other cell types are involved in infection beyond B cells. EBV has been reported to infect T cells[58–60], monocytes[61], and NK cells[62–64] in certain contexts. It is therefore possible that EBV bound by 72A1 allows for EBV infection of a non-B cell. NK cells and monocytes both display FcɣR that has a much higher affinity for IgG1 than the FcγR subtype displayed by B cells[65,66]. In theory this could lead to better binding of antibody/virus complexes to the cell, and in turn, more efficient infection.

Previous work has shown that NK cells are necessary for control of EBV in humanized mice, and depletion or perturbation of the NK cell subset led to enhanced viremia, splenomegaly, and earlier mortality[64]. As these results mirror what we observe with 72A1 in our work, we plan on investigating (1) whether EBV can infect NK cells in an Fc dependent manner *in vitro* and (2) if immune perturbations soon after challenge in humanized mice treated with 72A1.

Another noteworthy finding from our *in vitro* work is that the ability to mediate Fc-dependent infection seems limited to 72A1 (Fig. 4B). We tested mAbs against EBV gH/gL that are non-neutralizing against B cell infection, but did not observe any Fc-dependent infection. This could be due to gp350 being the most abundant protein on the virion surface[28], making 72A1 more efficient at mediating EBV attachment via FcɣR than antibodies against the less abundant gH/gL. 72A1 is the only mAb against EBV gp350 with a publicly available sequence. We are in the process of generating more neutralizing and non-neutralizing antibodies against EBV gp350, and hope to use these to further investigate the role antigen binding plays in the Fc-mediated infection we've observed.

It is possible that this antibody mediated enhancement of disease after EBV infection is an artefact of the humanized mouse model. It is true that while humanized mice develop human B cells, full immunophenotyping has not been performed using these mice. The effects seen here could be mediated by atypical immune populations that arise in this mixed species immune model. However, if this is the case it is still important to understand. Humanized mice are the primary small animal model used to study EBV, and have been used for efficacy studies of different EBV mAbs and vaccine candidates[46,67,68]. However, if this Fc mediated infection can occur in humans, this would be very important to know and understand. If antibodies against gp350 fail to protect because of an ability to mediate attachment to host immune cells in a manner that allows for downstream infection, this is very important to know when designing prophylactic vaccines. As mentioned previously in this thesis, gp350 has historically been the

major target of vaccine design[19,21,69–72], and many vaccines being developed still include gp350 as a target antigen (NCT04645147, NCT05164094). The work described here and the work currently underway will help further characterize an important animal model for EBV, and the potential role of antibodies against a major vaccine target.

4.5 Methods:

Antibody production:

pTT3-derived antibody expression plasmids encoding antibody heavy and light chains (as described previously[50,56]) were co-transfected into 293E cells at a density of $1x10^6$ cells/ml in Freestyle 293 media using the 293Free transfection reagent according to the manufacturer's instructions. Expression was carried out in Freestyle 293 media for 6 days, after which cells and cellular debris were removed by centrifugation at 4,000xg followed by filtration through a 0.22 µm filter. Clarified cell supernatant containing recombinant antibodies was passed over Protein A Agarose, followed by washing with PBS, and elution with 1 mL of Pierce IgG Elution Buffer, pH 2.0, into 0.1 mL of Tris HCl, pH 8.0. Purified antibodies were then buffer exchanged into PBS and sterile filtered before use.

Silent Fc 72A1 HC plasmid was produced by cloning the variable heavy chain of 72A1 into a pre-existing silent Fc[54] construct by Gibson assembly. For production of Silent Fc 72A1 mAbs, the Silent Fc 72A1 HC and WT 72A1 LC plasmids were co-transfected into 293E cells and antibody production carried out as described above.

Mice

NOD-scid Il2rgnull (NSG) and C57BL/6 mice were housed in a specific pathogen-free facility at FHCC. The facility is accredited by the Association for Assessment and Accreditation of

Laboratory Animal Care. Mice were handled in accordance with the NIH Guide for the Care and Use of Laboratory Animals, and experiments were approved by the FH Institutional Animal Care and Use Committee and Institutional Review Board. All C57BL/6 and NSG mice used in this study were female and 6 weeks old when experiments were initiated.

EBV infection in humanized mice

Twenty-five six week old NSG mice were irradiated (275R of total body irradiation) and received $1x10^6$ $CD34^+$ huPBSC in 200 µl PBS through i.v. injection. Eight weeks later, successful human cell engraftment was confirmed by the presence of human $CD45^+$ cells in peripheral blood by flow cytometry. Using 50 µl blood, RBCs were lysed and cells were stained using a BV510 viability dye, and the following antibodies at a 1:100 dilution unless otherwise noted: hCD45 FITC (eBioscience Cat. #5010066), mCD45 APC (eBioscience Cat. #17-0451-82) (1:500 dilution), hCD33 PE (BD Bioscience Cat. #555450), hCD19 BV711 (Biolegend Cat.# 302246), hCD4 AF700 (eBioscience Cat. #56-0048-82) and hCD8 BV421 (BD Bioscience Cat. #562429). Cells were stained for 30 min on ice, washed twice in FACS buffer, fixed in 200 µl of 10% formalin 15 min on ice, washed and resuspended in 200 µl FACS buffer for acquisition and analyzed on a BDFACS Celesta. 10 weeks post-engraftment, 500 µg of experimental or control antibodies were injected per humanized NSG mouse via intraperitoneal injection (i.p.). 24 hr later, mice were bled in the left eye to confirm passive transfer of IgG, and received a dose of EBV B95.8/F67 equivalent to 33,000 Raji infectious units or 50,000 Raji infectious units (depending on experiment) via retro-orbital injection in the right eye. Each group of mice receiving the same IgG preparation and/or EBV were housed separately from each other. Mice were weighed three times weekly. Beginning at two weeks post-infection, peripheral blood samples were collected to measure the presence of EBV DNA in whole blood. Twelve weeks post-challenge, or until mice lost 20% of their starting weight, mice were euthanized. Spleens

were photographed and weighed, then DNA was extracted from splenocytes utilizing the DNeasy Blood & Tissue Kit (QIAGEN) and according to the manufacturer's instructions for subsequent viral load analysis.

Quantitative PCR analysis EBV DNA in huCD34 engrafted mice

A primer-probe mix specific for the EBV BALF5 gene[73] was used to quantify EBV in DNA extracted from blood or spleen in hCD34 engrafted NSG recipient mice at the time points described. Each 25 µl qPCR reaction contained 12.5 µl QuantiTect Probe PCR Master Mix (QIAGEN), 600 nM of each primer and 300 nM of FAM-labeled probe (IDT), 1.25 µl of a TaqMan VIC-labeled RNase-P primer probe mix (Fisher Sci Cat. #4316844). For analysis of splenocytes, reactions contained 1 µg DNA extracted from splenocytes as template. To analyze EBV in peripheral blood, 50 µl of blood collected via cardiac puncture or retro-orbital bleed DNA extracted using the DNeasy Blood and Tissue Kit (QIAGEN) and eluted in 50 µl of Buffer AE (QIAGEN). 10 µl of extracted DNA was used as template in qPCR. Reactions were heated to 95ºC for 15 minutes to activate DNA polymerase followed by 50 cycles of 95ºC for 15 s 60ºC for 60 s, on an Applied Biosystems QuantStudio 7 Flex Real Time PCR System. Synthetic DNA fragments containing the BALF5 target gene as well as flanking genomic regions were synthesized as double stranded DNA gBlocks (IDT), and were used to generate a standard curve with known gene copy numbers ranging from 10^7-10^0 copies/µl. The copy number in extracted DNA was determined by interpolating from the standard curve. Serial dilutions of reference standard were used to experimentally determine a limit of detection of 6.25 copies, which corresponds to the amount of template that can be detected in > 95% of reactions. For graphical purposes, samples with no amplification or those yielding values below the limit of detection were assigned a value of 0.625 copies.

Plasmids

To generate CD21 lentiviral plasmid, the coding sequence for CD21 (GenBank ID BC090937.1) was codon optimized and cloned into pTwist Lenti SFFV Puro WPRE (Twist Biosciences).

Lentiviral Production:

5.46 µg of psPAX2, 2.73 µg of pMD2.G (both gifts from Didier Trono), and 11.05 µg of p156RRL-sinPPT-CMV-GFP-PRE/Nhe I FcgRiib plasmid (gift from Leslie Goo) or 11.05 µg of CD21 plasmid (Twist Bio) were mixed in 1.56mL PBS followed by 39 µL of 293-Free Transfection Reagent. The transfection mix was gently agitated, incubated at room temperature for 15 minutes, and added dropwise to 13 mL of suspension-adapted 293T cells at 2×10^6 cells/mL in a 125 mL flask. After 24 hours, an additional 15 mL of 293 Freestyle media containing 15 µg of valproic acid is added to the cell culture. After another 48 hours, the cell culture was centrifuged at 1000 × *g* for 3 minutes, the supernatant is passed through a 0.44 µm filter, aliquoted, and stored at -80ºC.

Lentiviral Transduction:

In a 6 well plate, 4 µg/mL polybrene was added to 3 mL of NALM6 cells at 3×10^6 cells/mL, along with 3 mL of supernatant containing either CD21 or FcɣRiib lentiviral particles. 24 hours following transduction, wells were moved to 25 ml TC flasks and 5mL fresh cRPMI added to the culture. After 72-96 hours, cells were stained for surface expression of FcɣR or CD21 by flow cytometry. A Guava easyCyte Flow Cytometer was used to monitor anti-CD21 (Biolegend Cat. #354903) or anti FcɣR (Biolegend Cat. #303206) staining. Cells were expanded and cultured with puromycin to select for transduced cells in culture.

Antibody mediated attachment staining

Biotinylated EBV gH/gL and gp350 (as described in Snijder et al.[56]) was conjugated to streptavidin-PE (Invitrogen Cat. #S866). 10 µg of protein was conjugated to 4 µl streptavidin-PE. NALM6 (transgenic or parental) cells were resuspended at $1x10^6$ cells/ml in FACS buffer, and 100 µl of each was transferred to 6x 2 ml FACS tubes for each cell type. For each cell type, one tube received either nothing, gH/gL alone, gH/gL with AMMO1, gp350 alone, gp350 with 72A1, and gp350 with silent Fc 72A1. Cells were stained on ice for 30 min in the dark, washed once in 2 ml FACS buffer, and fixed in 10% formalin. Cells were resuspended in 200 µl FACS buffer and the percentage of PE+ cells was determined using a Luminex Guava HT.

Preparation of EBV Reporter Viruses

To produce B-cell tropic GFP reporter viruses (B95-8/F), $5×10^6$ 293–2089 cells were seeded on a 100mm tissue culture dish in cRPMI containing 100 µg/ml hygromycin. 48 hr later the cells were washed with PBS, the media was replaced with cRPMI without hygromycin, and cells were transfected with 6 µg each of p509 and p2670 expressing BZLF1 and BALF4, respectively, using GeneJuice transfection reagent (SigmaAldrich Cat. #70967)[74,75]. 72 hr post transfection, the cell supernatant was collected and centrifuged at 500 × *g* for 3 min to pellet any cell debris, and passed through a 0.8 µm filter. Virions were concentrated 25-50-fold by centrifugation at 25,000 × *g* for 2 hr and re-suspended in PBS. Virus was stored at -80°C and thawed immediately before use.

Antibody mediated infection assay

Different mAbs were diluted to 20 µg/ml in cRPMI, and 20 µl cRPMI was added to a 96-well round-bottom plate in triplicate. 25 µl B95-8/F virus diluted to achieve an infection frequency of approximately 10-15% in Raji cells was added and plates were incubated for 1hr at 37°C. Following the incubation, 50 µl of cells at $1×10^6$ cells/ml was added to each well and incubated

for 72 hr at 37°C, 5% CO_2. After incubation, cells were fixed in 10% formalin and the percentage of GFP+ Raji cells was determined using a Luminex Guava HT or BDFACS Celesta. To account for any false positive cells due to auto-fluorescence in the GFP channel, the average %GFP^+ cells in negative control wells (n=5-10) was subtracted from each well. Each infection assay was repeated 3 times. Statistical differences were determined by Dunn's multiple comparison test using GraphPad Prism Version 10.1.1.

4.6 Chapter 4 Bibliography

1. Cohen, J. I. Epstein–Barr Virus Infection. *New England Journal of Medicine* **343**, 481–492 (2000).
2. Balfour, H. H. *et al.* Age-Specific Prevalence of Epstein–Barr Virus Infection Among Individuals Aged 6–19 Years in the United States and Factors Affecting Its Acquisition. *J Infect Dis* **208**, 1286–1293 (2013).
3. Henle, G., Henle, W. & Diehl, V. Relation of Burkitt's tumor-associated herpes-ytpe virus to infectious mononucleosis. *Proceedings of the National Academy of Sciences* **59**, 94–101 (1968).
4. Dunmire, S. K., Hogquist, K. A. & Balfour, H. H. Infectious Mononucleosis. in 211–240 (2015). doi:10.1007/978-3-319-22822-8_9.
5. Epstein, M. A., Achong, B. G. & Barr, Y. M. VIRUS PARTICLES IN CULTURED LYMPHOBLASTS FROM BURKITT'S LYMPHOMA. *The Lancet* **283**, 702–703 (1964).
6. Wong, Y., Meehan, M. T., Burrows, S. R., Doolan, D. L. & Miles, J. J. Estimating the global burden of Epstein-Barr virus-related cancers. *J Cancer Res Clin Oncol* **148**, 31–46 (2022).
7. Bjornevik, K., Münz, C., Cohen, J. I. & Ascherio, A. Epstein-Barr virus as a leading cause of multiple sclerosis: mechanisms and implications. *Nat Rev Neurol* **19**, 160–171 (2023).
8. Bjornevik, K. *et al.* Longitudinal analysis reveals high prevalence of Epstein-Barr virus associated with multiple sclerosis. *Science (1979)* **375**, 296–301 (2022).
9. Lanz, T. V. *et al.* Clonally expanded B cells in multiple sclerosis bind EBV EBNA1 and GlialCAM. *Nature* **603**, 321–327 (2022).
10. Balandraud, N. & Roudier, J. Epstein-Barr virus and rheumatoid arthritis. *Joint Bone Spine* vol. 85 165–170 Preprint at https://doi.org/10.1016/j.jbspin.2017.04.011 (2018).
11. Sorgato, C. C. *et al.* EBV and CMV viral load in rheumatoid arthritis and their role in associated Sjögren's syndrome. *Journal of Oral Pathology and Medicine* **49**, 693–700 (2020).
12. Callan, M. F. C. Epstein-Barr virus, arthritis, and the development of lymphoma in arthritis patients. *Curr Opin Rheumatol* **16**, 399–405 (2004).
13. Cohen, J. I. Vaccine Development for Epstein-Barr Virus. *Adv Exp Med Biol* **1045**, 477–493 (2018).
14. Plotkin, S. A. Correlates of Protection Induced by Vaccination. *Clinical and Vaccine Immunology* **17**, 1055–1065 (2010).
15. Sashihara, J., Burbelo, P. D., Savoldo, B., Pierson, T. C. & Cohen, J. I. Human antibody titers to Epstein–Barr Virus (EBV) gp350 correlate with neutralization of infectivity better than antibody titers to EBV gp42 using a rapid flow cytometry-based EBV neutralization assay. *Virology* **391**, 249–256 (2009).

16. Bu, W. *et al.* Kinetics of Epstein-Barr Virus (EBV) Neutralizing and Virus-Specific Antibodies after Primary Infection with EBV. *Clinical and Vaccine Immunology* **23**, 363–369 (2016).
17. Xiao, J., Palefsky, J. M., Herrera, R., Sunshine, C. & Tugizov, S. M. EBV-positive human sera contain antibodies against the EBV BMRF-2 protein. *Virology* **393**, 151–9 (2009).
18. Thorley-Lawson, D. A. & Poodry, C. A. Identification and isolation of the main component (gp350-gp220) of Epstein-Barr virus responsible for generating neutralizing antibodies in vivo. *J Virol* **43**, 730–736 (1982).
19. Gu, S. Y. *et al.* First EBV vaccine trial in humans using recombinant vaccinia virus expressing the major membrane antigen. *Dev Biol Stand* **84**, 171–7 (1995).
20. Moutschen, M. *et al.* Phase I/II studies to evaluate safety and immunogenicity of a recombinant gp350 Epstein–Barr virus vaccine in healthy adults. *Vaccine* **25**, 4697–4705 (2007).
21. Sokal, E. M. *et al.* Recombinant gp350 Vaccine for Infectious Mononucleosis: A Phase 2, Randomized, Double-Blind, Placebo-Controlled Trial to Evaluate the Safety, Immunogenicity, and Efficacy of an Epstein-Barr Virus Vaccine in Healthy Young Adults. *J Infect Dis* **196**, 1749–1753 (2007).
22. Rees, L. *et al.* A Phase I Trial of Epstein-Barr Virus Gp350 Vaccine for Children With Chronic Kidney Disease Awaiting Transplantation. *Transplantation* **88**, 1025–1029 (2009).
23. Hoffman, G. J., Lazarowitz, S. G. & Hayward, S. D. Monoclonal antibody against a 250,000-dalton glycoprotein of Epstein-Barr virus identifies a membrane antigen and a neutralizing antigen. *Proceedings of the National Academy of Sciences* **77**, 2979–2983 (1980).
24. Thorley-Lawson, D. A. & Geilinger, K. Monoclonal antibodies against the major glycoprotein (gp350/220) of Epstein-Barr virus neutralize infectivity. *Proceedings of the National Academy of Sciences* **77**, 5307–5311 (1980).
25. Fingeroth, J. D. *et al.* Epstein-Barr virus receptor of human B lymphocytes is the C3d receptor CR2. *Proceedings of the National Academy of Sciences* **81**, 4510–4514 (1984).
26. Ogembo, J. G. *et al.* Human Complement Receptor Type 1/CD35 Is an Epstein-Barr Virus Receptor. *Cell Rep* **3**, 371–385 (2013).
27. Bu, W. *et al.* Immunization with Components of the Viral Fusion Apparatus Elicits Antibodies That Neutralize Epstein-Barr Virus in B Cells and Epithelial Cells. *Immunity* **50**, 1305-1316.e6 (2019).
28. Edson, C. M. & Thorley-Lawson, D. A. Epstein-Barr virus membrane antigens: characterization, distribution, and strain differences. *J Virol* **39**, 172–184 (1981).
29. Pearson, G., Dewey, F., Klein, G., Henle, G. & Henle, W. Relation between neutralization of Epstein-Barr virus and antibodies to cell-membrane antigens-induced by the virus. *J Natl Cancer Inst* **45**, 989–95 (1970).
30. Sairenji, T. *et al.* Inhibition of Epstein-Barr virus (EBV) release from P3HR-1 and B95-8 cell lines by monoclonal antibodies to EBV membrane antigen gp350/220. *J Virol* **62**, 2614–2621 (1988).
31. Mutsvunguma, L. Z. *et al.* Identification of multiple potent neutralizing and non-neutralizing antibodies against Epstein-Barr virus gp350 protein with potential for clinical application and as reagents for mapping immunodominant epitopes. *Virology* **536**, 1–15 (2019).
32. Tugizov, S. M., Berline, J. W. & Palefsky, J. M. Epstein-Barr virus infection of polarized tongue and nasopharyngeal epithelial cells. *Nat Med* **9**, 307–314 (2003).
33. Turk, S. M., Jiang, R., Chesnokova, L. S. & Hutt-Fletcher, L. M. Antibodies to gp350/220 Enhance the Ability of Epstein-Barr Virus To Infect Epithelial Cells. *J Virol* **80**, 9628–9633 (2006).
34. Janz, A. *et al.* Infectious Epstein-Barr Virus Lacking Major Glycoprotein BLLF1 (gp350/220) Demonstrates the Existence of Additional Viral Ligands. *J Virol* **74**, 10142–10152 (2000).

35. Escalante, G. M. *et al.* A Pentavalent Epstein-Barr Virus-Like Particle Vaccine Elicits High Titers of Neutralizing Antibodies against Epstein-Barr Virus Infection in Immunized Rabbits. *Vaccines (Basel)* **8**, 169 (2020).
36. Perez, E. M., Foley, J., Tison, T., Silva, R. & Ogembo, J. G. Novel Epstein-Barr virus-like particles incorporating gH/gL-EBNA1 or gB-LMP2 induce high neutralizing antibody titers and EBV-specific T-cell responses in immunized mice. *Oncotarget* **8**, 19255–19273 (2017).
37. Cui, X. *et al.* Immunization with Epstein–Barr Virus Core Fusion Machinery Envelope Proteins Elicit High Titers of Neutralizing Activities and Protect Humanized Mice from Lethal Dose EBV Challenge. *Vaccines (Basel)* **9**, 285 (2021).
38. Molesworth, S. J., Lake, C. M., Borza, C. M., Turk, S. M. & Hutt-Fletcher, L. M. Epstein-Barr Virus gH Is Essential for Penetration of B Cells but Also Plays a Role in Attachment of Virus to Epithelial Cells. *J Virol* **74**, 6324–6332 (2000).
39. Kirschner, A. N., Omerović, J., Popov, B., Longnecker, R. & Jardetzky, T. S. Soluble Epstein-Barr Virus Glycoproteins gH, gL, and gp42 Form a 1:1:1 Stable Complex That Acts Like Soluble gp42 in B-Cell Fusion but Not in Epithelial Cell Fusion. *J Virol* **80**, 9444–9454 (2006).
40. Oda, T., Imai, S., Chiba, S. & Takada, K. Epstein–Barr Virus Lacking Glycoprotein gp85 Cannot Infect B Cells and Epithelial Cells. *Virology* **276**, 52–58 (2000).
41. Li, Q., Turk, S. M. & Hutt-Fletcher, L. M. The Epstein-Barr virus (EBV) BZLF2 gene product associates with the gH and gL homologs of EBV and carries an epitope critical to infection of B cells but not of epithelial cells. *J Virol* **69**, 3987–3994 (1995).
42. Mühe, J. & Wang, F. Host Range Restriction of Epstein-Barr Virus and Related Lymphocryptoviruses. *J Virol* **89**, 9133–9136 (2015).
43. Moghaddam, A., Koch, J., Annis, B. & Wang, F. Infection of Human B Lymphocytes with Lymphocryptoviruses Related to Epstein-Barr Virus. *J Virol* **72**, 3205–3212 (1998).
44. Yajima, M. *et al.* A new humanized mouse model of Epstein-Barr virus infection that reproduces persistent infection, lymphoproliferative disorder, and cell-mediated and humoral immune responses. *Journal of Infectious Diseases* **198**, 673–682 (2008).
45. Fujiwara, S., Imadome, K.-I. & Takei, M. Modeling EBV infection and pathogenesis in new-generation humanized mice. *Exp Mol Med* **47**, e135–e135 (2015).
46. Fujiwara, S. & Nakamura, H. Animal Models for Gammaherpesvirus Infections: Recent Development in the Analysis of Virus-Induced Pathogenesis. *Pathogens* **9**, 116 (2020).
47. Münz, C. EBV Infection of Mice with Reconstituted Human Immune System Components. in 407–423 (2015). doi:10.1007/978-3-319-22834-1_14.
48. Li, Y. & Di Santo, J. P. Probing Human NK Cell Biology Using Human Immune System (HIS) Mice. in 191–208 (2015). doi:10.1007/82_2015_488.
49. Schuhmachers, P. & Münz, C. Modification of EBV Associated Lymphomagenesis and Its Immune Control by Co-Infections and Genetics in Humanized Mice. *Front Immunol* **12**, (2021).
50. Singh, S. *et al.* Neutralizing Antibodies Protect against Oral Transmission of Lymphocryptovirus. *Cell Rep Med* **1**, 100033 (2020).
51. Zhu, Q.-Y. *et al.* A potent and protective human neutralizing antibody targeting a novel vulnerable site of Epstein-Barr virus. *Nat Commun* **12**, 6624 (2021).
52. Haque, T. *et al.* A Mouse Monoclonal Antibody against Epstein-Barr Virus Envelope Glycoprotein 350 Prevents Infection Both In Vitro and In Vivo. *J Infect Dis* **194**, 584–587 (2006).
53. Kim, J. *et al.* Epstein-Barr virus (EBV) hyperimmune globulin isolated from donors with high gp350 antibody titers protect humanized mice from challenge with EBV. *Virology* **561**, 80–86 (2021).
54. Moore, G. L. *et al.* A robust heterodimeric Fc platform engineered for efficient development of bispecific antibodies of multiple formats. *Methods* **154**, 38–50 (2019).

55. Bournazos, S., Gupta, A. & Ravetch, J. V. The role of IgG Fc receptors in antibody-dependent enhancement. *Nat Rev Immunol* **20**, 633–643 (2020).
56. Snijder, J. *et al.* An Antibody Targeting the Fusion Machinery Neutralizes Dual-Tropic Infection and Defines a Site of Vulnerability on Epstein-Barr Virus. *Immunity* **48**, 799-811.e9 (2018).
57. Tanner, J., Weis, J., Fearon, D., Whang, Y. & Kieff, E. Epstein-barr virus gp350/220 binding to the B lymphocyte C3d receptor mediates adsorption, capping, and endocytosis. *Cell* **50**, 203–213 (1987).
58. Coleman, C. B. *et al.* Epstein-Barr Virus Type 2 Latently Infects T Cells, Inducing an Atypical Activation Characterized by Expression of Lymphotactic Cytokines. *J Virol* **89**, 2301–2312 (2015).
59. Coleman, C. B. *et al.* Epstein-Barr Virus Type 2 Infects T Cells in Healthy Kenyan Children. *J Infect Dis* **216**, 670–677 (2017).
60. Jones, J. F. *et al.* T-Cell Lymphomas Containing Epstein–Barr Viral DNA in Patients with Chronic Epstein–Barr Virus Infections. *New England Journal of Medicine* **318**, 733–741 (1988).
61. Tugizov, S. *et al.* Epstein-Barr virus (EBV)-infected monocytes facilitate dissemination of EBV within the oral mucosal epithelium. *J Virol* **81**, 5484–96 (2007).
62. Kimura, H. *et al.* EBV-associated T/NK–cell lymphoproliferative diseases in nonimmunocompromised hosts: prospective analysis of 108 cases. *Blood* **119**, 673–686 (2012).
63. Kim, W. Y., Montes-Mojarro, I. A., Fend, F. & Quintanilla-Martinez, L. Epstein-Barr Virus-Associated T and NK-Cell Lymphoproliferative Diseases. *Front Pediatr* **7**, (2019).
64. Chijioke, O. *et al.* Human natural killer cells prevent infectious mononucleosis features by targeting lytic Epstein-Barr virus infection. *Cell Rep* **5**, 1489–98 (2013).
65. Bruhns, P. *et al.* Specificity and affinity of human Fcγ receptors and their polymorphic variants for human IgG subclasses. *Blood* **113**, 3716–3725 (2009).
66. Dekkers, G. *et al.* Affinity of human IgG subclasses to mouse Fc gamma receptors. *MAbs* **9**, 767–773 (2017).
67. Kanekiyo, M. *et al.* Rational Design of an Epstein-Barr Virus Vaccine Targeting the Receptor-Binding Site. *Cell* **162**, 1090–100 (2015).
68. Malhi, H. *et al.* Immunization with a self-assembling nanoparticle vaccine displaying EBV gH/gL protects humanized mice against lethal viral challenge. *Cell Rep Med* **3**, 100658 (2022).
69. Epstein, M. A., Morgan, A. J., Finerty, S., Randle, B. J. & Kirkwood, J. K. Protection of cottontop tamarins against Epstein–Barr virus-induced malignant lymphoma by a prototype subunit vaccine. *Nature* **318**, 287–289 (1985).
70. Jackman, W. T., Mann, K. A., Hoffmann, H. J. & Spaete, R. R. Expression of Epstein-Barr virus gp350 as a single chain glycoprotein for an EBV subunit vaccine. *Vaccine* **17**, 660–8 (1999).
71. Morgan, A. J., Finerty, S., Lovgren, K., Scullion, F. T. & Morein, B. Prevention of Epstein-Barr (EB) virus-induced lymphoma in cottontop tamarins by vaccination with the EB virus envelope glycoprotein gp340 incorporated into immune-stimulating complexes. *J Gen Virol* **69 (Pt 8)**, 2093–6 (1988).
72. Epstein, M. A., Morgan, A. J., Finerty, S., Randle, B. J. & Kirkwood, J. K. Protection of cottontop tamarins against Epstein–Barr virus-induced malignant lymphoma by a prototype subunit vaccine. *Nature* **318**, 287–289 (1985).
73. Kimura, H. *et al.* Quantitative Analysis of Epstein-Barr Virus Load by Using a Real-Time PCR Assay. *J Clin Microbiol* **37**, 132–136 (1999).
74. Delecluse, H.-J., Hilsendegen, T., Pich, D., Zeidler, R. & Hammerschmidt, W. Propagation and recovery of intact, infectious Epstein–Barr virus from prokaryotic to human cells. *Proceedings of the National Academy of Sciences* **95**, 8245–8250 (1998).

75. Neuhierl, B., Feederle, R., Hammerschmidt, W. & Delecluse, H. J. Glycoprotein gp110 of Epstein–Barr virus determines viral tropism and efficiency of infection. *Proceedings of the National Academy of Sciences* **99**, 15036–15041 (2002).

Chapter 5. Concluding Remarks on EBV gH/gL Vaccines

EBV is a ubiquitous virus with a global burden of disease, and a vaccine to prevent infection and associated disease has the potential have immense public health benefit. Our group has focused on developing vaccines targeting gH/gL, as antibodies against gH/gL can neutralize infection *in vitro* and *in vivo*. As described in this thesis, using both protein nanoparticles in rhesus macaques (chapter 2) and repRNA immunizations in mice (chapter 3), these vaccines are immunogenic and can elicit antibodies capable of neutralizing EBV infection of B cells and epithelial cells *in vitro*. *In vivo*, one of four rhesus macaques was protected from challenge with the orthologous rhLCV, and humanized mice receiving vaccine-elicited IgG had reduced detectable EBV DNA and were protected from lethal EBV challenge.

Approaches to optimize vaccines are detailed in chapter 1.6. As detailed in this thesis, adjuvant selection, dosing, and antigen design all influence immunogenicity of a vaccine. In chapter 3 we tested various repRNA gH/gL constructs. Another potential path to improve vaccine immunogenicity that was not done in this work is to include other EBV proteins as vaccine targets. In chapters 2 and 3, our gH/gL vaccine elicited lower B cell neutralizing titers than epithelial cell titers. To improve this we could target EBV proteins involved in B cell infection, like gp350 and gp42. In chapter 4 I show preliminary data in a humanized mouse model, where mice given a mAb against gp350 prior to EBV challenge develop worsened disease. However the implications of this are unclear, as more work is needed to understand how this effect is being mediated (the Fc region of the mAb appears to be involved) and whether or not this effect is limited to the humanized mouse model.

Additionally, work in this thesis highlights the limitations of animal models for EBV. As detailed in chapter 2, there was an unexpected degree of antigenic disparity between the vaccine antigen (EBV gH/gL) and the challenge strain (rhLCV gH/gL). While these two viruses

are closely related, our work has shown that there is enough difference to limit the utility of rhLCV challenge to model EBV vaccine elicited protection. Potential ways to work around this could be to make hybrid rhLCV challenge strains that express EBV proteins[1], or to immunize with the rhLCV version of proteins instead of EBV. In contrast, use of humanized mice allows us to model EBV infection *in vivo*, but not by the typical oral route, and only B cell infection is recapitulated[2]. Additionally, these animals do not develop typical immune responses to vaccination, requiring passive transfer studies to look at the role of vaccine elicited antibodies in protection from infection. These limitations must be considered when evaluating EBV vaccines. However, with these caveats in mind, they are still useful tools for preclinical evaluation of EBV vaccines. The work outlined in this thesis describes the immunogenicity and protection mediated by two next-generation vaccines targeting EBV gH/gL, and validates gH/gL as being an important vaccine target. Further optimization of gH/gL vaccines by changing the vaccine platform, adjuvants, dosing, or introducing additional antigens should be explored further.

If a promising vaccine candidate is identified through preclinical studies in animal models, setting up clinical trials in humans is the next step in development. However this raises questions about how to evaluate vaccines in humans. In addition to determining safety, immunogenicity, and optimal dosing, how do you determine if a vaccine against EBV is actually effective? If a population of EBV negative individuals is evaluated, this allows investigation of whether or not the candidate vaccine is protective against acquisition of the virus and additionally development of IM. However, as mentioned previously, most adults are seropositive for EBV and have lifelong infection with the virus, so finding a suitable study population could be a challenging endeavor. Additionally, secondary endpoints determining protection mediated by candidate vaccines against development of EBV associated malignancies and MS are important to evaluate. Given these conditions can take decades to develop after initial EBV infection makes evaluation of these secondary endpoints during a clinical trial complicated and difficult.

Designing additional trials with specific study cohorts can give researchers a proxy for difficult to measure benefits. For example, vaccinating populations at higher risk of EBV-associated malignancies that are relatively quick to develop (i.e. EBV-negative patients undergoing transplantation and at risk of PTLD or those with certain primary immunodeficiencies linked to EBV malignancies)[3]. While human trials with candidate EBV vaccines present unique challenges and obstacles, they also presents a critical opportunity to further develop vaccines that could have enormous impact on human health by reducing the morbidity and mortality driven by IM, MS, and EBV-associated malignancy[3].

Chapter 5 Bibliography

1. Mühe, J. *et al.* Neutralizing antibodies against Epstein-Barr virus infection of B cells can protect from oral viral challenge in the rhesus macaque animal model. *Cell Rep Med* **2**, 100352 (2021).
2. Fujiwara, S. & Nakamura, H. Animal Models for Gammaherpesvirus Infections: Recent Development in the Analysis of Virus-Induced Pathogenesis. *Pathogens* **9**, 116 (2020).
3. Cohen, J. Vaccine Development for Epstein-Barr Virus. *Adv Exp Med Biol*. 1045 (2018)